

## **CHAPTER-4**

### **RESULT AND DISCUSSION**

---

The main objective of the present investigation is to understand the effect of different frequencies and amplitudes of oscillation during the solidification on mechanical and metallurgical properties of A356 and A319 aluminum alloy casting. The chapter presents the experimental results obtained during the investigation. The frequency varies from 0 Hz to 400Hz and amplitude of oscillation ranged from 0 $\mu$ m to 15 $\mu$ m. The castings prepared under oscillatory conditions have the different value of ultimate tensile strength, yield strength, percentage elongation, impact strength and hardness for different frequencies and amplitudes of oscillation during casting. The microstructure of the castings has also been found to vary with the variation in frequency and amplitude of oscillation.

The experimental results were compared with that of the properties of the stationary casting, and the conclusions were derived. The detailed experimental procedures involved in each stage of this experimental work are briefed in the following sections. To achieve the main objectives of the present experimental investigation, the experimental research work was planned in the following sequence:-

1. Evaluation and investigation of the chemical composition, and inter-metallic phase determination after solidification of A356 and A319 aluminum alloy.
2. Evaluation of the mechanical properties and comparison of oscillatory casting with the stationary casting.

3. Evaluation of the metallurgical characteristics and comparison of the oscillatory casting with stationary casting.
4. Evaluation of Tensile Fracture Surface (SEM Image) to identify fracture mode from the microscopic appearance or morphology of resulting fracture surface.

#### 4.1 Evaluation and investigation of the chemical composition and inter-metallic phase determination after solidification of A356 and A319 aluminum alloy

##### 4.1.1 SEM/EDS of A356

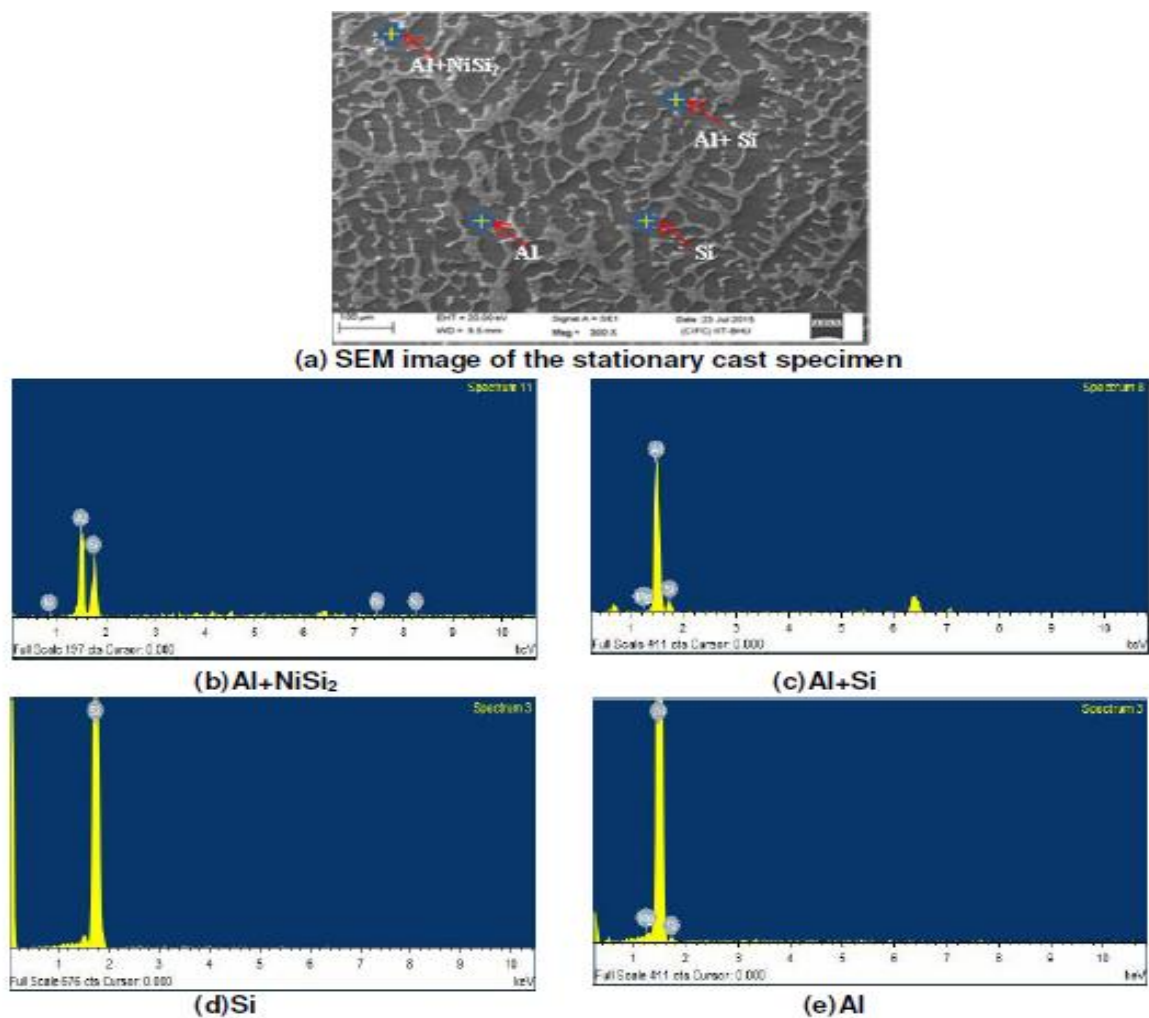
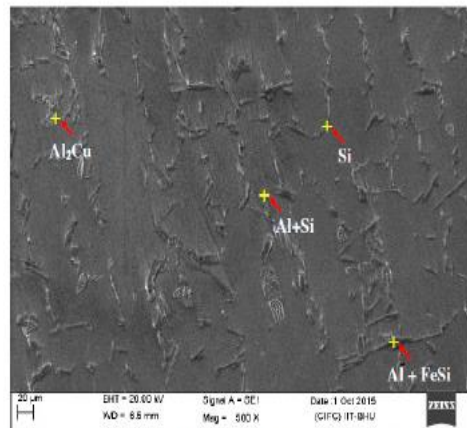
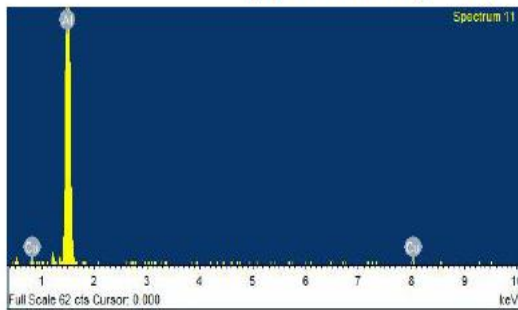


**Figure 4.1 SEM and Corresponding EDS (Energy Dispersive Spectroscopy) spectra (b-e) of Al+NiSi<sub>2</sub>, Al + Si, Al and Si respectively showing phases present in the Cast specimen of A356 aluminum alloy**

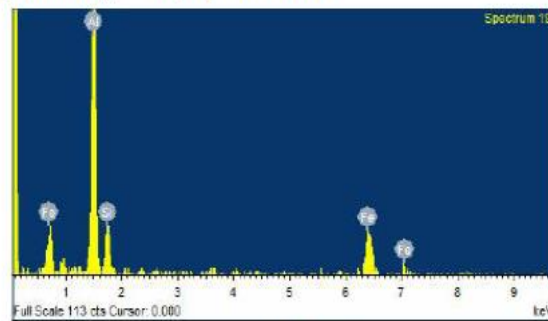
#### 4.1.2 SEM/EDS of A319



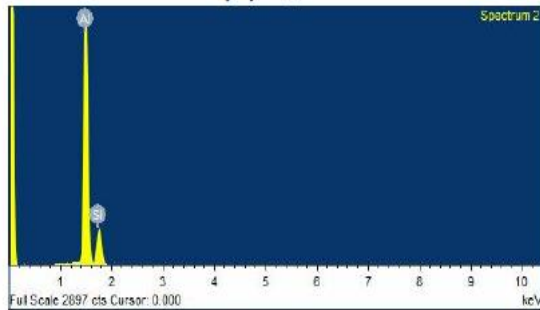
(a) SEM image of the stationary cast specimen



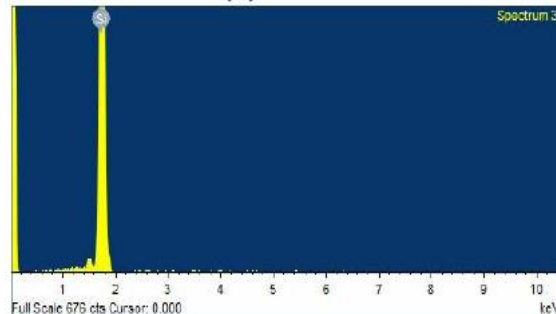
(b) Al<sub>2</sub>Cu



(c) Al+FeSi



(d) Al + Si



(e) Si

**Figure 4.2 SEM and Corresponding EDS (Energy Dispersive Spectroscopy) spectra (b-e) of Al<sub>2</sub>Cu, Al+FeSi, Al + Si and Si respectively showing phases present in the cast specimen of A 319 aluminum alloy**

For the fast measurements of the local chemical composition of the metals EDS mode of x-ray micro-analyzer was used. The elemental analyses of casting were studied using SEM coupled with energy dispersive x-ray spectroscopy (EDS) software. The aim was to understand the element composition (weight % and Atomic%) and corresponding EDS spectrum present at area of interest represented in the Figures 4.2 (a) and Figure 4.2

(b).The SEM was primarily used to capture image of the sample's surface, while the EDS scan was performed in order to characterize element present. In the examined surface are Al-K, Si-K, Mg-K, Fe-K, Ti-K , Mn-L, Fe-L Ni-L, Cu-L and Zn-L elements are found along with O. Which indicates the possible formation of oxides likes  $\text{SiO}_2$ , MgO and  $\text{Al}_2\text{O}_3$  as shown in Figure 1(a).

Similarly for A319 the elements found in the examined surface are Al-K, Si-K, Mg-K, Mn-L, and Cu-L along with the possible formation of intermetallic phase likes  $\text{Mg}_2\text{Si}$ ,  $\text{Al}_2\text{Cu}$ ,  $\text{Al}_5\text{FeSi}$ , and  $\text{Al}_5\text{Cu}_2\text{Mg}_8\text{Si}_5$  in the scanned microstructure as shown in Figure 4.3.

#### **4.1.3 X-RAY Diffraction Analysis**

X-ray diffraction analysis (XRD) was performed on A356 and A319 aluminum alloy casting to identify various phases present on the sample surface.XRD analysis was carried out using PAN analytical's X'Pert PRO Materials Research Diffractometer (Holland) with Cu K- $\alpha$  radiation and nickel filter at 40mA under a voltage of 45kV at Central Research Facility ,IIT(BHU) Varanasi(India).The specimens were scanned with a scanning speed of 1kcps and intensities were recorded at a chart speed of 1cm/min with  $2^\circ/\text{min}$  as goniometer speed. The diffractometer interfaced with X'Pert High Score plus X-ray diffraction software provides d-spaced values directly on the diffraction patterns. These 'd' values from observed XRD patterns were then used for identification of individuals crystalline phase using the ICDD-PDF database.

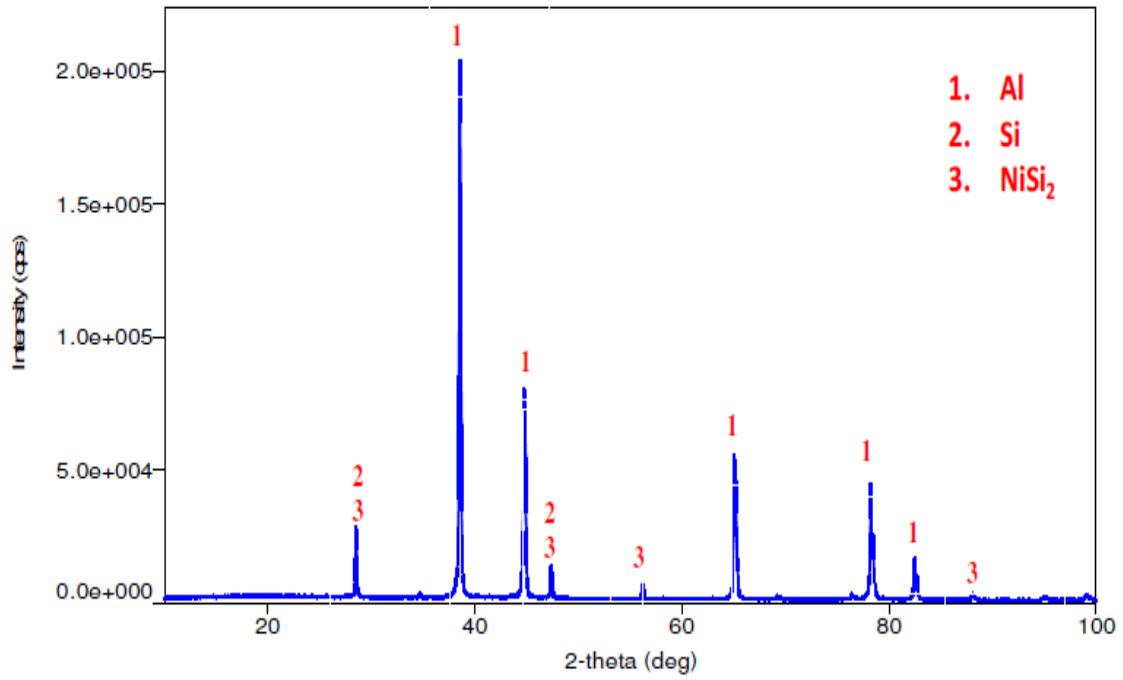


Figure 4.3 XRD Pattern of A356 aluminum alloy

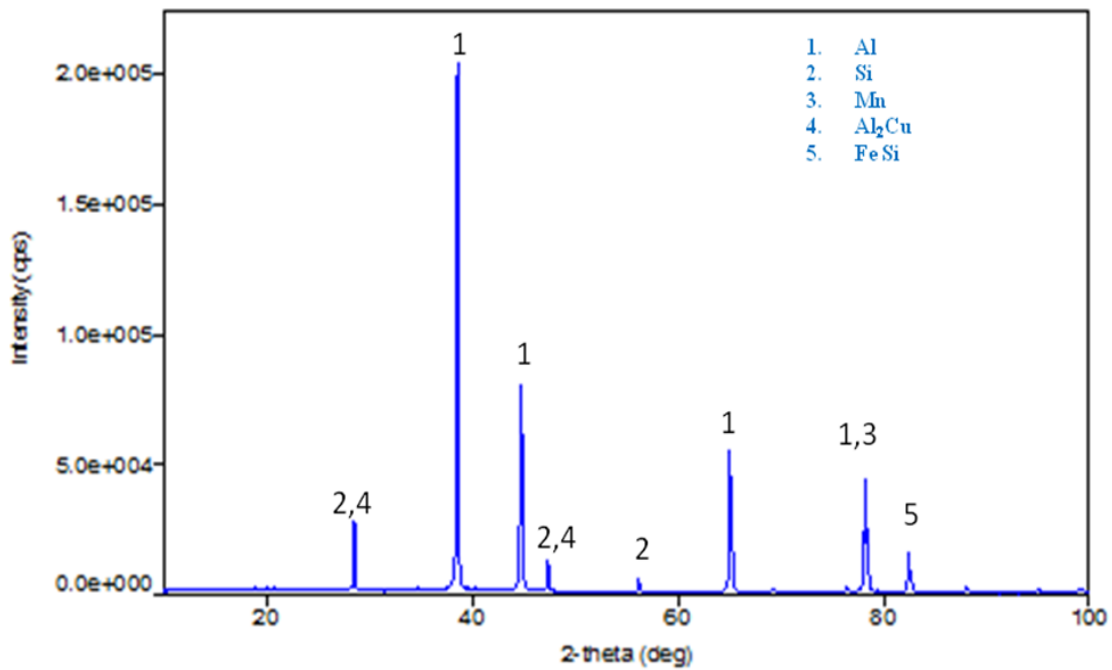


Figure 4.4 XRD Pattern of A319 aluminum alloy

XRD patterns of A356 and A319 of aluminum alloys are shown in Figure 4.4 and Figure 4.5 respectively. The search result showed mainly Al, Si, Cu, Mg and Ni are the main element on the surface of the specimens. The identified XRD peaks on A356 surface revealed that  $Mg_2Si$  and  $NiSi_2$  phases are present in area of interest. The presence of aluminum, Magnesium and Silicon has also been identified as main phase. Small traces of  $SiO_2$ ,  $MgO$  and  $Al_2O_3$  are also present as weak phase. Peaks pertaining  $SiO_2$ ,  $MgO$  and  $Al_2O_3$  are seen in the XRD signature may be due to very low relative portion on the surface of the sample. A few small peaks of low intensity were unidentifiable. The fairly sharp peaks in the XRD pattern clearly indicate that sample surface has a crystalline microstructure.

Similarly for identification of XRD peaks of A319 sample surface revealed that have  $Al_2Cu$ ,  $Al_2CuMg$ , and  $Fe_{1.7}Al_4Si$  phase are present in area of interest. The presence of aluminum, Copper and Silicon has been also identified as main phase. Several small peaks are of low intensity were also unidentifiable. The fairly sharp peaks are also present as A356 in the XRD pattern which clearly indicates that sample surface has a crystalline microstructure.

**Gopikrishna, S., & Binu, C. Y. [113]** reported that the size, morphology and the distribution of silicon particles could affect the hardness of the eutectic mixture. They also suggested that a solutioning temperature of  $500^\circ C$  is suitable for A319 alloy due to mutual inter-metallic precipitation formation of  $Al_2Cu$  and  $Mg_2Si$  at this temperature. Hardness of A319 also increases because of these precipitate.

**Rincon, E. et al [114]** depicted that the fracture behavior of A319 aluminum alloy is controlled by the brittle fracture of inter-metallic  $Al_2Cu$  and  $Al_5FeSi$  phases and Si eutectic. They have also stated that UTS and Yield strength are improved due to a lower

area fraction of inter-metallic precipitate,  $\text{Al}_2\text{Cu}$  and  $\text{Al}_5\text{FeSi}$  phases present after solution and solution plus aging heat treatment.

**Lasa, L., and J. M. Rodriguez-Ibabe. [115]** observed that magnesium bearing phases containing magnesium such as  $\text{Mg}_2\text{Si}$  or  $\text{Al}_5\text{Mg}_8\text{Cu}_2\text{Si}_6$  are present in A319 type aluminum alloy. The  $\text{Al}_5\text{Mg}_8\text{Cu}_2\text{Si}_6$  and  $\text{Al}_2\text{Cu}$  phase precipitates in clusters near the solidus point of the alloy. They also found that the magnesium bearing phases improve the strength of A319 type alloys particularly in the metastable state, obtained after solution heat treatment and aging.

**Tash, M., et al. [116]** investigated the impact of metallurgical parameters on the hardness of as-cast and heat treated 356 and 319 aluminum alloys. They are trying to discuss the metallurgical characterization of 356, and 319 aluminum alloys containing  $\alpha$ -Fe or  $\beta$ -Fe intermetallics with same Mg-containing concentration of as-cast and heat treated conditions. A319 alloys exhibit greater hardness values than the A356 alloys at all aging times and temperatures, regardless of their modification state. The remarkable improvement in the hardness with the increase in Mg content in these 319 alloys occurs by combining precipitation of  $\text{Al}_2\text{Cu}$  and  $\text{Mg}_2\text{Si}$  phase particles, compared to only  $\text{Mg}_2\text{Si}$  precipitation in the case of the 356 alloys.

**Mohedano, M., et al. [117]** characterized the microstructure of the rheocast A356 Al alloy by fine and rounded particles of  $\alpha$ -Al phase with the eutectic silicon and intermetallic compounds placed at the interglobular regions. The intermetallics were recognized as  $\beta$ -AlFeSi,  $\pi$ -AlFeSiMg and  $\text{Mg}_2\text{Si}$ . A notable change was also observed in the morphology and dispersion of silicon particles and  $\beta$ -AlFeSi intermetallic compared to the A356 gravity-cast alloy

## **4.2 Evaluation and Comparison of the mechanical properties of oscillatory prepared casting and stationary casting**

Applying mechanical mold oscillation with different frequencies and amplitude during permanent mold casting enhances nucleation and improves mold-casting heat transfer. In the number of published research papers in this area attracted little attention to correlating the vibration parameters of frequency and amplitude with the metallurgical and mechanical properties of casting. In this experimental investigation to the effect of mold oscillation on microstructure refinement and mechanical properties of casting has been observed. Mold-oscillation was given at different frequencies (100 Hz, 200Hz, 300Hz and 400 Hz, and 2000 Hz) and amplitudes (5 $\mu$ m, 10 $\mu$ m and 15 $\mu$ m). The tensile test was carried out on samples prepared as per ASTM standards, from work pieces by keeping a fixed strain rate of 1 mm/min using the computerized tensile testing machine (INSTRON). The test was conducted on three specimens for both alloys in a given condition, and average values of the ultimate tensile strength (UTS), Yield Strength along with percentage elongation were analyzed in the present study. The Charpy impact test machine was used for estimating the absorbed energy of the samples as impact strength. The standard Charpy test samples 10  $\times$  10  $\times$  55 mm with a 2 mm V-notch were prepared for Impact strength testing. The Vickers hardness test was carried out using a load of 50 N with 30 seconds dwell period on samples according to ASTM standards. All the experiments were conducted at room temperature. Scanning electron microscope (SEM) was employed for the examination of tensile fractured surface of the selected samples under different conditions.

#### 4.2.1 Effect of Oscillation on Ultimate Tensile Strength

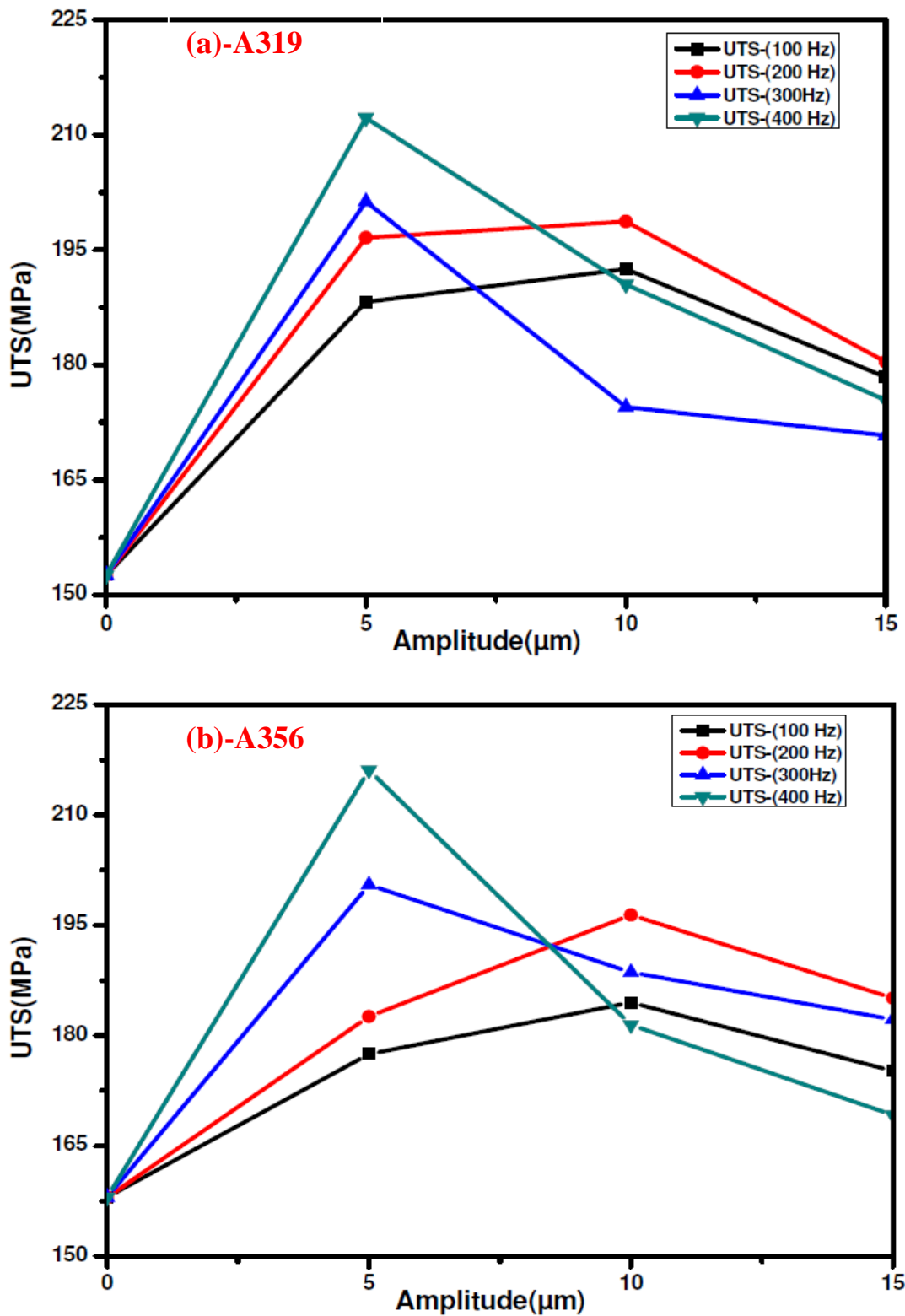


Figure 4.5 Effect of amplitude on ultimate tensile strength of (a) A319 and (b) A356 aluminum alloys casting

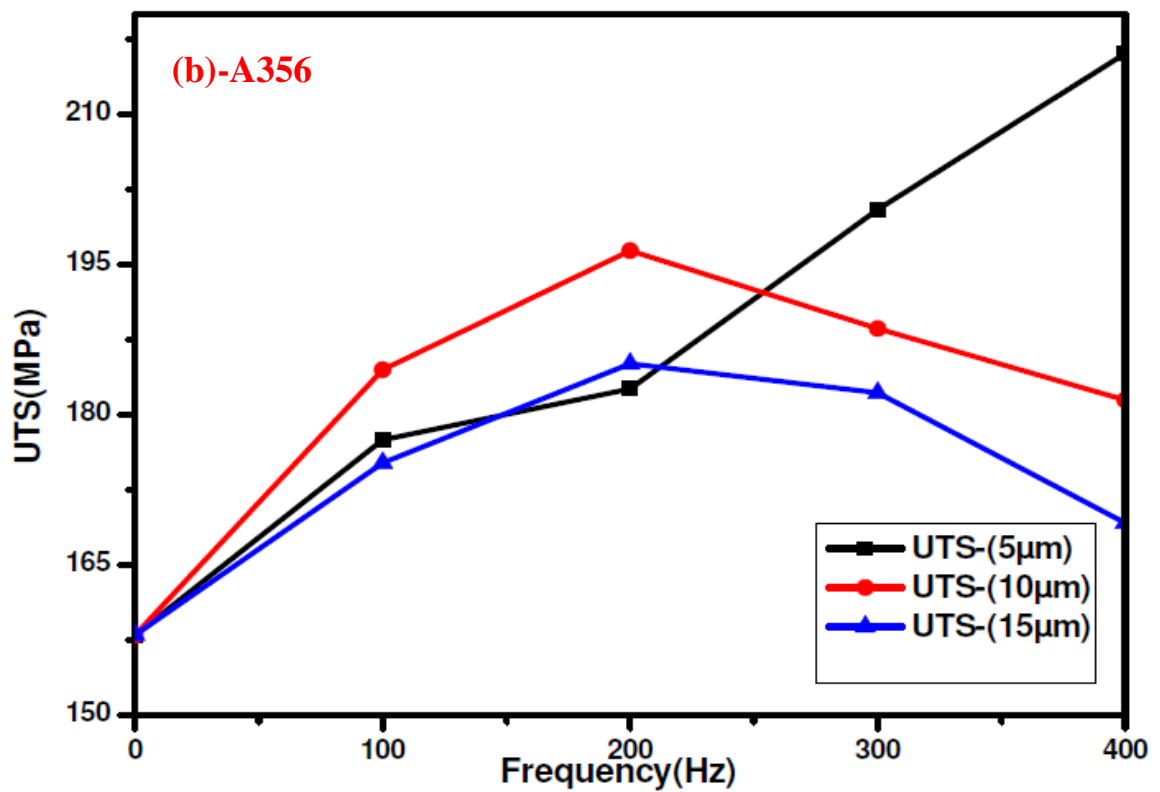
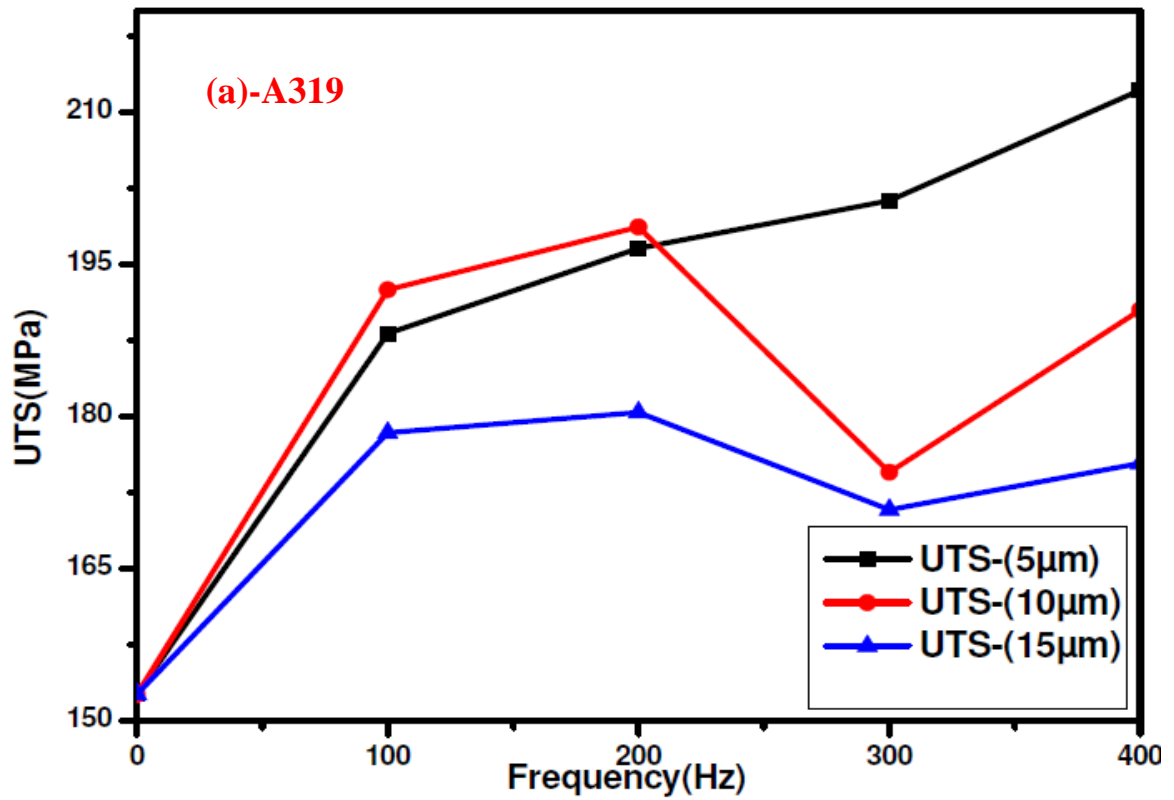


Figure 4.6 Effect of frequency on ultimate tensile strength of (a) A319 and (b) A356 aluminum alloys casting

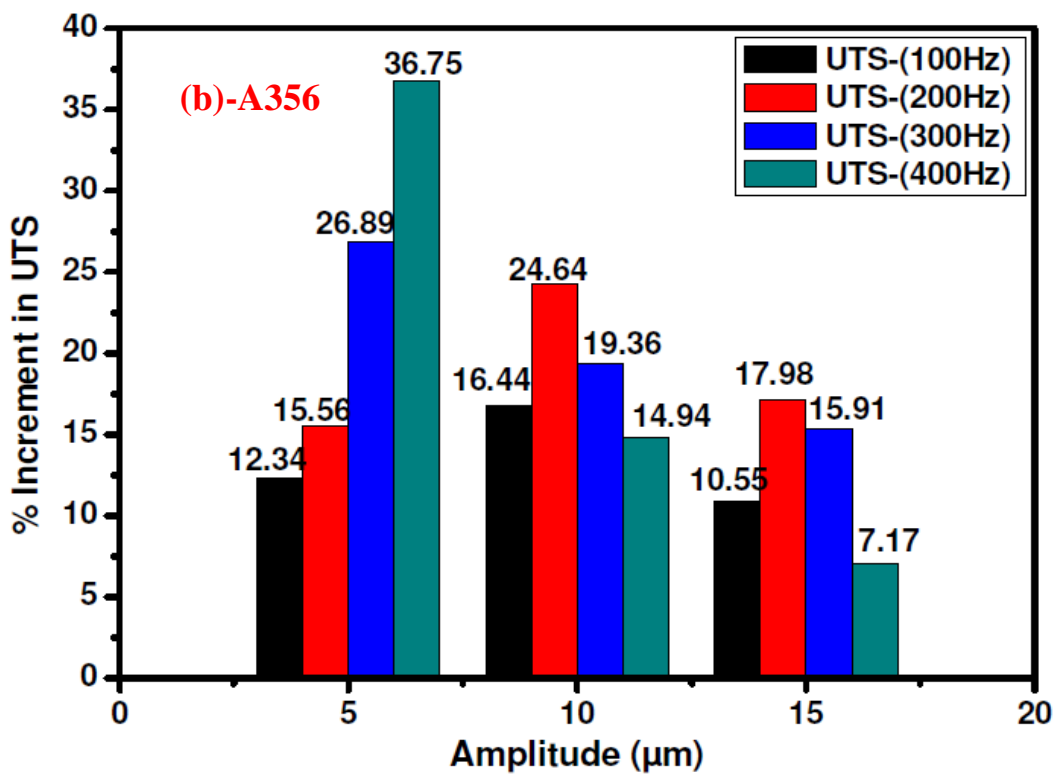
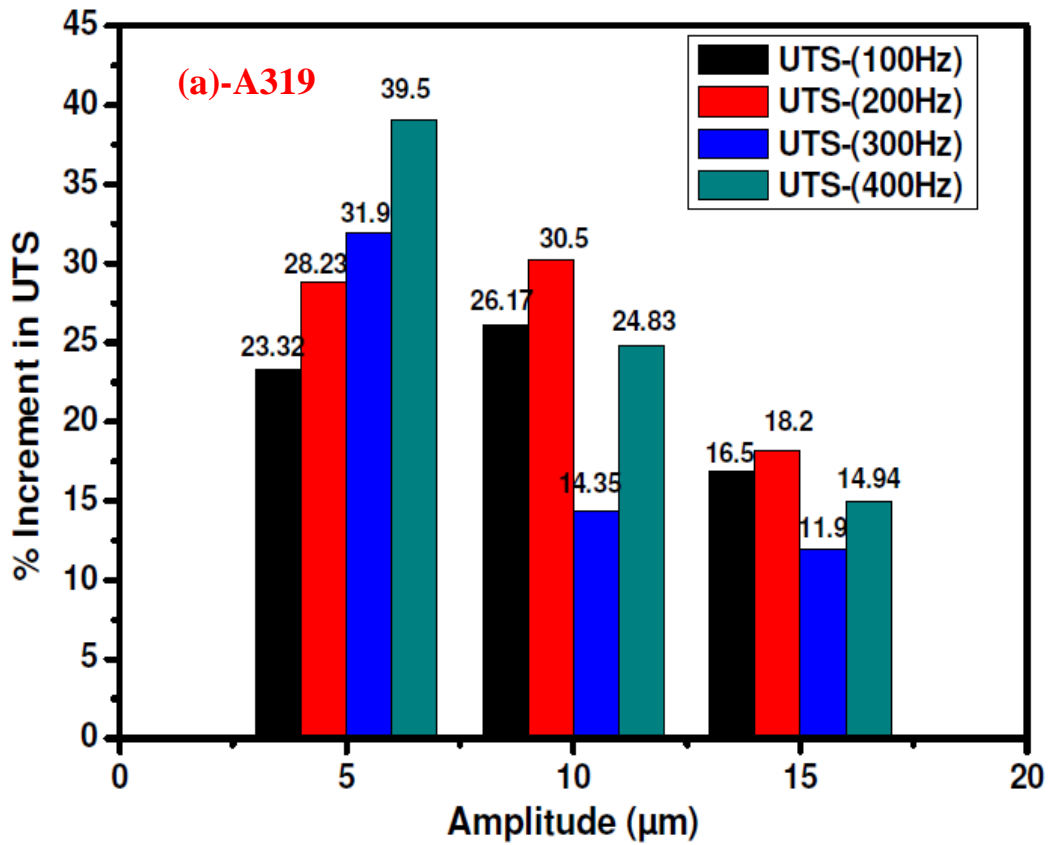


Figure 4.7 Comparison of percentage change in ultimate tensile strength (a) A319 and (b) A356 aluminum alloys casting

#### 4.2.2 Effect of Oscillation on Yield Strength

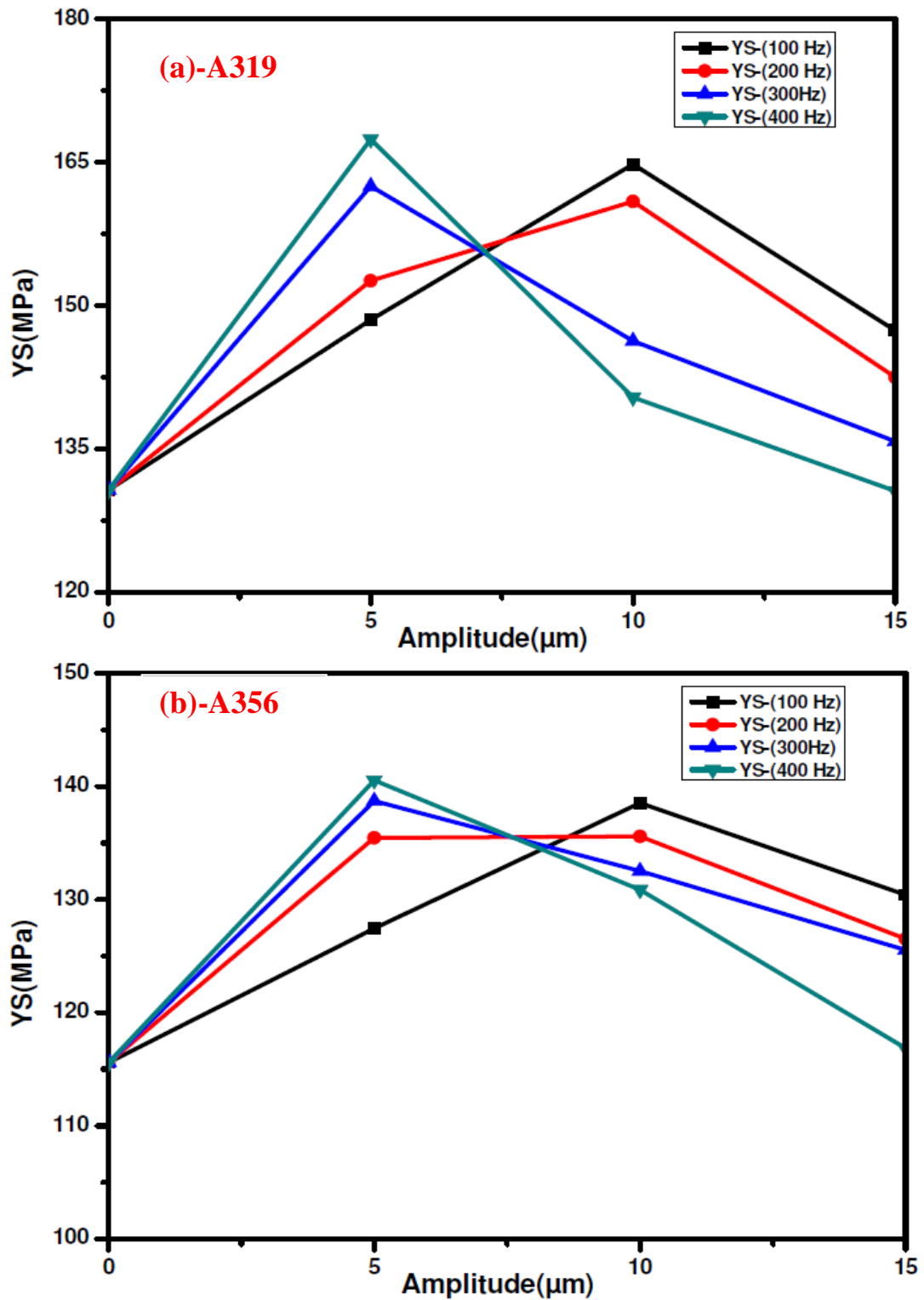


Figure 4.8 Effect of amplitude on yield strength of (a) A319 and (b) A356 aluminum alloys casting

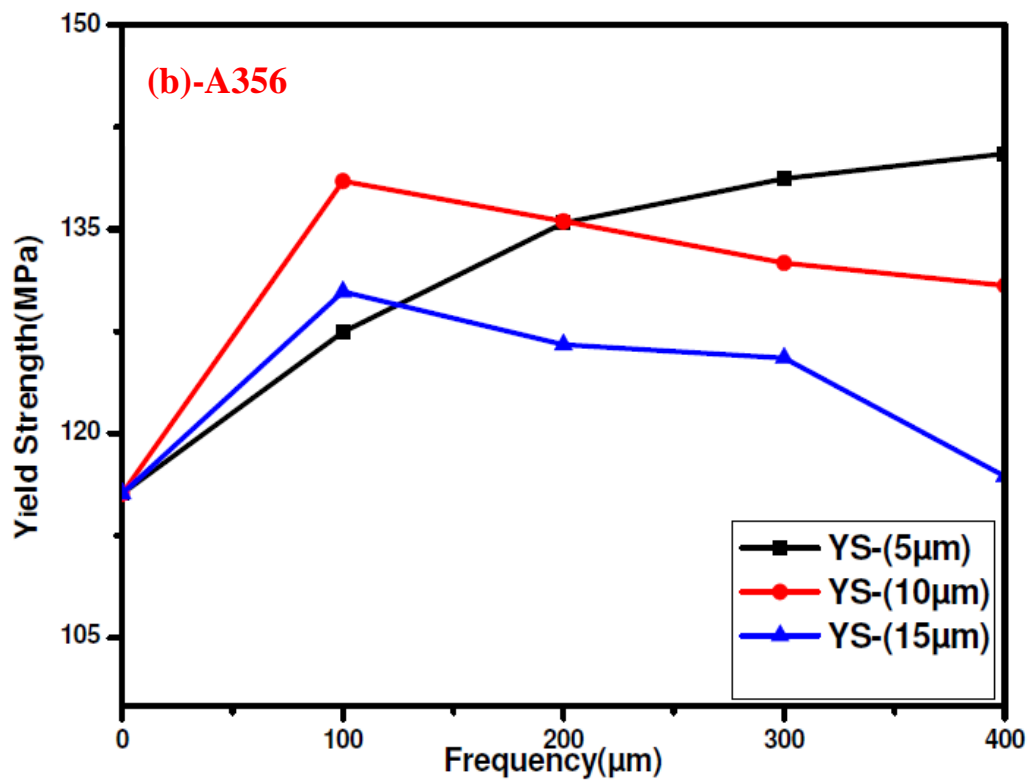
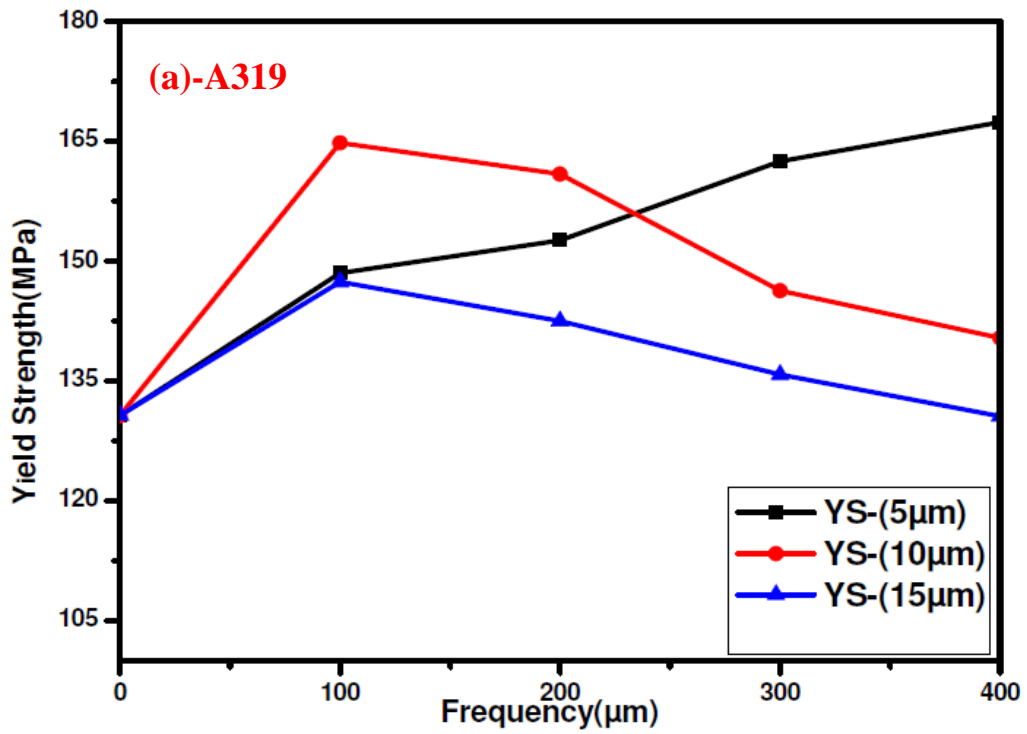


Figure 4.9 Effect of frequency on yield strength of (a) A319 and (b) A356 Aluminum Alloys Casting

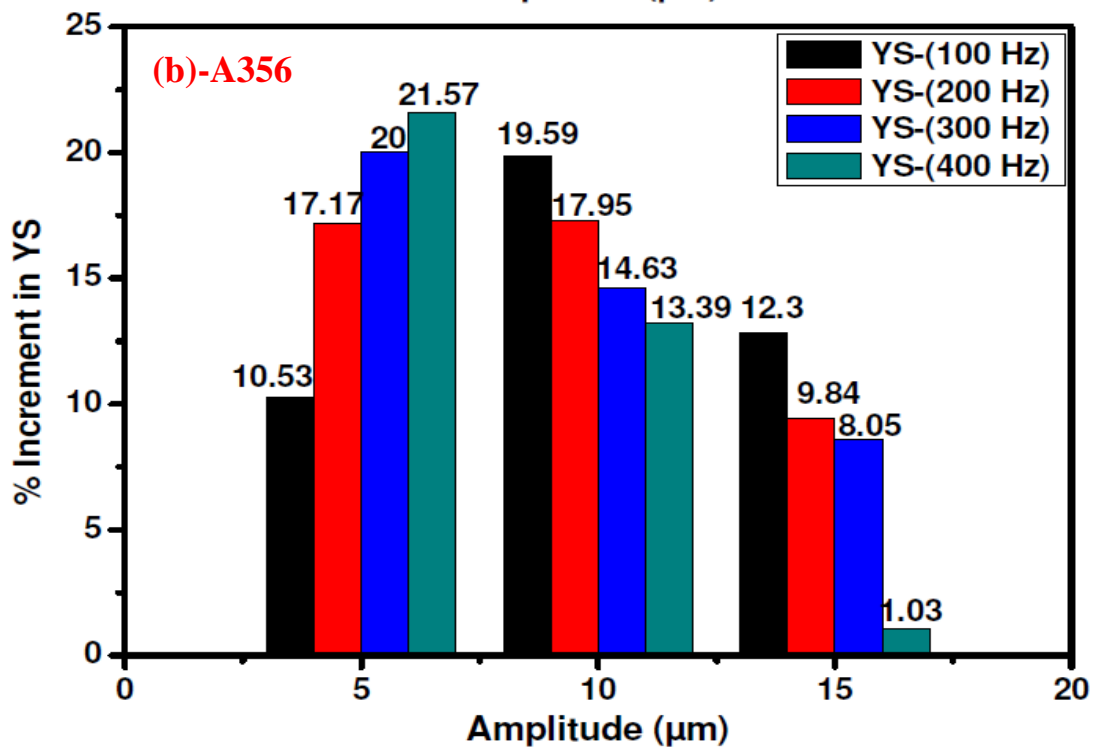
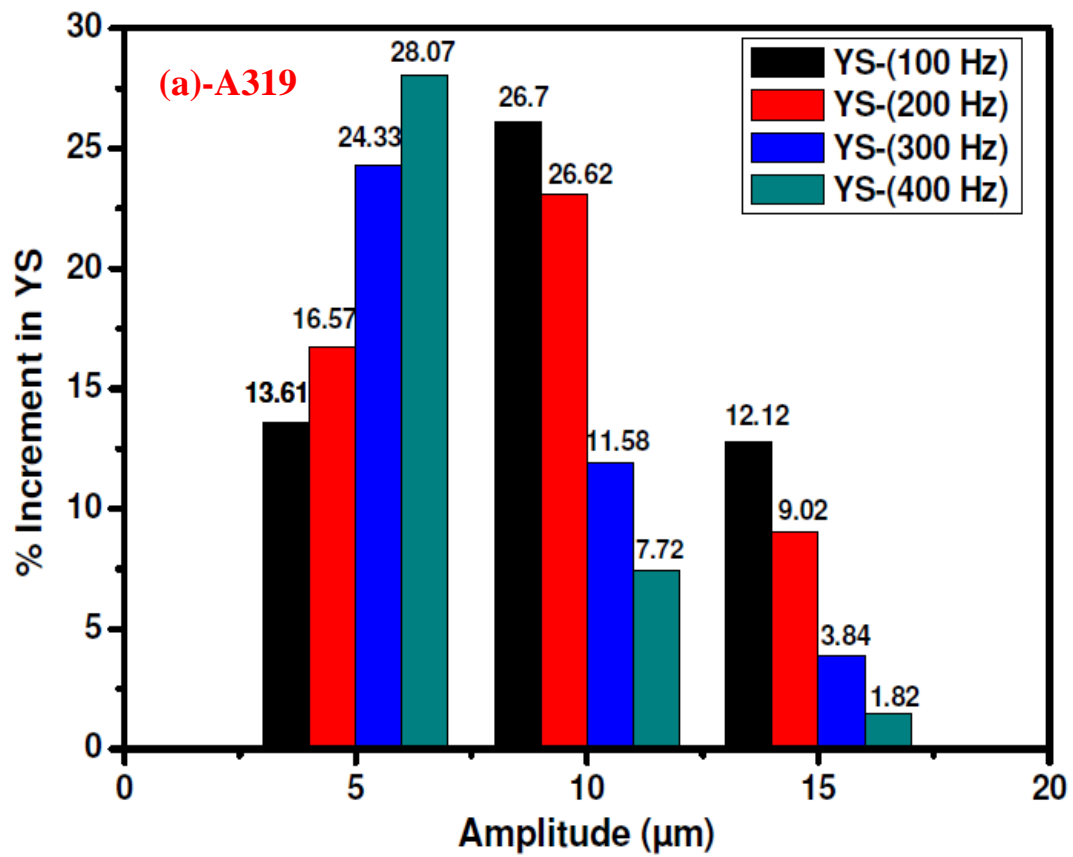


Figure 4.10 Comparison of percentage change in yield strength (a) A319 and (b) A356 aluminum alloys casting

### 4.2.3 Effect of Oscillation on % Elongation

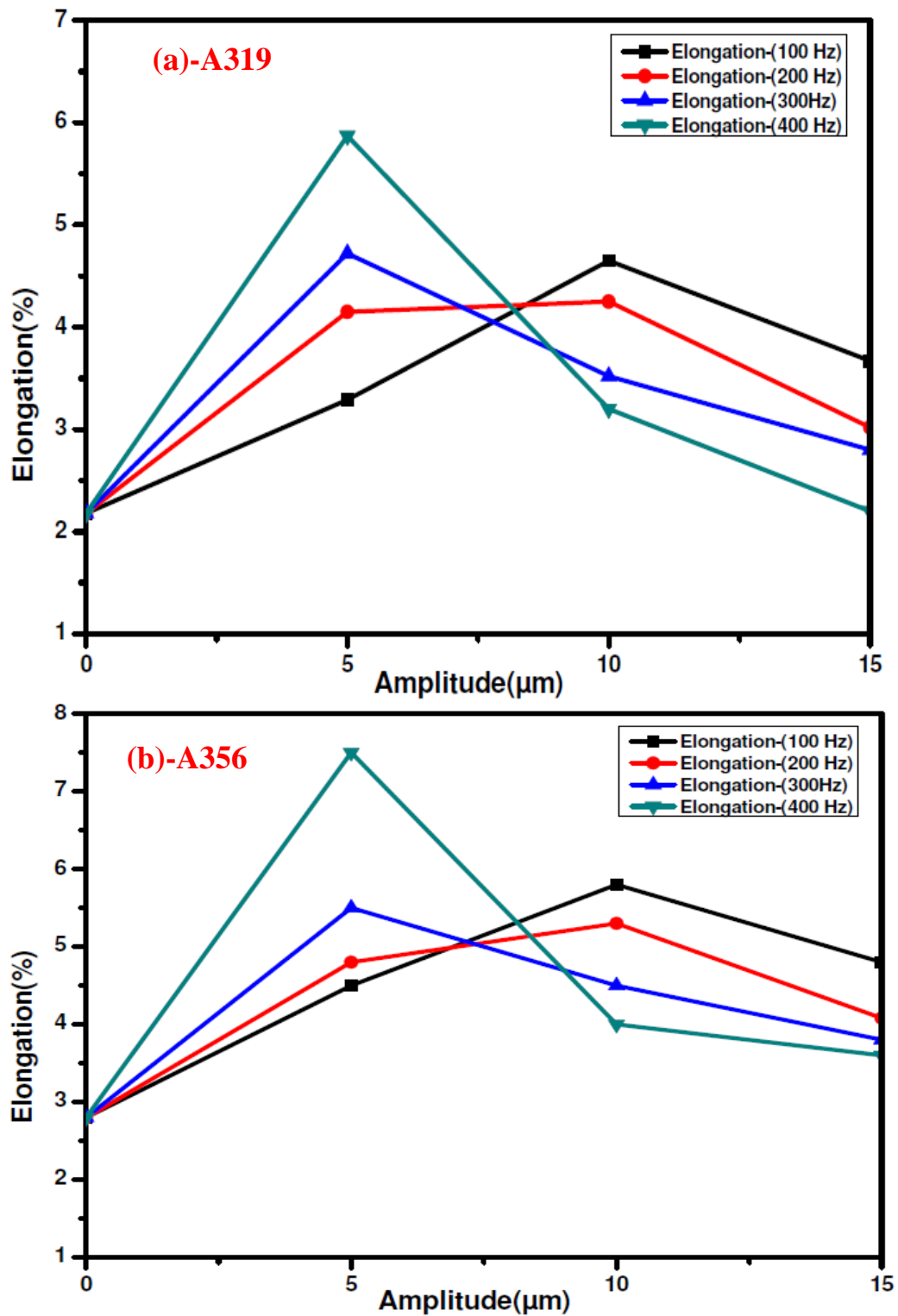


Figure 4.11 Effect of amplitude on %Elongation of(a) A319 and (b) A356 aluminium alloys casting

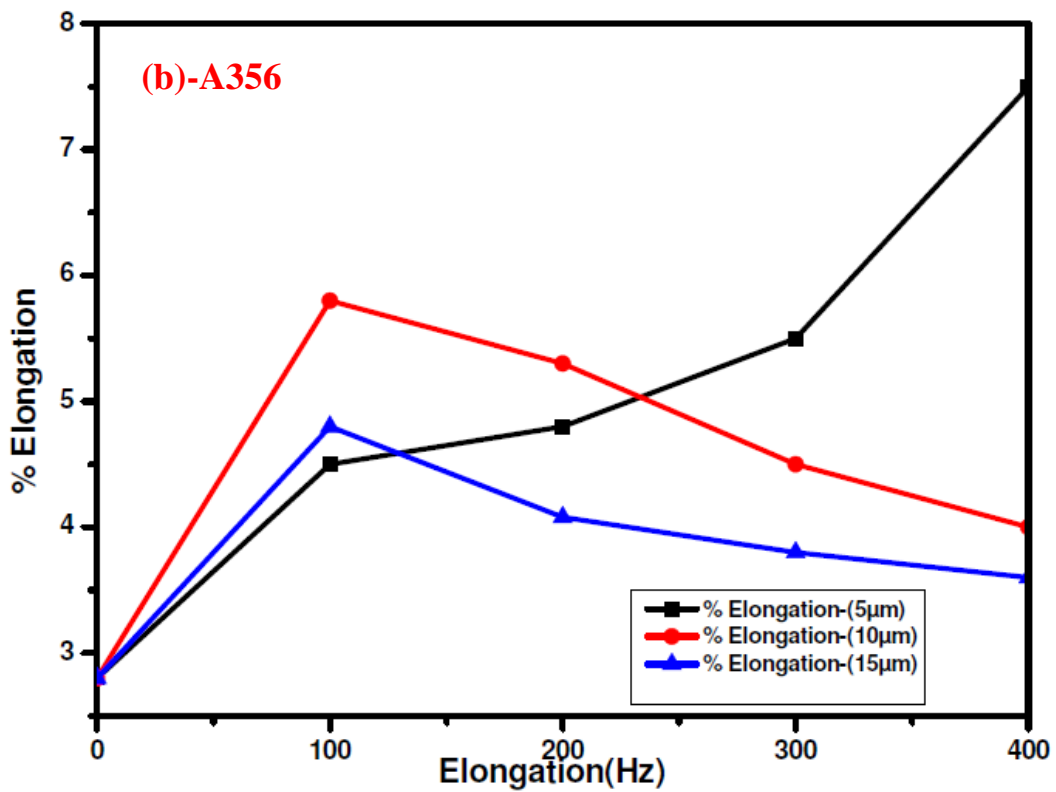
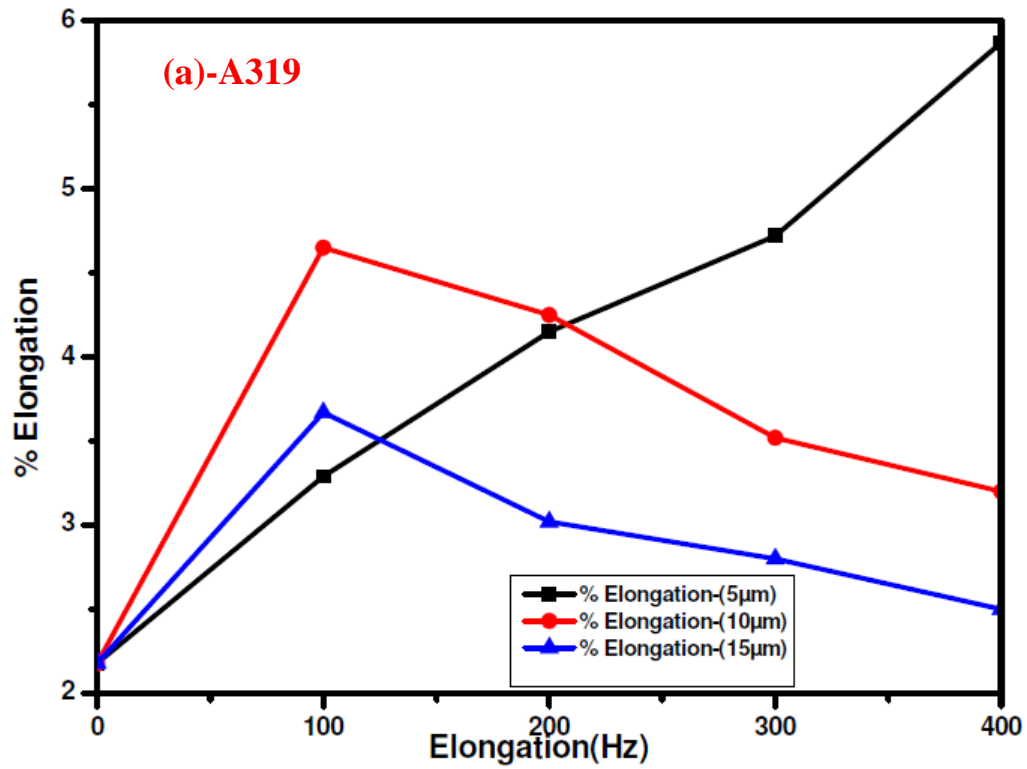


Figure 4.12 Effect of frequency on % Elongation of (a) A319 and (b) A356 aluminum alloys casting

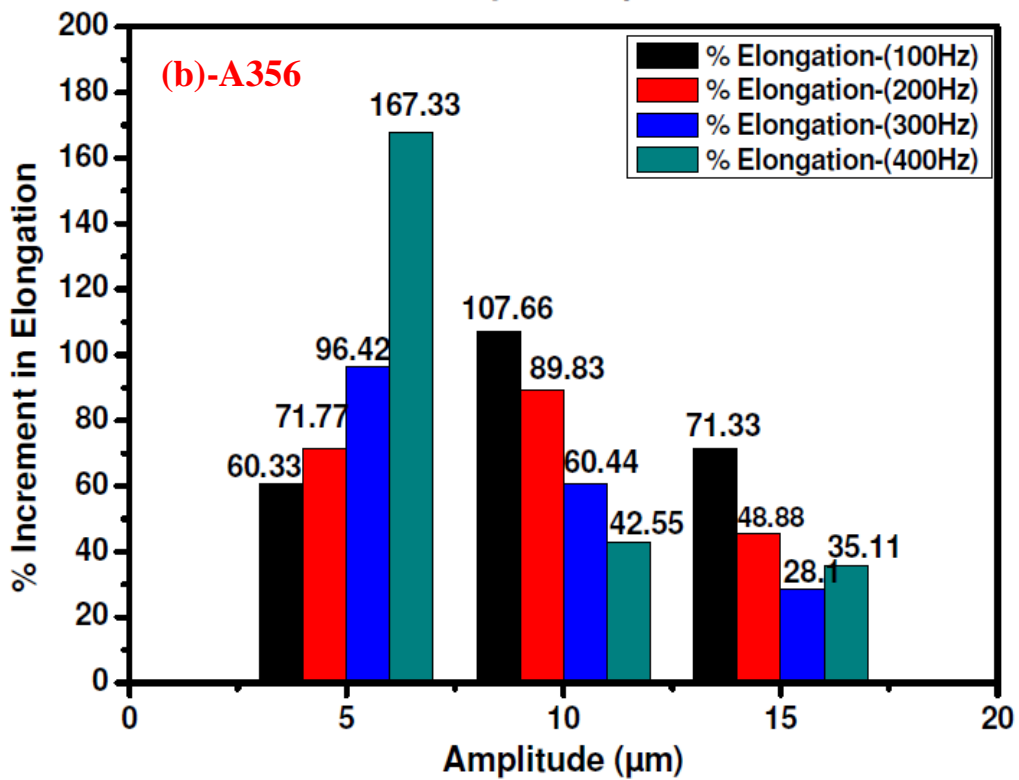
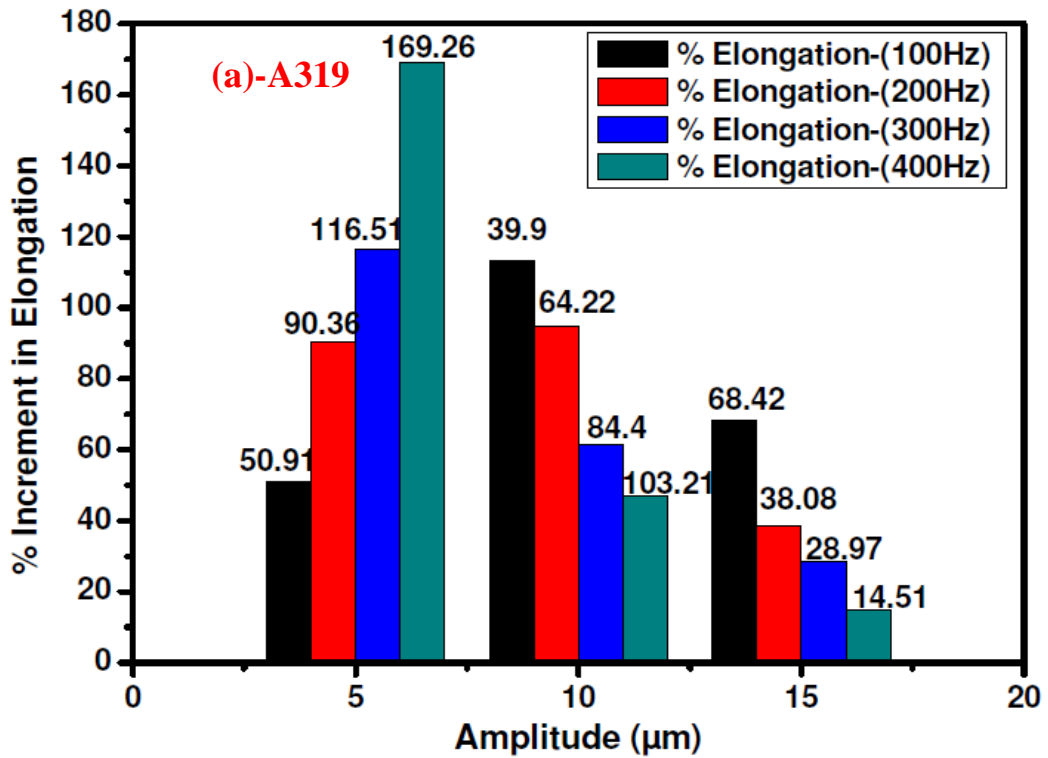


Figure 4.13 Comparison of percentage change in yield strength (a) A319 and (b) A356 aluminum alloys casting

#### 4.2.4 Effect Of Oscillation on Micro-Hardness(HV)

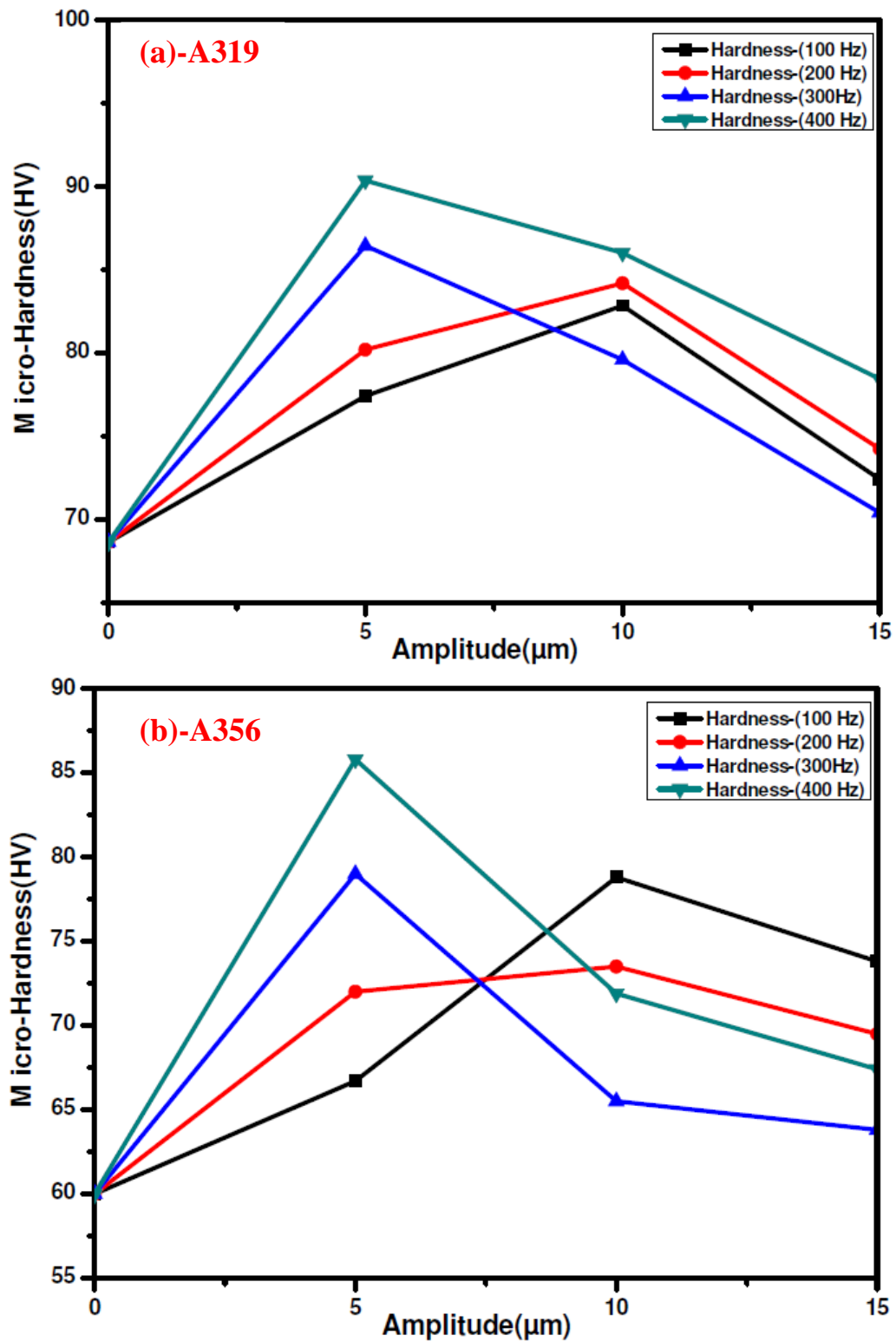
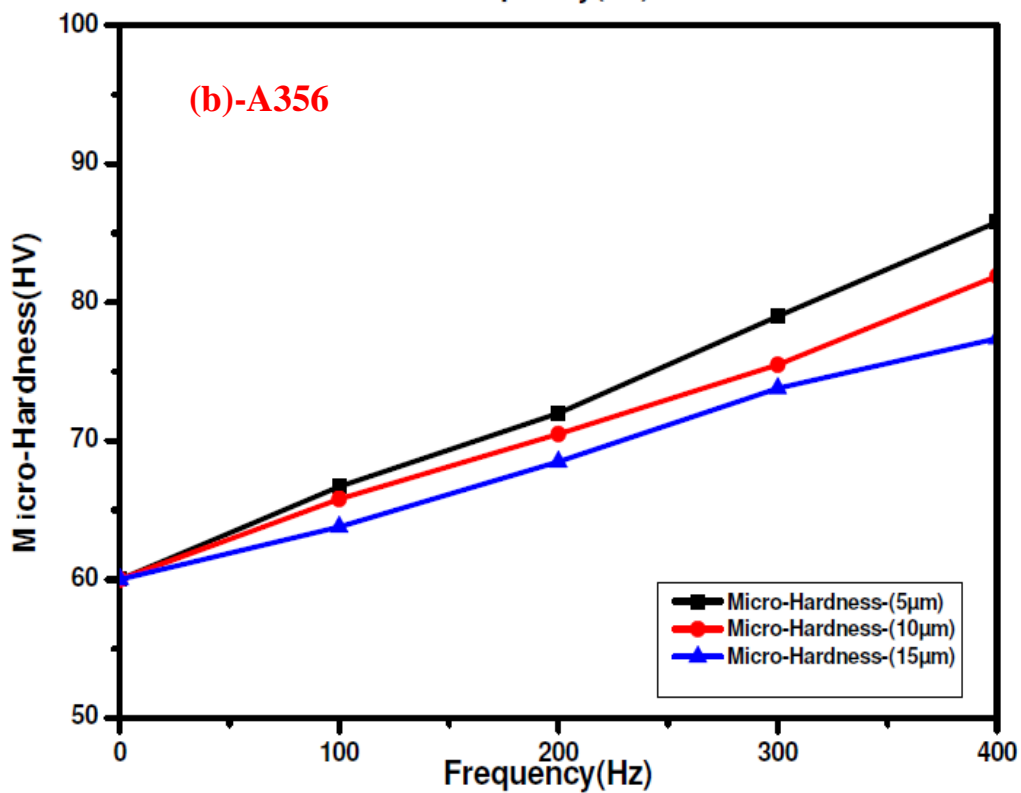
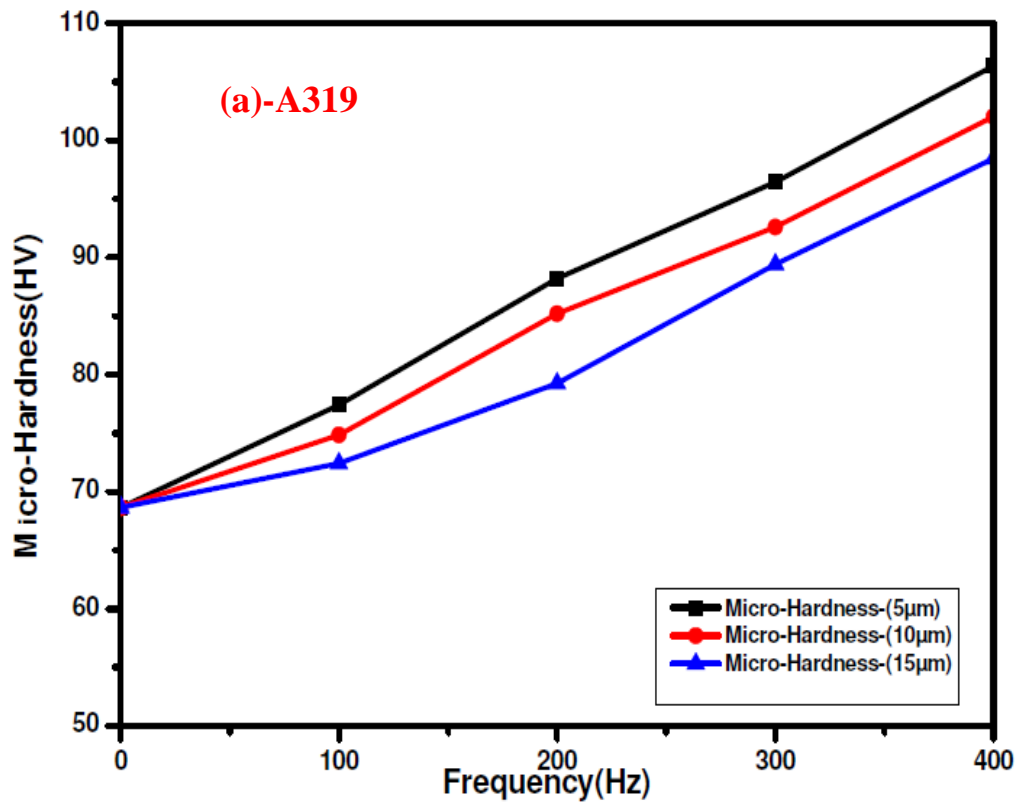


Figure 4.14 Effect of amplitude on Micro-Hardness of (a) A319 and (b) A356 aluminium alloys casting



**Figure 4.15 Effect of frequency on Micro-Hardness of (a) A319 and (b) A356 aluminium alloys casting**

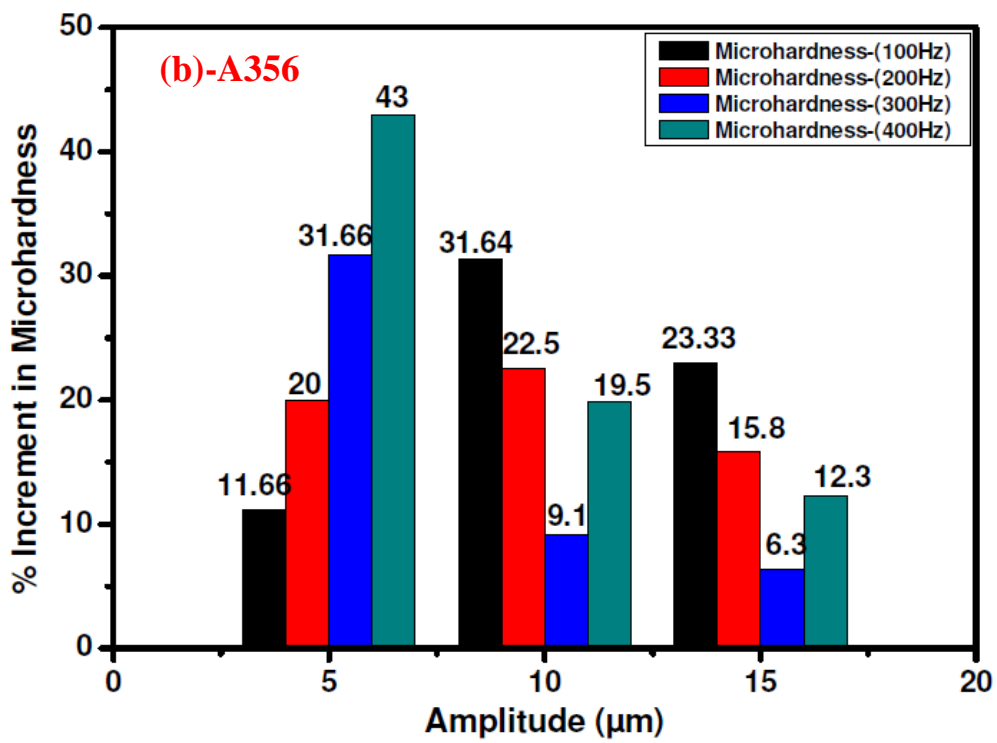
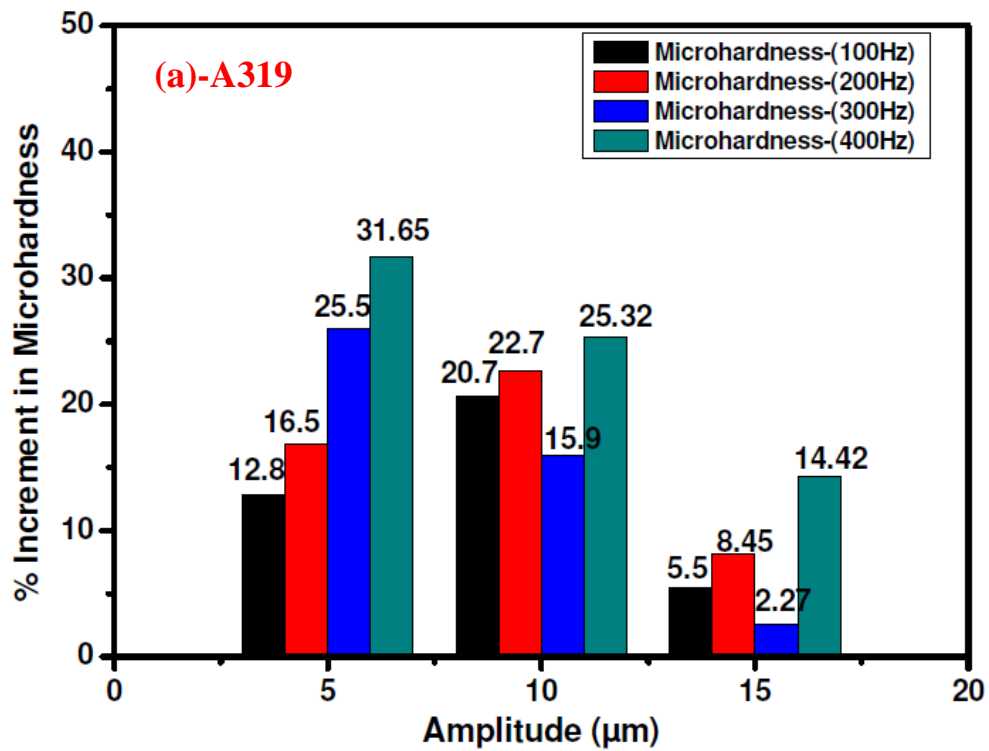


Figure 4.16 Comparison of percentage change in Micro-Hardness (a) A319 and (b) A356 aluminum alloys casting

#### 4.2.5 Effect of Oscillation on Toughness (Joule)

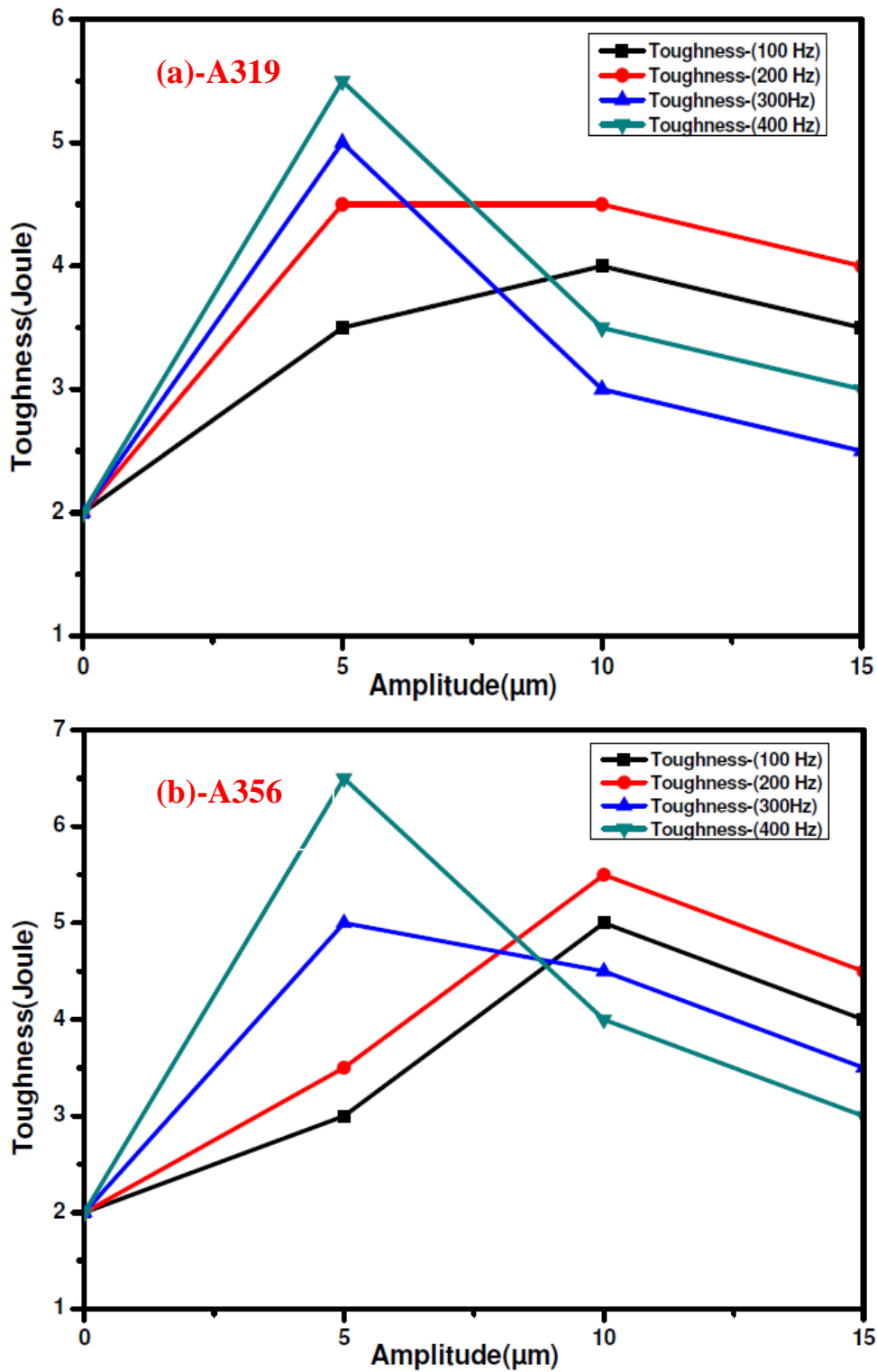
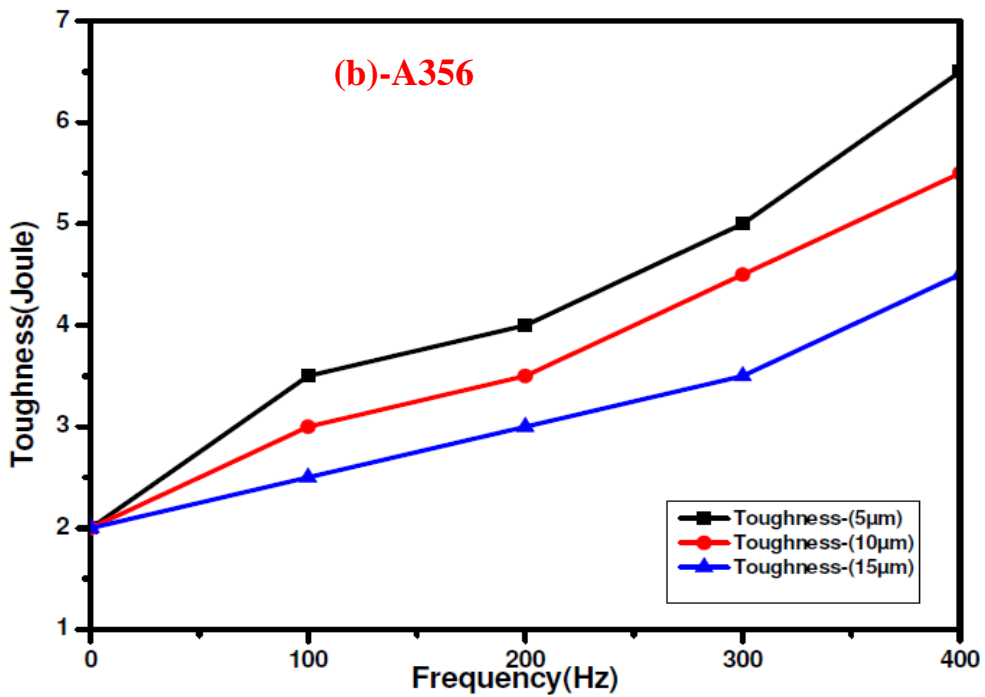
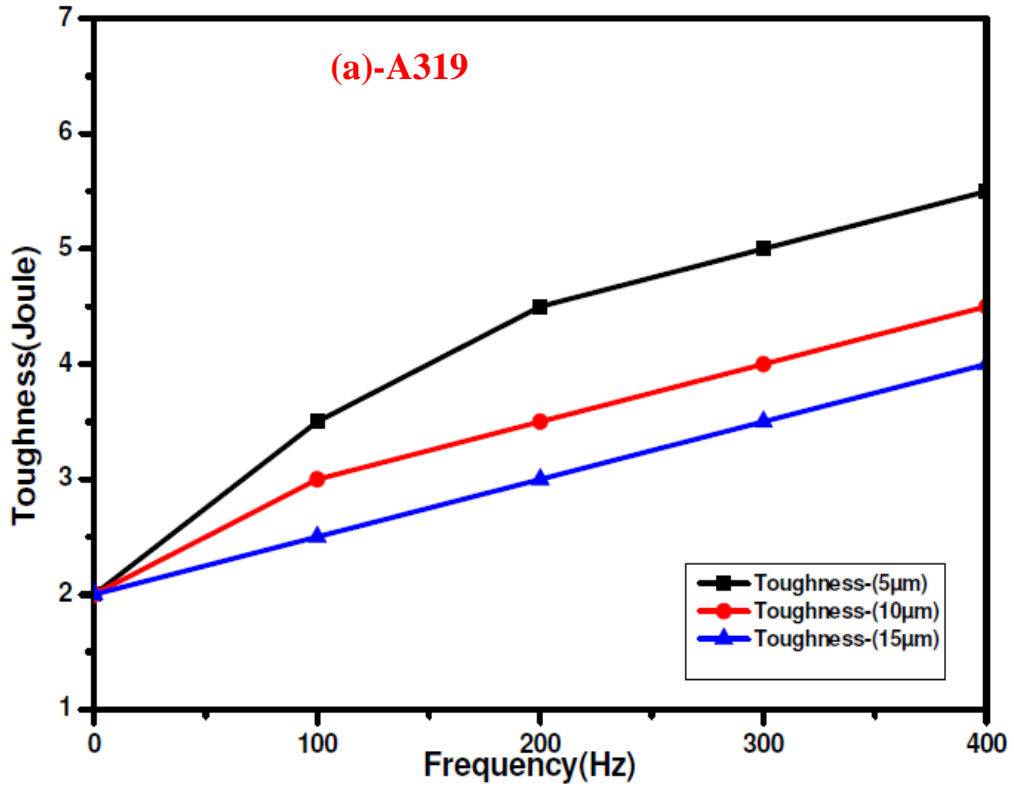


Figure 4.17 Effect of amplitude on Toughness (Joule) of (a) A319 and (b) A356 aluminium alloys casting



**Figure 4.18 Effect of frequency on Toughness(Joule) of (a) A319 and (b) A356 aluminium alloys casting**

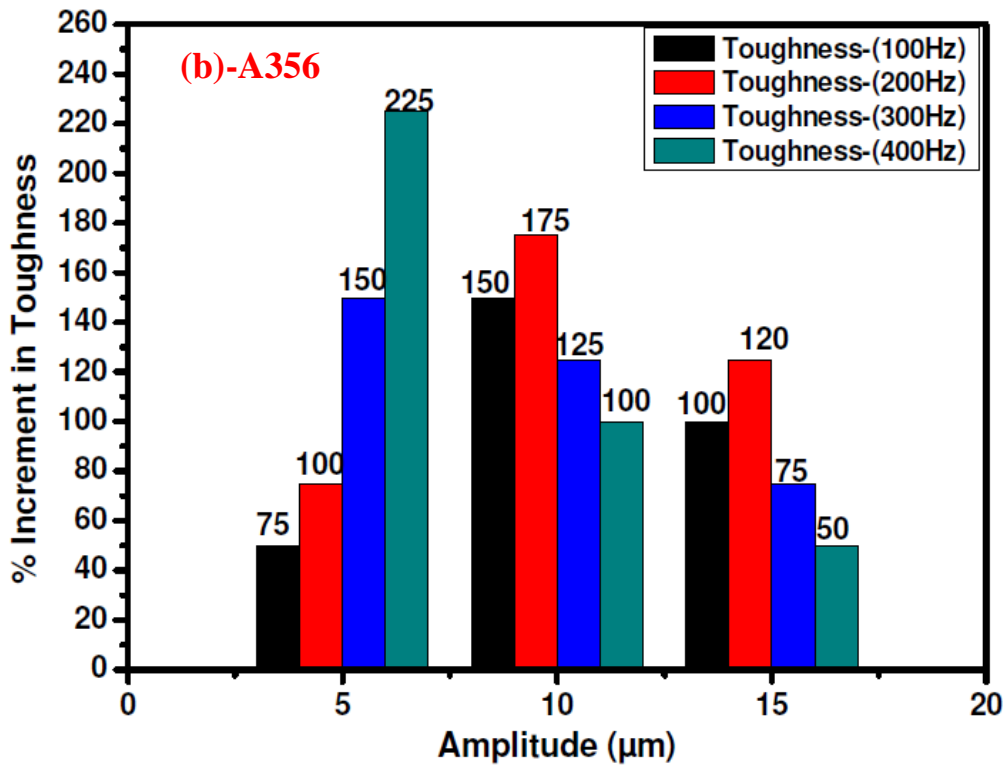
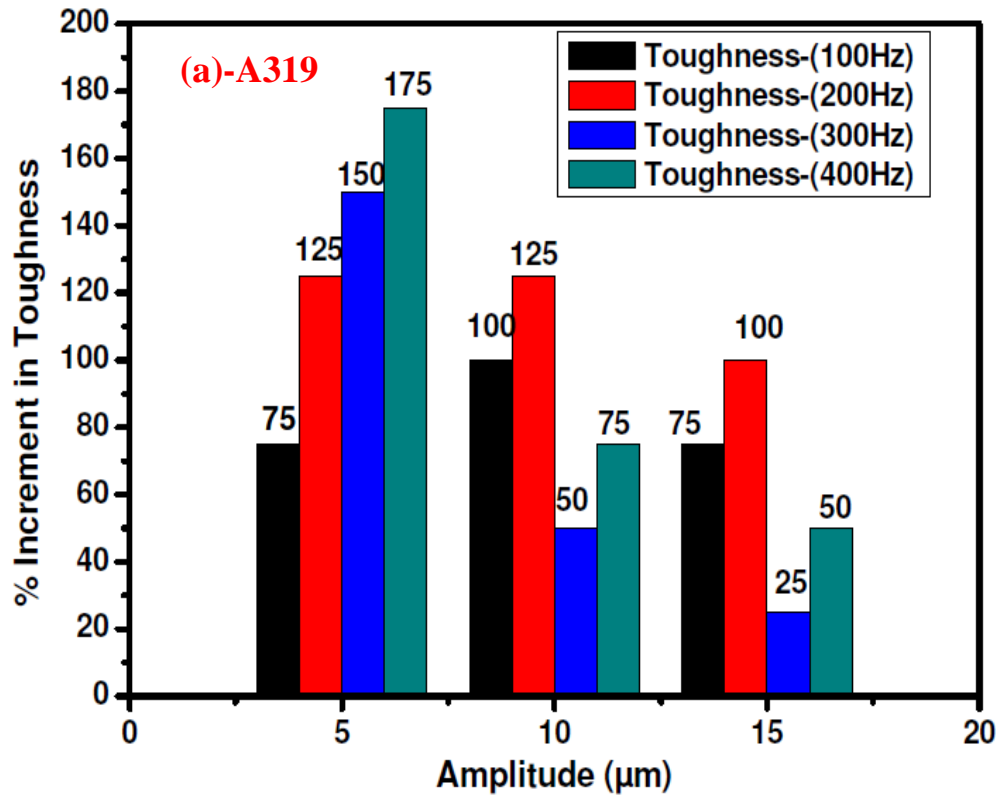


Figure 4.19 Comparison of percentage change in Micro-Hardness of (a) A319 and (b) A356 aluminum alloys casting

## 4.3 Discussion and Characterizations of Mechanical Properties

### 4.3.1 Ultimate Tensile Strength

#### 1) A319 Aluminum alloy Casting:

The ultimate tensile strength is improved by mold oscillation during the solidification and varies for oscillated test specimens when compared to stationary cast specimen. The UTS at stationary and at 100,200,300,400Hz with 5 $\mu$ m amplitude are 152,188.2, 196.6, 201.3 and 212.2MPa respectively. Similarly, the UTS at stationary and at 100,200,300,400Hz with 10 $\mu$ m amplitude are 152,160.5, 165.7, 174.5 and 190.5 MPa respectively and similarly for the UTS at stationary and at 100,200,300,400Hz with 15 $\mu$ m amplitude are 152,156.4, 160.4, 170.8 and 175.4MPa respectively. It can be observed that in general the ultimate tensile strength increase with increase in frequency of oscillation and decrease with increase in amplitudes of oscillation as shown in **Figure 4.7(a)** and **Figure 4.6(a)** respectively.

The percentage increase in ultimate tensile strength for oscillated test specimens when compared to stationary cast specimen are 39.03 % at 400Hz ,31.9% at 300Hz ,28.33% at 200Hz and 23.32% at 100Hz frequencies of oscillation with 5 $\mu$ m amplitude .Similarly, 24.83 % at 400Hz ,14.35 % at 300Hz ,8.58% at 200Hz and 5.17% at 100Hz frequencies of oscillation with 10 $\mu$ m amplitude and 14.94% at 400Hz ,11.9 % at 300Hz ,5.11% at 200Hz and 2.5% at 100Hz frequencies of oscillation with 15 $\mu$ m amplitude. It can be observed from this **Figure 4.8 (a)** that in general the ultimate tensile strength increase with increase in frequency of oscillation and decrease with increase in amplitudes of oscillation.

#### 2) A356 Aluminum alloy Casting:

Similarly A319 aluminum alloy casting mold was given oscillation with different frequencies and amplitude during the solidification of A356 aluminum alloy casting .Due

to mold oscillation casting enhances nucleation and improves mold-casting heat transfer. In this experimental investigation, the effect of mold oscillation parameter on microstructure refinement and mechanical properties of casting were observed. Mold-oscillation at different frequencies of experimentation of A319 i.e. 100 Hz, 200Hz, 300Hz and 400 Hz, and 2000 Hz and amplitudes are 5 $\mu$ m, 10 $\mu$ m and 15 $\mu$ m were investigated.

The ultimate tensile strength is improved by mold oscillation during the solidification and varies for oscillated test specimens when compared to stationary cast specimen. The UTS at stationary and at 100,200,300 and 400Hz with 5 $\mu$ m amplitude are 158,177.5, 182.6, 200.5 and 216.08MPa respectively. Similarly, the UTS at stationary and at 100,200,300 and 400Hz with 10 $\mu$ m amplitude are 158,174.5, 176.4, 188.6 and 208.47 MPa respectively and similarly for the UTS at stationary and at 100,200,300 and 400Hz with 15 $\mu$ m amplitude are 158,165.2, 180.3, 186.3 and 196.2MPa respectively. It can be observed that in general the ultimate tensile strength increase with increase in frequency of oscillation and decrease with increase in amplitudes of oscillation as shown in **Figure 4.7(b)** and **Figure 4.6(b)** respectively.

The percentage increase in ultimate tensile strength for oscillated test specimens when compared to stationary casted specimen are 36.75 % at 400Hz ,26.89% at 300Hz ,15.56% at 200Hz and 12.34% at 100Hz frequencies of oscillation with 5 $\mu$ m amplitude .Similarly, 31.94% at 400Hz ,19.36 % at 300Hz ,11.64% at 200Hz and 10.44% at 100Hz frequencies of oscillation with 10 $\mu$ m amplitude and 24.17% at 400Hz ,17.91 % at 300Hz ,13.98% at 200Hz and 4.55% at 100Hz frequencies of oscillation with 15 $\mu$ m amplitude. It can be observed from the **Figure 4.8(b)** that in general the ultimate tensile strength increase with increase in frequency of oscillation and decrease with increase in amplitudes of oscillation.

### 4.3.2 Yield Strength

#### 1) A319 Aluminum alloy Casting

The yield strength is improved by mold oscillation during the solidification and varies for oscillated test specimens when compared to that of stationary cast specimen. The yield strength at stationary and at 100,200,300,400Hz with 5 $\mu$ m amplitude are 130.7, 148.5, 152.6, 162.5 and 167.4 MPa respectively. Similarly, the yield strength at stationary and at 100,200,300,400Hz with 10 $\mu$ m amplitude are 130.7, 140.8, 145.9, 156.3 and 160.4 MPa respectively and similarly for the yield strength at stationary and at 100,200,300,400Hz with 15 $\mu$ m amplitude are 130.7,137.4, 142.5, 148.8 and 153.6 MPa respectively. It can be observed that in general the yield strength increase with increase in frequency of oscillation and decrease with increase in amplitudes of oscillation as shown in **Figure 4.10(a)** and **Figure 4.9(a)** respectively.

The percentage increase in yield strength for oscillated test specimens when compared to that of stationary cast specimen are 28.07 % at 400Hz ,24.33% at 300Hz ,16.75% at 200Hz and 13.61% at 100Hz frequencies of oscillation with 5 $\mu$ m amplitude .Similarly the increases is, 22.72 % at 400Hz ,19.58 % at 300Hz ,11.62% at 200Hz and 7.7% at 100Hz frequencies of oscillation with 10 $\mu$ m amplitude and 17.52% at 400Hz ,13.84 % at 300Hz ,9.02% at 200Hz and 5.12% at 100Hz frequencies of oscillation with 15 $\mu$ m amplitude. It can be observed from this **Figure 4.11(a)** that in general the yield strength increase with increase in frequency of oscillation and decrease with increase in amplitudes of oscillation.

#### 2) A356 Aluminum alloy Casting

The yield strength is improved by mold oscillation during the solidification and varies for oscillated test specimens when compared to stationary cast specimen. The yield strength at stationary and at 100,200,300 and 400Hz with 5 $\mu$ m amplitude are 115.60, 127.45,

135.46, 138.72 and 140.54 MPa respectively. Similarly, the yield strength at stationary and at 100,200,300 and 400Hz with 10 $\mu$ m amplitude are 115.60, 125.54, 130.58, 132.8 and 136.87 MPa respectively and similarly for the yield strength at stationary and at 100,200,300 and 400Hz with 15 $\mu$ m amplitude are 115.60, 119.42, 126.57, 129.54 and 132.86 MPa respectively. It can be observed that in general the yield strength increase with increase in frequency of oscillation and decrease with increase in amplitudes of oscillation as shown in **Figure 4.10(b)** and **Figure 4.9(b)** respectively.

The percentage increase in yield strength for oscillated test specimens when compared to stationary cast specimen are 21.57 % at 400Hz ,20% at 300Hz ,17.17% at 200Hz and 10.25% at 100Hz frequencies of oscillation with 5 $\mu$ m amplitude .Similarly, 18.39 % at 400Hz ,14.63 % at 300Hz ,12.95% at 200Hz and 8.59% at 100Hz frequencies of oscillation with 10 $\mu$ m amplitude and 14.93% at 400Hz ,12.05% at 300Hz ,9.48% at 200Hz and 3.30% at 100Hz frequencies of oscillation with 15 $\mu$ m amplitude. It can be observed from this **Figure 4.11 (b)** that in general the yield strength increase with increase in frequency of oscillation and decrease with increase in amplitudes of oscillation.

### **4.3.3 % Elongation**

#### **1) A319 Aluminum alloy Casting:**

The percentage increase in % Elongation for oscillated test specimens when compared to stationary cast specimen are 169.26 % at 400Hz ,116.51% at 300Hz ,90.36% at 200Hz and 50.91% at 100Hz frequencies of oscillation with 5 $\mu$ m amplitude .Similarly, 103.21 % at 400Hz ,84.40 % at 300Hz ,64.40% at 200Hz and 39.9% at 100Hz frequencies of oscillation with 10 $\mu$ m amplitude and 87.15% at 400Hz ,66.97 % at 300Hz ,49.08% at 200Hz and 24.47% at 100Hz frequencies of oscillation with 15 $\mu$ m amplitude. It can be observed that in general the %elongation increases with increase in frequency of

oscillation and decrease with increase in amplitudes of oscillation as shown in **Figure 4.13(a)** and **Figure 4.12(a)** respectively.

## 2) A356 Aluminum alloy Casting

The percentage increase in % Elongation for oscillated test specimens when compared to stationary cast specimens are 108.33 % at 400Hz ,52.77% at 300Hz ,33.33% at 200Hz and 25% at 100Hz frequencies of oscillation with 5 $\mu$ m amplitude .Similarly, 80.55 % at 400Hz ,44.44 % at 300Hz ,20.83% at 200Hz and 16.66% at 100Hz frequencies of oscillation with 10 $\mu$ m amplitude and 61.11% at 400Hz ,38.88 % at 300Hz ,13.33% at 200Hz and 5% at 100Hz frequencies of oscillation with 15 $\mu$ m amplitude. It can be observed that in general the %elongation increase with increase in frequency of oscillation and decrease with increase in amplitudes of oscillation as shown in **Figure 4.13(b)** and **Figure 4.12(d)** respectively.

Ductility of oscillatory casting is more than stationary casting because of fine grain size and fine dispersion of second phase particles within the material. Very fine and homogeneous microstructure has been observed throughout the ingots.

### 4.3.4 Micro-Hardness

#### 1) A319 Aluminum alloy Casting:

Hardness of casting surface improved because of high cooling rate (due to mould oscillation) and due to inter-metallic phase  $Al_2Cu$  ,  $Fe_{1.7}Al_4Si$  and  $Al_2CuMg$  precipitate formation and its uniform dispersion throughout within the ingot and on the surface of the castings.

The hardness of castings is improved due to mold oscillation during the solidification and varies for oscillated test specimens when compared to stationary cast specimens. The micro-hardness at stationary and at 100,200,300 and 400Hz with 5 $\mu$ m amplitude are

68.46, 77.42, 88.2, 96.5 and 106.36 HV respectively. Similarly, the micro-hardness at stationary and at 100,200,300 and 400Hz with 10 $\mu$ m amplitude are 68.46, 74.85, 85.2, 92.6 and 102.02 HV respectively and similarly for the micro-hardness at stationary and at 100,200,300 and 400Hz with 15 $\mu$ m amplitude are 68.46, 72.42, 79.25, 89.42 and 98.45HV respectively. It can be observed that in general the micro-hardness increase with increase in frequency of oscillation and decrease with increase in amplitudes of oscillation as shown in **Figure 4.16(a)** and **Figure 4.15(a)** respectively.

The percentage increase in ultimate tensile strength for oscillated test specimens when compared to stationary cast specimens are 54.95 % at 400Hz ,40.51% at 300Hz ,28.49% at 200Hz and 12.79% at 100Hz frequencies of oscillation with 5 $\mu$ m amplitude .Similarly, 48.63 % at 400Hz ,34.90 % at 300Hz ,24.12% at 200Hz and 9.04% at 100Hz frequencies of oscillation with 10 $\mu$ m amplitude and 43.42% at 400Hz ,30.27 % at 300Hz ,15.45% at 200Hz and 5.5% at 100Hz frequencies of oscillation with 15 $\mu$ m amplitude. It can be observed from the **Figure 4.17(a)** that in general the micro-hardness increase with increase in frequency of oscillation and decrease with increase in amplitudes of oscillation.

## 2) **A356 Aluminum alloy Casting:**

Hardness of casting surface improved because of high cooling rate(due to mould oscillation) and due to inter-metallic phase Mg<sub>2</sub>Si and NiSi<sub>2</sub> precipitate formation and its uniform dispersion throughout within the ingot and on the surface of the castings.

The hardness of castings is improved due to mold oscillation during the solidification and varies for oscillated test specimens when compared to stationary cast specimens. The micro-hardness at stationary and at 100,200,300 and 400Hz with 5 $\mu$ m amplitude are 60, 66.7,72, 79 and 85.8 HV respectively. Similarly, the micro-hardness at stationary and at 100,200,300 and 400Hz with 10 $\mu$ m amplitude are 60, 65.8, 70.5, 75.5 and 81.9 HV

respectively and similarly for the micro-hardness at stationary and at 100,200,300 and 400Hz with 15 $\mu$ m amplitude are 60, 63.8, 68.5, 73.8 and 77.4 HV respectively. It can be observed that in general the micro-hardness increase with increase in frequency of oscillation and decrease with increase in amplitudes of oscillation as shown in **Figure 4.16(b)** and **Figure 4.15(b)** respectively.

The percentage increase in micro-hardness for oscillated test specimens when compared to stationary cast specimens are 43 % at 400Hz ,31.66% at 300Hz ,20% at 200Hz and 11.66% at 100Hz frequencies of oscillation with 5 $\mu$ m amplitude .Similarly increase is 36.5 % at 400Hz ,25.33 % at 300Hz ,17.5% at 200Hz and 9.66% at 100Hz frequencies of oscillation with 10 $\mu$ m amplitude and 29% at 400Hz ,23 % at 300Hz ,14.16% at 200Hz and 6.33% at 100Hz frequencies of oscillation with 15 $\mu$ m amplitude. It can be observed from this **Figure 4.17(b)** that in general the micro-hardness increase with increase in frequency of oscillation and decrease with increase in amplitudes of oscillation.

#### **4.3.5 Toughness (Joule)**

##### **1) A319 Aluminum alloy Casting:**

The toughness of casting is improved due to mold oscillation during the solidification and varies for oscillated test specimens when compared to stationary cast specimens. The toughness at stationary and at 100,200,300 and 400Hz with 5 $\mu$ m amplitude are 2, 3.5, 4.5, 5 and 5.5 Joule respectively. Similarly, the toughness at stationary and at 100,200,300 and 400Hz with 10 $\mu$ m amplitude are 2, 3, 3.5,4 and 4.5 Joule respectively and similarly for the toughness at stationary and at100, 200,300 and 400Hz with 15 $\mu$ m amplitude are 2, 2.5, 3, 3.5 and 4 Joule respectively. It can be observed that in general the toughness (Impact Strength) increase with increase in frequency of oscillation and

decrease with increase in amplitudes of oscillation as shown in **Figure 4.19(a)** and **Figure 4.18(a)** respectively.

The percentage increase in ultimate tensile strength for oscillated test specimens when compared to stationary cast specimens are 175 % at 400Hz ,150% at 300Hz ,125% at 200Hz and 75% at 100Hz frequencies of oscillation with 5 $\mu$ m amplitude .Similarly, 125 % at 400Hz ,100 % at 300Hz ,75% at 200Hz and 50 at 100Hz frequencies of oscillation with 10 $\mu$ m amplitude and 100% at 400Hz ,75 % at 300Hz ,50% at 200Hz and 25% at 100Hz frequencies of oscillation with 15 $\mu$ m amplitude. It can be observed from this **Figure 4.20(a)** that in general the toughness (Impact Strength) increase with increase in frequency of oscillation and decrease with increase in amplitudes of oscillation.

## 2) **A356 Aluminum alloy Casting:**

The toughness of castings are improved due to mold oscillation during the solidification and varies for oscillated test specimens when compared to stationary cast specimens. The toughness at stationary and at 100,200,300 and 400Hz with 5 $\mu$ m amplitude are 2, 3.5,4, 5 and 6.5 Joule respectively. Similarly, the toughness at stationary and at 100,200,300 and 400Hz with 10 $\mu$ m amplitude are 2, 3, 3.5, 4.5 and 5.5 Joule respectively and similarly for the toughness at stationary and at 100,200,300 and 400Hz with 15 $\mu$ m amplitude are 2, 2.5, 3, 3.5 and 4.5 Joule respectively. It can be observed that in general the toughness (Impact Strength) increase with increase in frequency of oscillation and decrease with increase in amplitudes of oscillation as shown in **Figure 4.19(b)** and **Figure 4.18(b)** respectively.

The percentage increase in ultimate tensile strength for oscillated test specimens when compared to stationary casted specimen are 255% at 400Hz ,150% at 300Hz ,100% at 200Hz and 75% respectively at 100Hz frequencies of oscillation with 5 $\mu$ m amplitude .Similarly, 175 % at 400Hz ,125% at 300Hz ,75% at 200Hz and 50% at 100Hz

frequencies of oscillation with 10 $\mu$ m amplitude and 125% at 400Hz, 75% at 300Hz, 50% at 200Hz and 25% at 100Hz frequencies of oscillation with 15 $\mu$ m amplitude. It can be observed from the **Figure 4.20(b)** that in general the toughness (Impact Strength) increase with increase in frequency of oscillation and decrease with increase in amplitudes of oscillation. Impact toughness depend on the shape, type, size and size distribution of  $\alpha$ -Al grains, silicon particles and CuAl<sub>2</sub> phases in the matrix. The increase in impact toughness consists of two parts: The breakage of the elongated primary  $\alpha$ -Al grains into more uniformly distributed  $\alpha$ -Al grains by refinement. The plate-like eutectic silicon to fine broken particles of silicon and massive particles to fine micro constituent of CuAl<sub>2</sub> by modification.

Mechanical properties of the A319 and A356 aluminum cast alloys mainly depend on the shape, size, and size distribution of the  $\alpha$ -Al grains, eutectic silicon morphology, bonding between the hard silicon crystals and soft aluminum matrix and precipitation level of A319 (Al<sub>2</sub>Cu, Fe<sub>1.7</sub>Al<sub>4</sub>Si and Al<sub>2</sub>CuMg) and A356(Mg<sub>2</sub>Si and NiSi<sub>2</sub>) particles. **Figures 4.5– Figure 4.19** present the variation of UTS, YS, %EL, hardness, and impact strength values obtained from the samples of the A319 and A356 cast alloys with different aforesaid conditions. The unmodified (Stationary Cast Alloys) consist of large elongated  $\alpha$ -Al grains and plate-like (acicular) eutectic silicon which reduces ductility of the cast alloys. Acicular silicon structure acts as internal stress riser and provides easy path for fracture, which is the primary reason for the poor mechanical properties of these alloys.

The increase in mechanical properties can be attributed to the wavy motion experienced by the molten metal due to vibration during solidification. The improvements are also due to the fragmentation of the silicon flakes, suppression of undesirable dendritic and columnar zones, development of a fine-grained equiaxed structure, and reduced porosity

due to vibration. The increase in the amount of eutectic composition apart from grain refinement observed in the case of modified-vibrated alloys may also have contributed to the enhancement of mechanical properties. The improvement in strength of the matrix and enhancement in mechanical properties of the alloys are due to the combined effects of fracturing of eutectic Si particle and finer grain size together with fine A319 ( $\text{Al}_2\text{Cu}$ ,  $\text{Fe}_{1.7}\text{Al}_4\text{Si}$  and  $\text{Al}_2\text{CuMg}$ ) and A356 ( $\text{Mg}_2\text{Si}$  and  $\text{NiSi}_2$ ) particles inter-metallic phase formed along the inter-dendritic region, due to vibration during solidification. The results (UTS, YS, %EL, and hardness) obtained in the present investigation are plotted. **Anilkumar, T., et al. [104]** investigated the influence of vibration during the solidification on the mechanical properties of the Al-Si alloy castings. Grain structure gets reduced, when the alloy is subjected to vibration frequency varying from 0 to 12Hz. For 12Hz frequency, the percentage increase in UTS and the percentage increase in the hardness in comparison to the ascast are about 16% and 7.5% respectively. And this indicates that vibration has an influence on the mechanical properties of the Al-Si alloy castings.

**Patel, V. R. (103)** suggested that eutectic silicon particles in eutectic aluminium-silicon alloys can be modified with the help of mechanical mold vibration during the solidification. With the help of mold vibration during the solidification pattern of the eutectic silicon particles tends to become more uniform. The tensile strength and impact strength of vibratory prepared casting are higher than that of stationary prepared casting. Mold vibration method also affects the morphology of eutectic Si-particle and refinement of  $\alpha$ -Al dendrites of eutectic Al-Si alloy..

**K G Basavakumar and P G Mukunda Bull [101]** examined the influence of melt treatment on microstructure and impact properties of Al-7Si and Al-7Si-2.5Cu cast alloys. The alloys showed enhanced impact toughness in as cast condition when

compared to those employed by the only addition of grain refiner or modifier. The enhancement of impact toughness of Al-7Si-2.5Cu alloys are related to fracture of the large aluminum grains and uniform dispersion of eutectic silicon and fine CuAl<sub>2</sub> particles in the interdendritic region produced from the combined effect of refinement and modification.

**Sayuti, M., et al.[100]** investigated the effect of mechanical vibration on solidifying particulate(TiC) reinforced aluminum alloy(LM6) matrix composite formed by various particulate weight fraction of titanium dioxide. They found several sources of vibration which modified the casting property. A mechanical vibration method is used for producing vibration resulting in improved mechanical properties, such as toughness property and the microstructure. Microstructure investigations were carried out to determine the impact strength and density. Preliminary works confirm that the mechanical properties have been enhanced by using mold vibration during solidification as compared to gravity castings without vibration.

**Jiang, W., et al.[99]** investigated the influences of vibration frequency on fracture behavior, metallurgical, and mechanical properties of the A356 aluminum alloy. For aforesaid mentioned effect, they used vibration frequency of 100Hz. The tensile strength, yield strength, % elongation and hardness of the A356 alloy sample were more than 35%, 42%, 57% and 28% respectively than that of stationary prepared casting. Also, the mechanical vibration turned the fractograph of the A356 alloy from brittle fracture nature of the alloy without vibration to a prominent dimple fracture nature, and with the increase of vibration frequency, the dimples were quite deep and well dispersed with a high density.

**Chaturvedi, V., & Pandel, U. [98]** studied the influences of mechanical vibrations on the mechanical properties of AZ91 magnesium alloy. This was tested at constant frequency of 40Hz and at varied amplitudes from 0 to 2 mm. With increasing vibration acceleration from 2.5 to 19 m s<sup>2</sup>, the yield strength increased from 71 to 122 MPa. Increased amplitude of mechanical vibration during solidification causes refinement of the grain in the alloy. Tensile strength improved upto a certain point with increasing amplitude and start decreasing with further increment in the amplitude of vibrations. This refinement of the grain also results in an increased percentage of elongation and hardness of the alloy samples.

**Guo, H. M., et al. [97]** found the mechanical vibration during the solidification of AZ31 magnesium alloy casting can significantly enhance mechanical performance, with a simultaneous improvement in both strength and elongation. With increasing vibration acceleration from 2.5 to 19 m s<sup>2</sup>, the ultimate tensile strength improved from 152 to 213 MPa, the yield strength increased from 71 to 122 MPa, and the elongation increased from 4.8 to 11.5 percent. These conclusions are consistent with the grain size, where the maximum strength and elongation correspond to the lowest grain size achieved under vibratory prepared casting.

**Kumar, R., et al. [95]** examined and understand the modification in microstructure and mechanical properties of Al-Cu alloys castings solidified under mold vibration. The mold was made of graphite and frequencies varied from 40 to 150 Hz. One more cast also was made under stationary condition to compare the results of castings with vibration. The test results revealed significant grain refinement. The improvement in hardness of castings with mold vibration during solidification are compatible with the determined grain size. The maximum tensile strength and elongation correspond to the smallest grain size obtained.

**P.A.O. Adegbuyi et al.,[84]** suggested that each composition of Aluminum-Copper alloys grain refinements that led to improved properties by specimens were vibrated at different frequencies during solidification (Casting) .The tensile stress (strength) increases with of frequency.of vibration of the material.

**W. Dai et al., [53]** investigated the effects of rheo-squeeze casting parameters on microstructure and mechanical properties of AlCuMnTi alloy and the semisolid slurry of AlCu<sub>5</sub>MnTi alloy castings were prepared by indirect ultrasonic vibration (IUV). The tensile strength was 326.5 MPa, which was improved by 6.5% and the elongation was 11%, which was improved by 47% as compared with conventional squeeze casting samples.

#### **4.4 Microstructure Photographs:**

##### **4.4.1 Evaluation of metallurgical characterization of A319 and A356 aluminum alloy casting with the help of their optical microstructure image**

In general, applying vibration to the solidifying melt results in two significant effects. Firstly, it improves the wetting of the mold surface by the molten metal, improving faster heat removal from the molten metal through the mold surface. Under normal conditions, it is challenging to expect uniform contact between molten metal and mold wall due to the presence of oxide films on the melt surface. Application of vibration fractures these covering oxide films, thus forming the melt more wet-table with the mold wall and improving the contact between them. This aids in improving nucleation of crystals and formation of finer grains at mold surface. Secondly, vibration leads to microstructure changes to both the eutectic composition and dendritic structure of aluminum. Vibration successfully breaks the dendritic structure into small islands of aluminum. More over the application of external energy works on “crystal multiplication” phenomenon. It is

important to note that by subjecting molten aluminum melts to vibration has also shortened the solidification time and some amount of reduction in gas content. Vibration also accelerates the spheroidisation of grains during heat-treatment due to decrease in diffusion distance.

These mechanisms are responsible for grain refinement and due to grain refinement there is appreciable increase in mechanical and metallurgical properties of casting prepared under oscillatory conditions than that of stationary casting.

The influence of change in morphology of silicon on the ultimate tensile strength and ductility is largely governed. Optical microstructure Images of A319 and A356 Alloy casting are shown in **Figure (4.21-4.23)** and **Figure (4.24-4.26)** respectively. Due to different conditions of oscillation it affects the grain size, Silicon particle morphology and distribution of silicon particles accordingly. Fine and spheroidised phases are known to contribute more to increased strength and ductility than the acicular and irregular shape particles. The size and shape of the second phase silicon particles governs the nucleation and growth of crack in this type of alloys. Small and homogeneously rounded evenly distributed eutectic silicon particles results in high ductility and strength.

The microstructure of oscillatory castings of the alloy where high degree of refining of dendrite cells and eutectic silicon are seen. It favors to yield strength of oscillatory casting more than stationary casting. This is possible only when fine grain size and fine dispersion of second phase particles within the material are achieved.

1) Comparison of Change in Metallurgical Properties of Stationary Casting With Oscillatory Casting of A319 aluminum alloy with the help of Optical Micrograph

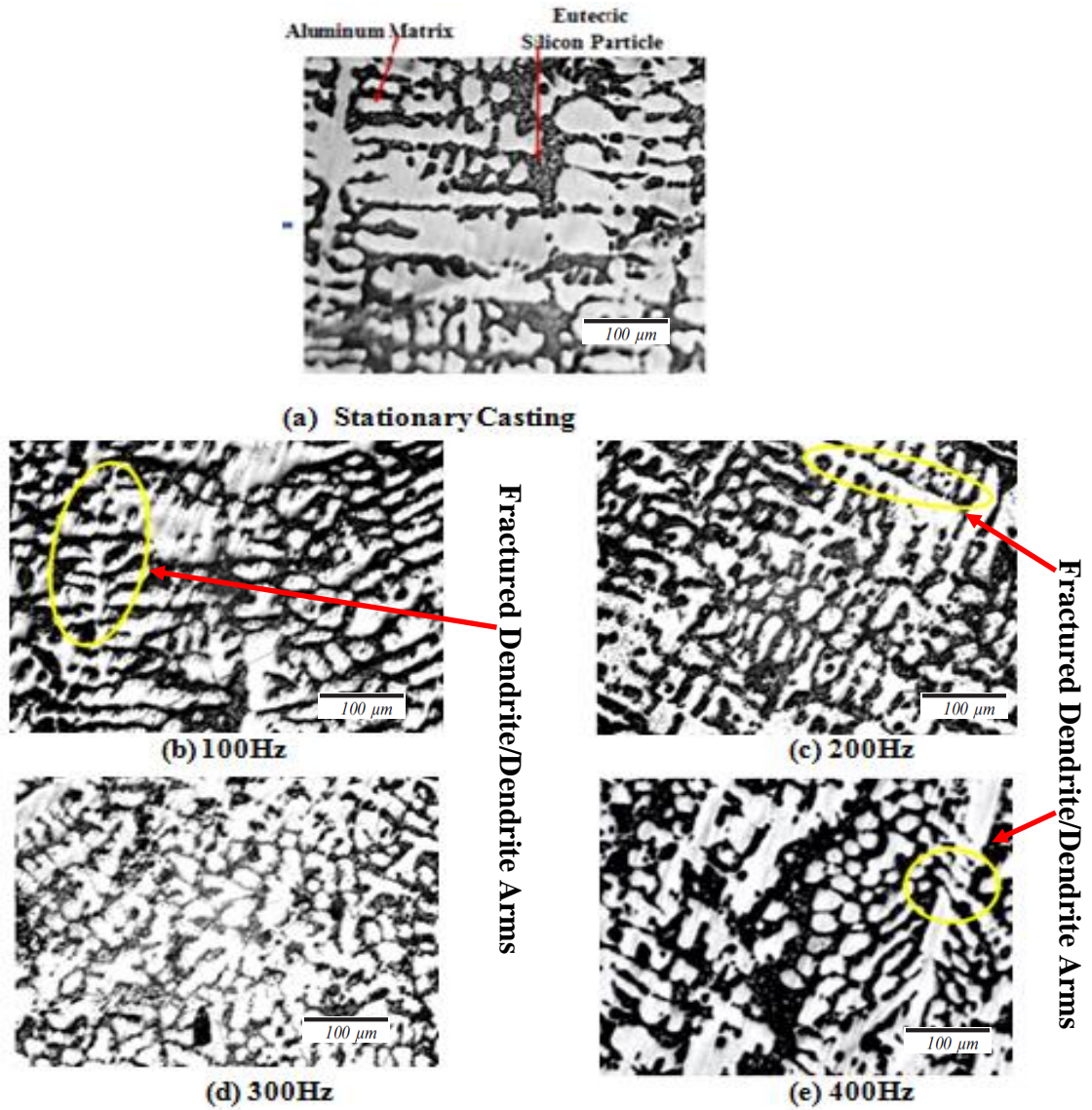
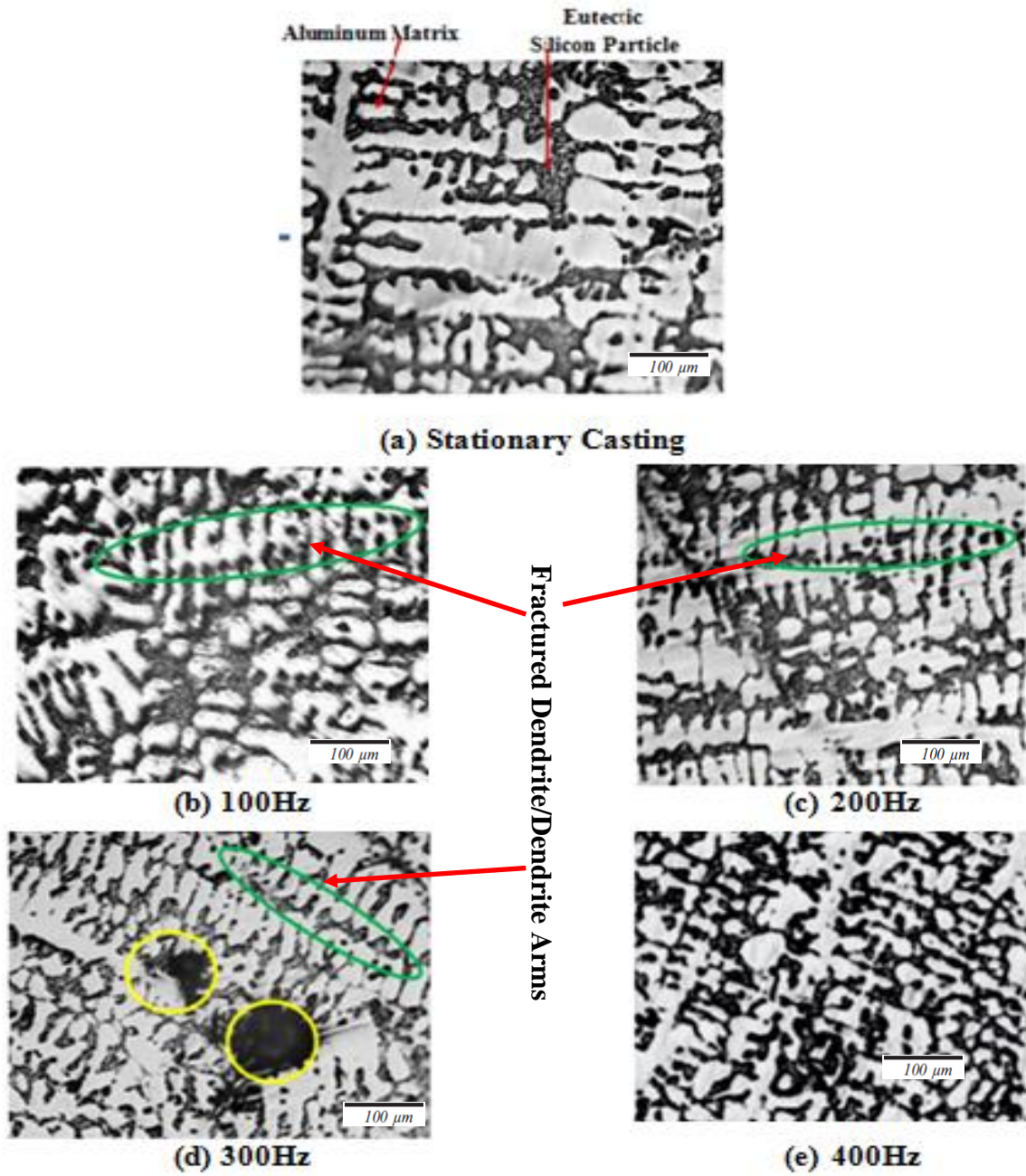
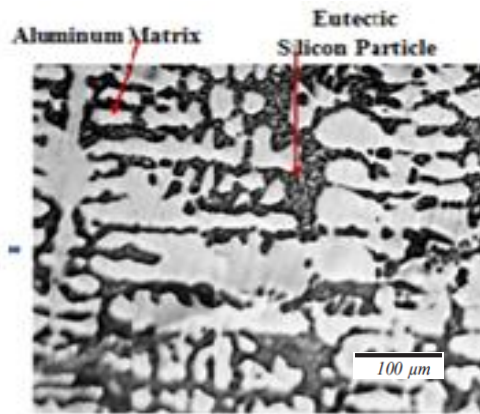


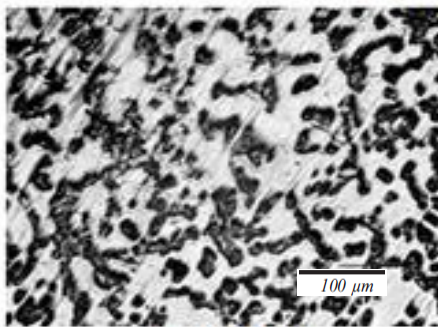
Figure 4.20 Optical micrographs (A319) order place with increase in frequency of mold oscillation (Constant Amplitude=5μm)



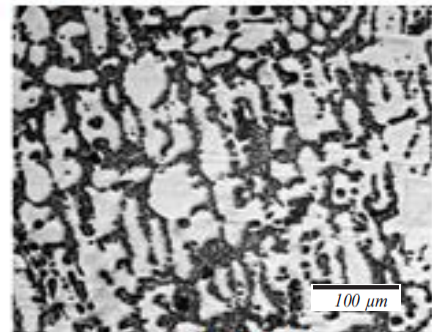
**Figure 4.21** Optical micrographs (A319) order place with increase in frequency of mold oscillation (Constant Amplitude=10 $\mu\text{m}$ )



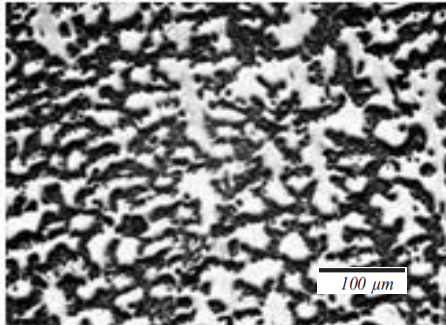
(a) Stationary Casting



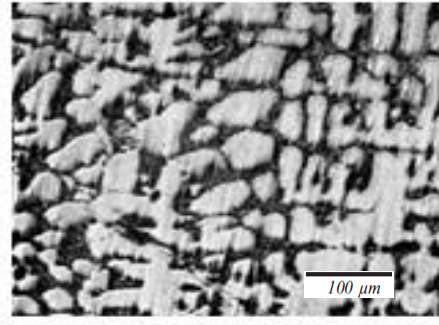
(b) 100Hz



(c) 200Hz



(d) 300Hz



(e) 400Hz

**Figure 4.22 Optical micrographs (A319) order place with increase in frequency of mold oscillation (Constant Amplitude=15 $\mu\text{m}$ )**

2) Comparison of Change in Metallurgical Properties of Stationary Casting With Oscillatory Casting of A356 aluminum alloy with the help of Optical Micrograph

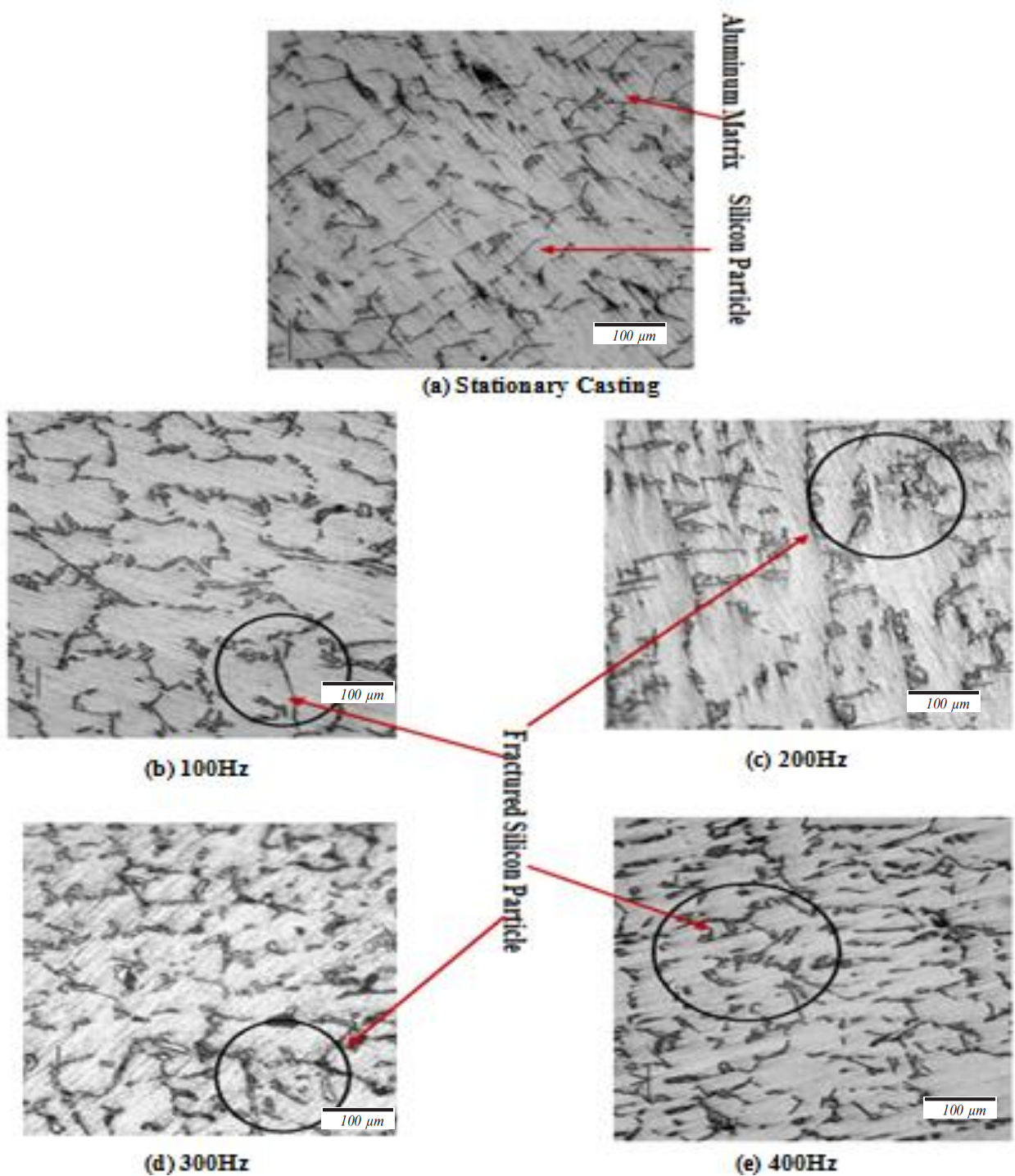
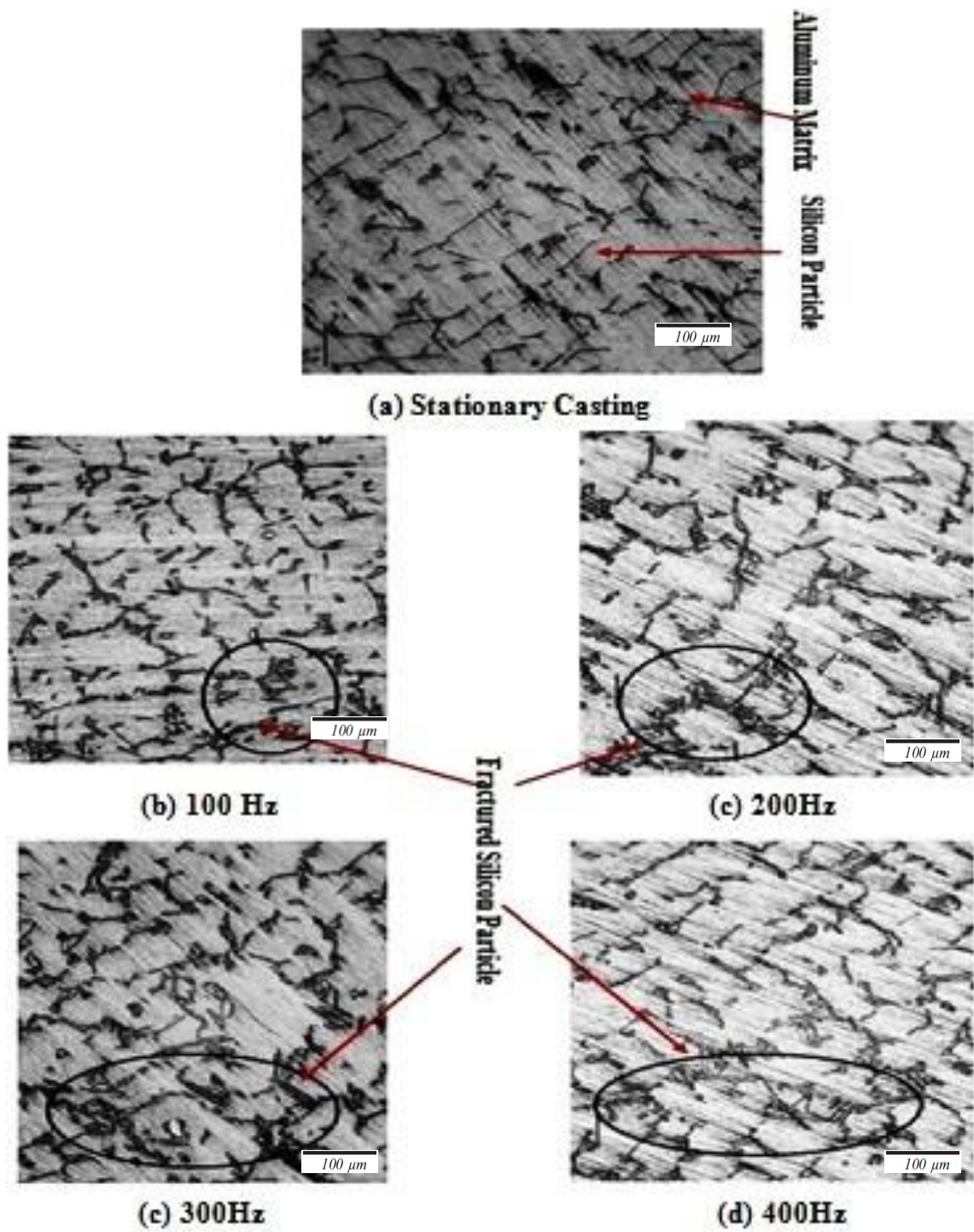
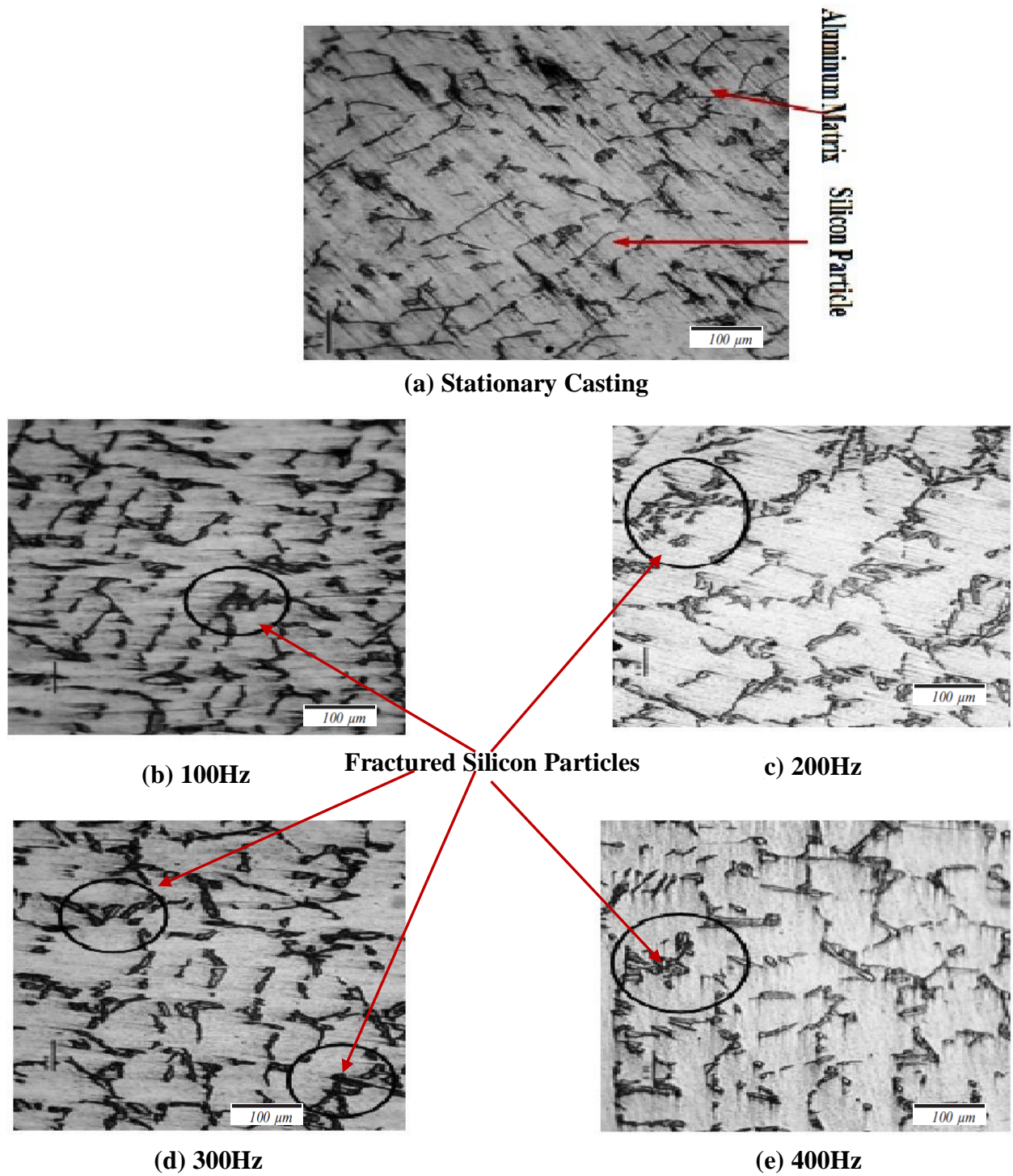


Figure 4.23 Optical micrographs (A356) order place with increase in frequency of mold oscillation (Constant Amplitude=5μm)



**Figure 4.24** Optical micrographs (A356) order place with increase in frequency of mold oscillation (Constant Amplitude=10μm)



**Figure 4.25** Optical micrographs (A356) order place with increase in frequency of mold oscillation (Constant Amplitude=15 $\mu\text{m}$ )

In general, applying vibration to the solidifying melt results in promoting nucleation of crystals and generation of finer grains at mould surface. Secondly, vibration leads to microstructure changes to both the eutectic composition and dendritic structure of aluminum. Vibration successfully breaks the dendritic structure into small islands of aluminum. More over the application of external energy works on “crystal multiplication” phenomenon. It is important to note that by subjecting molten aluminum melts to vibration has also shortened the solidification time and some amount of reduction in gas content. These mechanisms are responsible for grain refinement and due to grain refinement there is appreciable increase in mechanical and metallurgical properties of casting prepared under oscillatory conditions than stationary casting.

Metallurgical properties of the A319 and A356 aluminum cast alloys mainly depend on the shape, size, and size distribution of the  $\alpha$ -Al grains, eutectic silicon morphology, bonding between the hard silicon crystals and soft aluminum matrix and precipitation level of  $\text{Al}_2\text{Cu}$  and  $\text{Al}_2\text{CuMg}$  particles in A319 and  $\text{Mg}_2\text{S}$  and  $\text{NiSi}_2$  in A356 Aluminum alloy Casting.

The variation of Grain Size, DAS, silicon particle roundness, silicon particle area, aspect ratio and %porosity are observed from the samples of the A319 and A356 cast alloys with different conditions of oscillation are shown in order from Figure 2.27 to Figure 4.43. The unmodified alloys consist of large elongated  $\alpha$ -Al grains and plate-like (acicular) eutectic silicon which reduces ductility of the cast alloys. Acicular silicon structure acts as internal stress riser and provides easy path for fracture, which is the primary reason for the poor mechanical properties of these alloys.

#### **A319 Aluminum Alloy:**

The optical microstructures of the eutectic zone were obtained with different mold oscillation frequencies in order to demonstrate a substantial microstructure difference in

the size and morphology of eutectic silicon particles. In the microstructure obtained from the sample without vibration, it is clear that the rod-like silicon particles are observed, and the eutectic silicon particles show a non-uniform distribution, as shown in **Figure 4.21(a)**, **Figure 4.22(a)** and **Figure 4.23(a)**. Optical Micrographs order place with increase in Frequency of mold oscillation are shown in **Figure 4.21(b-e)**, **Figure 4.22(b-e)** and **Figure 4.23(b-e)**. With the application of mechanical vibration, by increasing vibration frequency from 100Hz up to 400 Hz. The eutectic silicon particles obviously exhibit a short rod and granular structure, and the coarse plate-like silicon particles have disappeared and the sizes of eutectic silicon particles are much finer than those of the sample without vibration. These mechanisms are responsible for globular silicon particle and due to Globularisation of Silicon Particle there is appreciable increase in roundness of silicon particle of casting prepared under oscillatory conditions than stationary casting.

#### **A356 Aluminium Alloy:**

In the microstructure obtained from the sample without vibration, it is clear that the long dendrite cell with large grain size and the eutectic silicon particles show a non-uniform distribution, as shown in **Figure 4.24(a)**, **Figure 4.25(a)** and **Figure 4.25(a)**. Optical Micrographs order place with increase in Frequency of mold oscillation are shown in **Figure 4.24(b-e)**, **Figure 4.25(b-e)** and **Figure 4.23(b-e)**. Application of mechanical vibration was made by increasing vibration frequency from 100Hz up to 400 Hz during the solidification of casting. The grain detachment mechanism is also operative due to mold oscillation during the solidification, where partially melted grains are loosely held together by liquid film between them. They are separated due to mold oscillation and survive like dendrite fragments and work as nuclei for the formation of new grains in the casting. The grain multiplication (dendrite fragmentation) and fracture of silicon particle are observed. Due to the increase in vibration frequency, dendrite structure is gradually

broken down with an increase in frequency and amplitude along with coarsening of aluminum grains obtained. These mechanisms are responsible for grain refinement and due to grain refinement there is appreciable decrease in grain size of casting prepared under oscillatory conditions than stationary casting..

**GUO Hong-min, et al. [46]** investigated combined effects of vibration and grain refiner on the microstructure of semisolid slurry of hypoeutectic Al-Si alloy. They were found that the primary  $\alpha(\text{Al})$  particles become finer and rounder with the increase of vibration frequencies. Intense convection can be produced in the melt by vibration during the solidification. Non-dendrite primary  $\alpha(\text{Al})$  crystals become finer and rounder with the increase of vibration frequency. Combined effect of vibration and grain refiner on the slurry can be prepared with EPD(equivalent particle diameter) of primary  $\alpha(\text{Al})$  about 90  $\mu\text{m}$  and ASC(average shape coefficient) above 0.5 under the vibration of 20 Hz.

**S. Wu et al. [48]** developed the a technique of introducing mechanical vibration during isothermal holding period of hypoeutectic A356 Al alloy to prepare semi-solid slurry and examine the formation of non-dendritic microstructure under aforesaid condition. The above technique used mechanical vibration to agitate the melt this was held at a temperature below its liquidus in a crucible. Development of the nucleation and formation of a non-dendritic microstructure within the semi-solid slurry due to melt convection by mechanical vibration together with under cooling of melts was investigated.

**C. Limmaneevichitr et al., [51]** studied about the metallurgical structure of A356 aluminum alloy solidified under mechanical vibration. They found the fracture of dendrites. Fractured dendrites are uniformly disturbed and fragmented into the melted alloy with a larger solid fraction at lower pouring temperatures.

**N. Abu-Dheir et al. [57]** investigated effect of mold vibration on Silicon morphology in the eutectic Al–Si alloy. They found modification in microstructure with the increasing of the vibration amplitude as compared to gravity castings. However, they also stated that by exceeding a critical value of vibration amplitude, the silicon tends to coarsen.

**W. Wang et al.[77]** investigated and studied the effect of vibration on crystal nucleation and chilling solid surface. They suggested that this technique is an effective way to produce lots of nuclei for forming equiaxed grains microstructure. It is possible only by preventing the solidifying shell to form and promoting fracturing of dendrites not only from the free liquid surface but also from the chilling solid surface. For finer equiaxed grains, it is required to increase synchronously vibration frequency as well as amplitude..

**Piwonka T S [83]** described the effect of vibration during solidification of alloys. In this handbook it is given that the vibration during solidification is the main reason for a zone of low-melting liquid exists immediately adjacent to the main crystal growth. Nucleation can happen, and if disturbed by vibration, banding results. This method additionally states that growth takes place from these new nuclei in such a way as to form a sandwich of liquid metal enclosed by solid metal, which is isolated from the liquid bath at the bore.

**Jiang, W., et al. [91]** found that the mechanical vibration greatly increased the mechanical properties, density of A356, the size, morphology, distribution of  $\alpha$ -Al primary phase, eutectic silicon particles, and SDAS. They found that with increasing vibration frequency, the grain size and SDAS continuously decreased, and the shape factor gradually increased with the increase of vibration frequency.

**Radjai et al. [87]** investigated the impact of such a vibration on the refinement of Al - 17 wt.% Si and decided that electromagnetic vibration caused a cavitation effect that fractured the primary silicon particles into smaller pieces

**Kumar, R., et al. [95]** examined and understood the modification in microstructure and mechanical properties of Al-Cu alloys castings solidified under mold vibration. The mold was made of graphite and frequencies varied from 40 to 150 Hz. One more cast also was made under stationary condition to compare the results of castings with vibration. The test results show significant grain refinement, and the improvement in hardness of castings with mold vibration during solidification are compatible with the determined grain size. The maximum tensile strength and elongation correspond to the smallest grain size obtained.

**Chaturvedi, V., & Pandel, U. [98]** studied the influences of mechanical vibrations on the mechanical properties of AZ91 magnesium alloy. This was tested at constant frequency of 40Hz and varied amplitude from 0 to 2 mm. Increased amplitude of mechanical vibration during solidification causes refinement of the grain in the alloy. Tensile strength improved upto a certain point with increasing amplitude and start decreasing with further increment in the amplitude of vibrations. This refinement of the grains also results in an increased percentage elongation and hardness of the alloy samples.

**Jiang, W., et al.[99]** examined the impacts of the mold vibration frequency of 100 Hz on microstructure, mechanical properties, and fracture behavior of the A356 aluminum alloy. Obtained results such as the grain size, and SDAS decreased by 32 and 19 %, respectively, and the shape factor increased by 262 percent compared to stationary prepared casting. The additional results like morphological properties of Si-particle such as the average length, width, and aspect ratio of the silicon particles decreased by 45, 6, and 42 %, respectively, compared to stationary prepared casting. Similarly, mechanical properties

such as the tensile strength, yield strength, elongation, and hardness of the A356 alloy sample were, respectively, 35, 42, 57, and 28 % higher than those of stationary prepared casting. The mechanical vibration also modified the fractograph of the A356 alloy from a clear, brittle fracture nature of the alloy without vibration to dimple fracture nature with the increase of vibration frequency, the dimples were very deep and well distributed with a high density.

**Jianbo Yu et. al [102]** studied the solidification structure of eutectic Al-Si alloy experimentally under electromagnetic vibration and high magnetic field. They found that solidification structure of eutectic Al-Si alloy more refined under high magnetic field than electromagnetic vibration. Polyhedral Si grains and nondendritic  $\alpha$ -Al appeared when the electromagnetic vibration strength was strong. These high electromagnetic vibrations may break co-operative growth of eutectic phases to form polyhedral Si grains and non-dendritic  $\alpha$ -Al.

**Patel, V. R. [103]** recommended that mechanical mold vibration has a significant impact on the alternative film of eutectic silicon particles in eutectic Al-Si alloys. The eutectic silicon particles reveal significant modification, and their dispersion tends to become more uniform when the casting is solidified with vibration. The maximum tensile strength and impact strength is obtained by casting prepared under vibration as compared to that of stationary. Melt treatment along with vibration proves modification in size of eutectic silicon & refinement of  $\alpha$ -Al dendrites of eutectic Al-Si alloy.

#### 4.5 Evaluation of the Metallurgical Properties and Comparison of oscillatory casting with the stationary casting.

##### 4.5.1 Effect of Oscillation on $\alpha$ -Al Grain Size ( $\mu\text{m}$ )

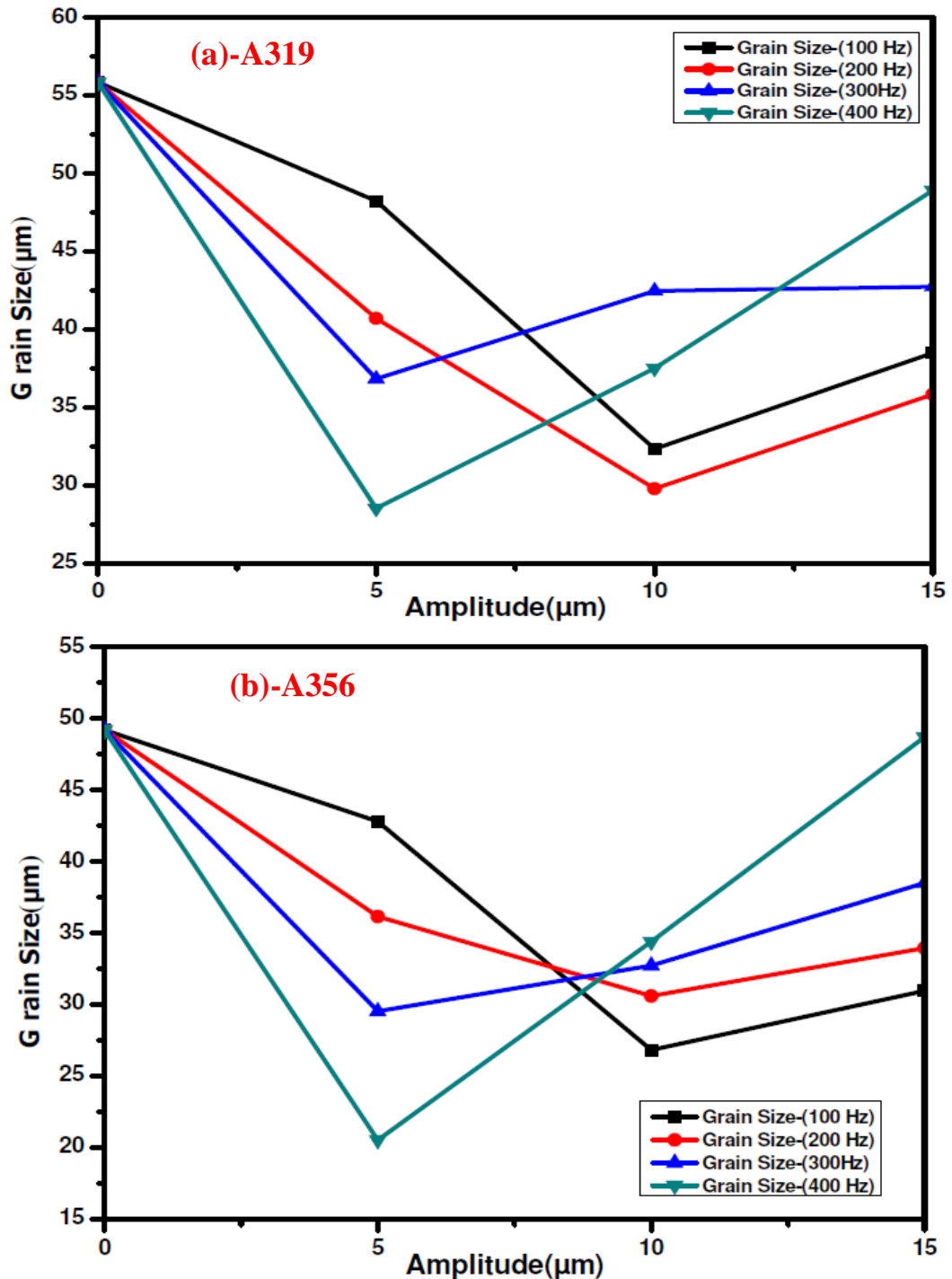
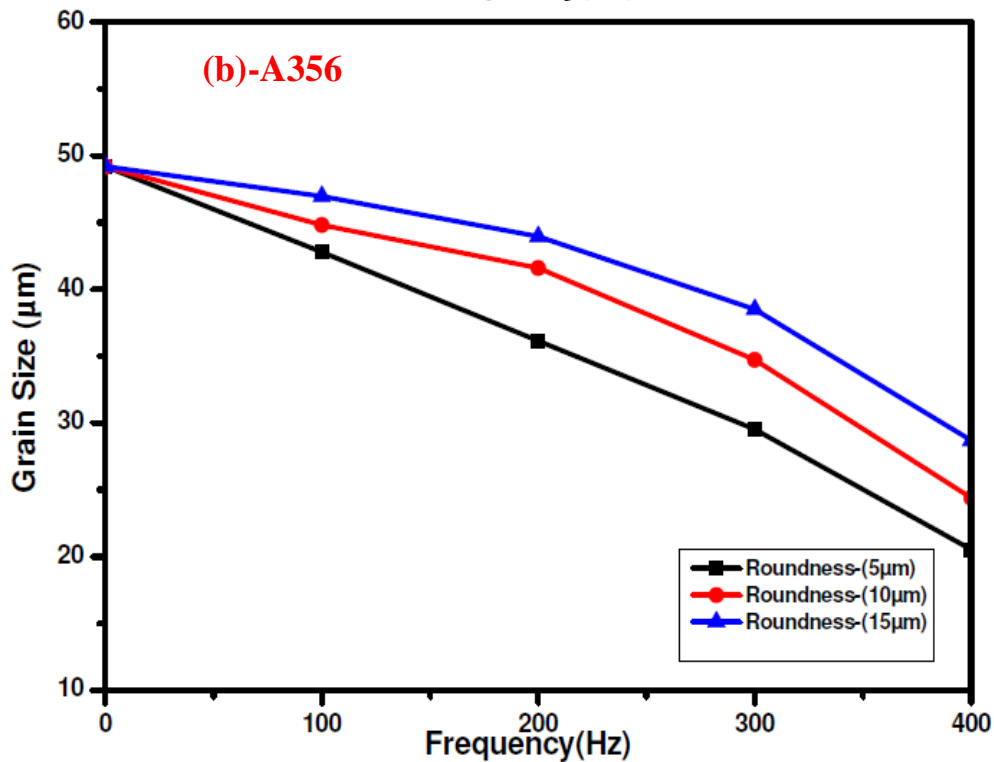
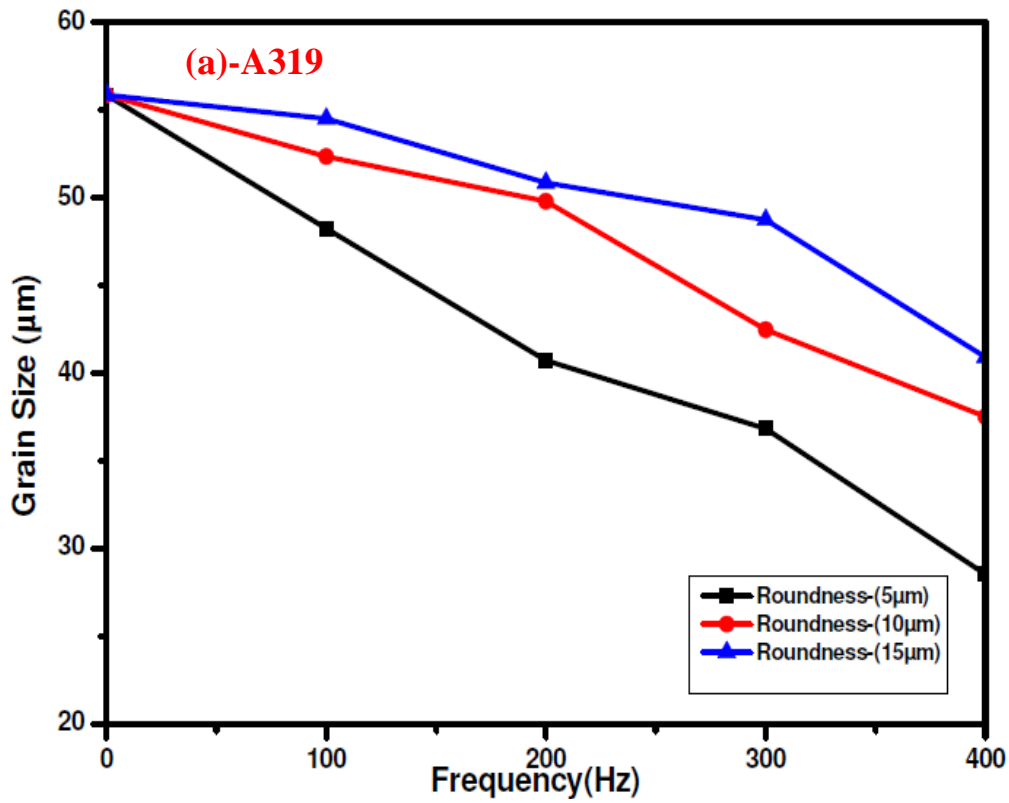


Figure 4.26 Effect of amplitude on grain size of (a) A319 and (b) A356 aluminium alloys casting



**Figure 4.27 Effect of frequency on grain size of (a) A319 and (b) A356 aluminium alloys casting**

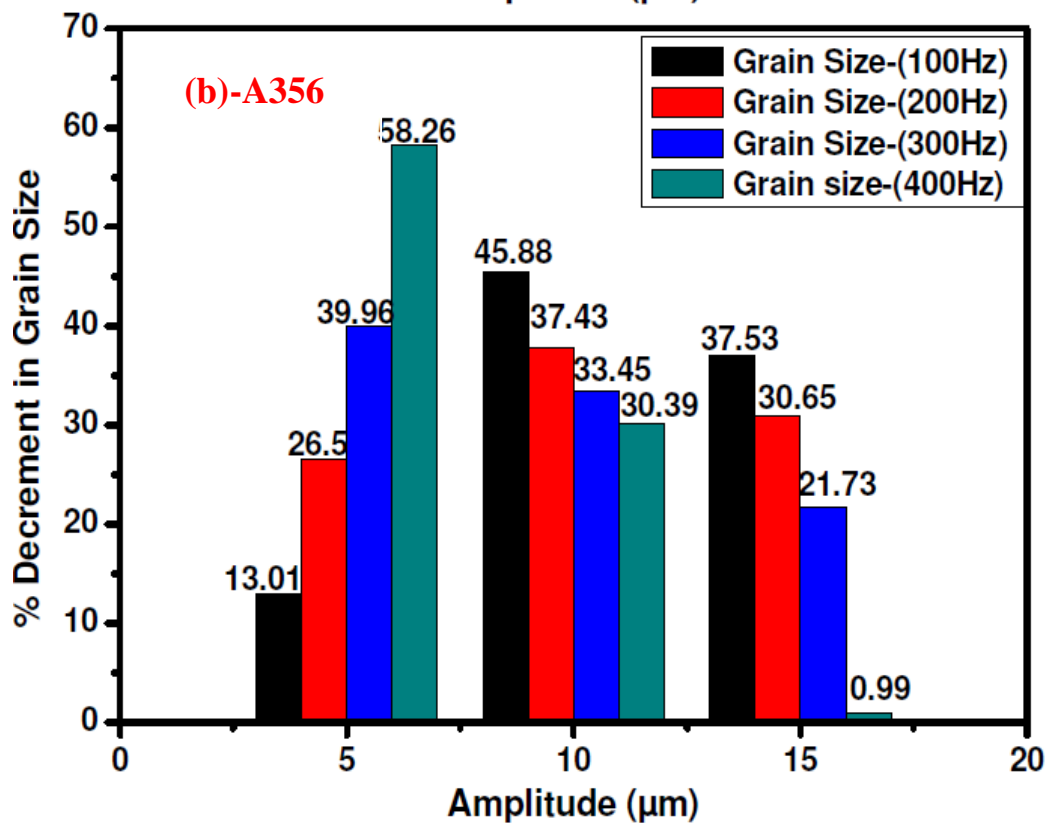
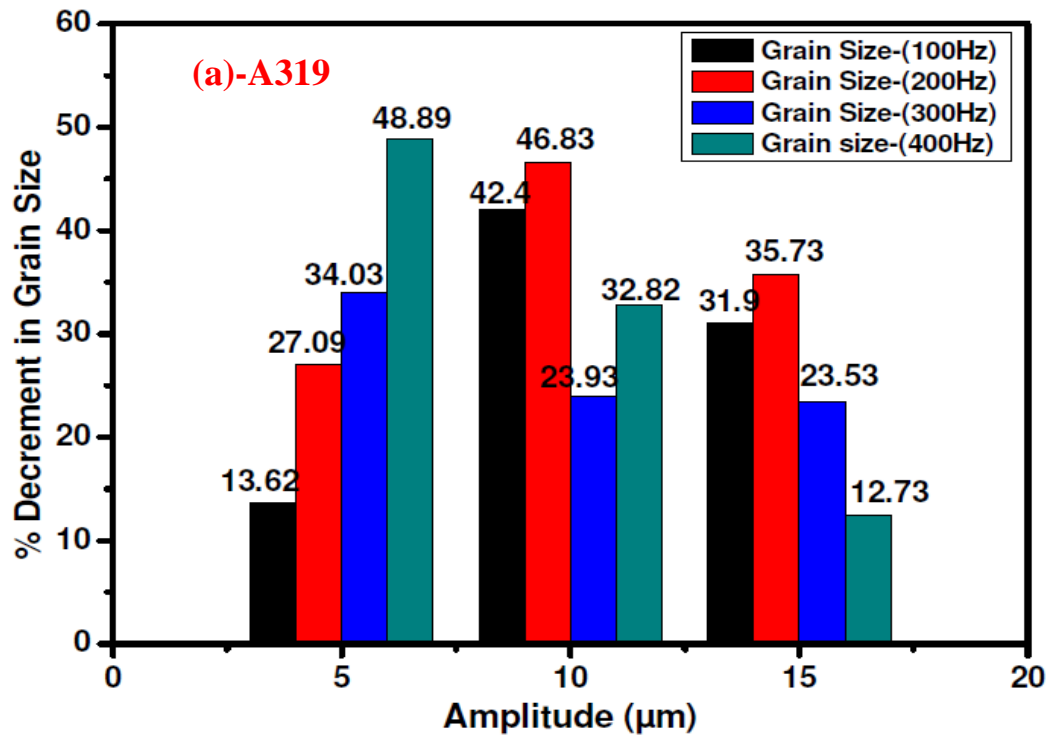


Figure 4.28 Comparison of percentage change in grain size (a) A319 and (b) A356aluminium alloys casting

#### 4.5.2 Effect Of Oscillation on Dendrite Arm Spacing ( $\mu\text{m}$ )

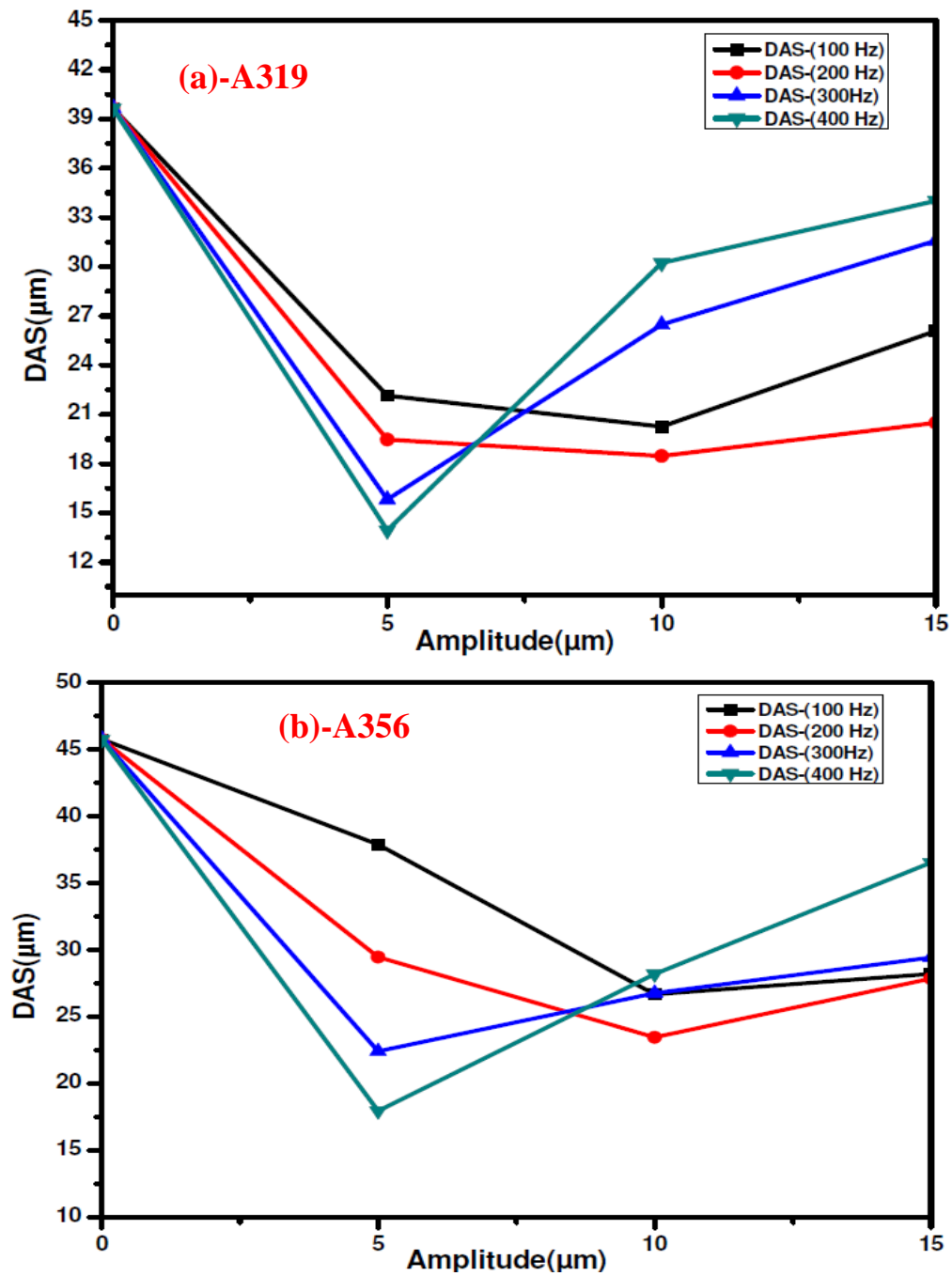


Figure 4.29 Effect of amplitude on DAS of (a) A319 and (b) A356 aluminium alloys casting

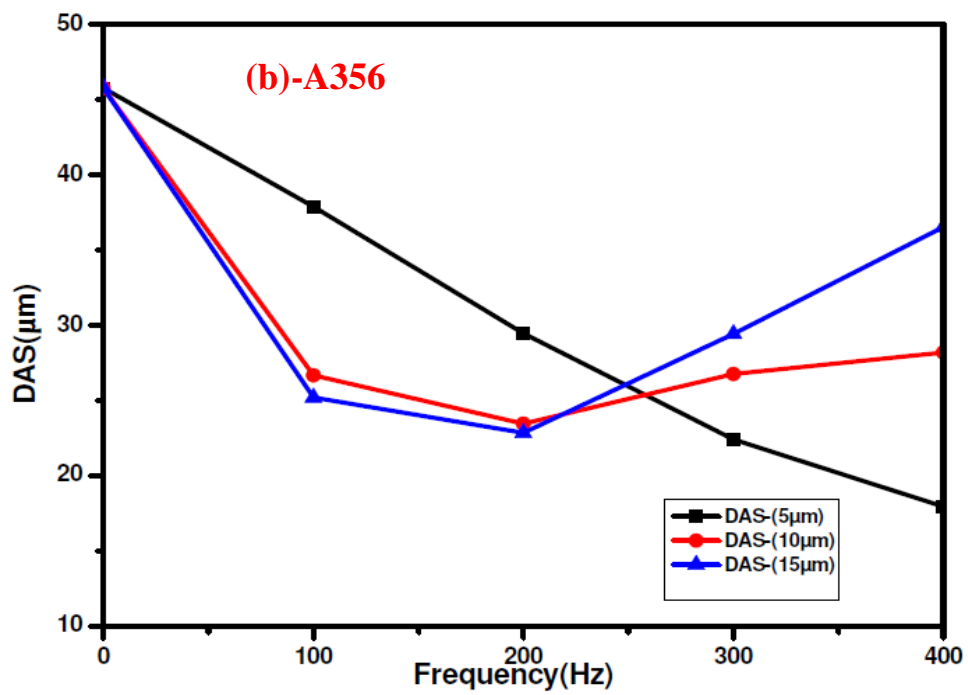
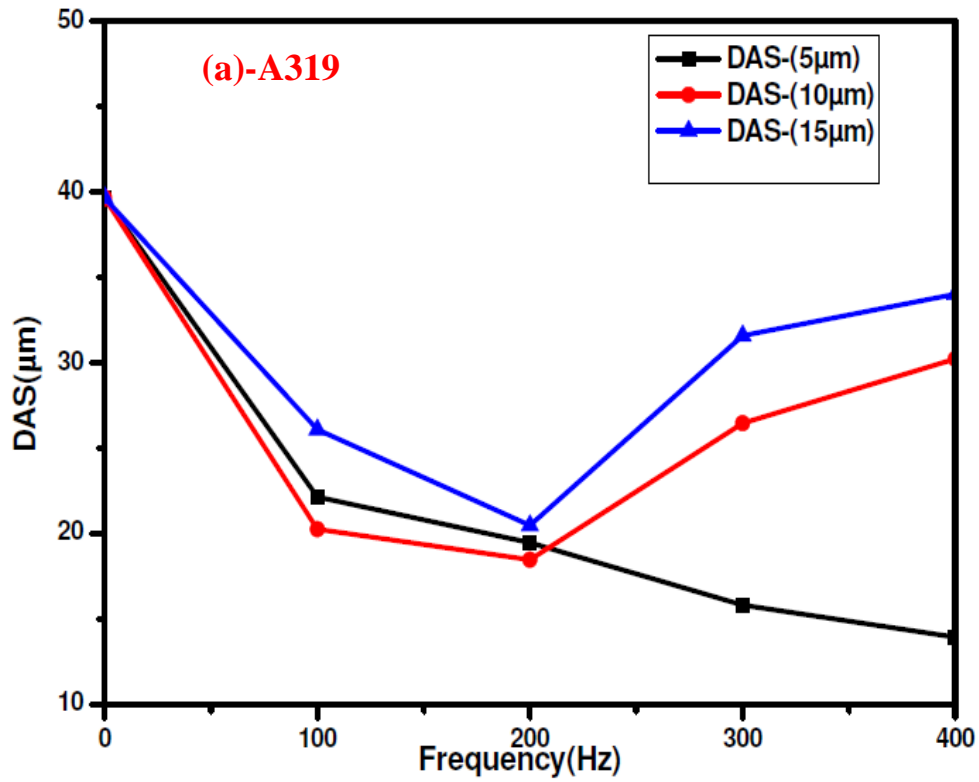


Figure 4.30 Effect of frequency on DAS of (a) A319 and (b) A356 aluminium alloys casting

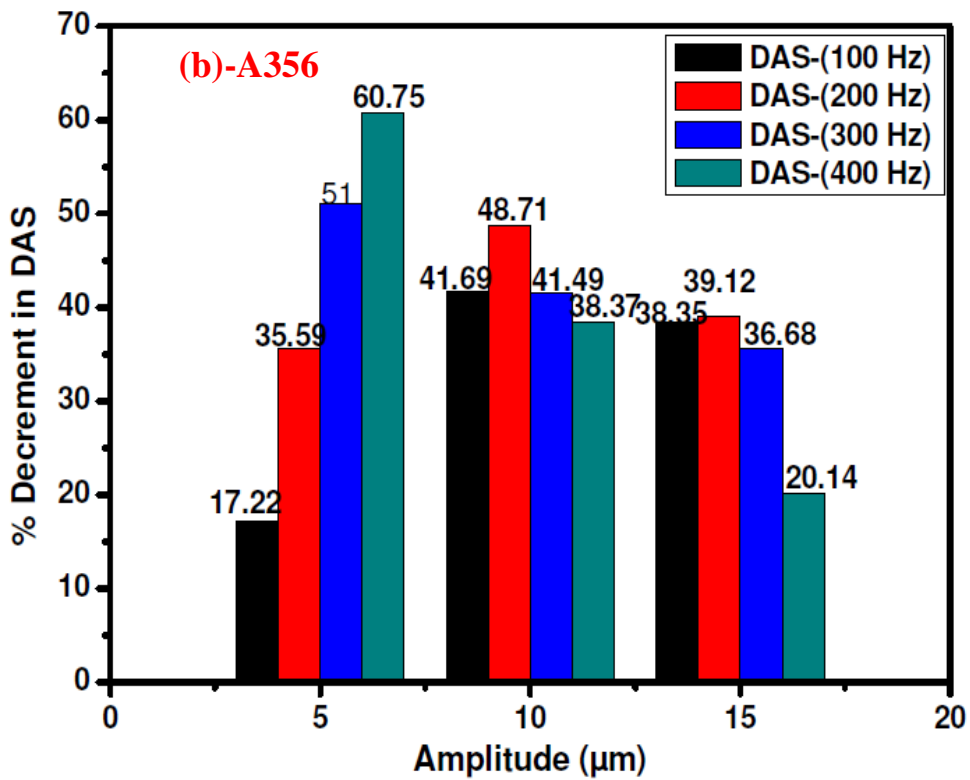
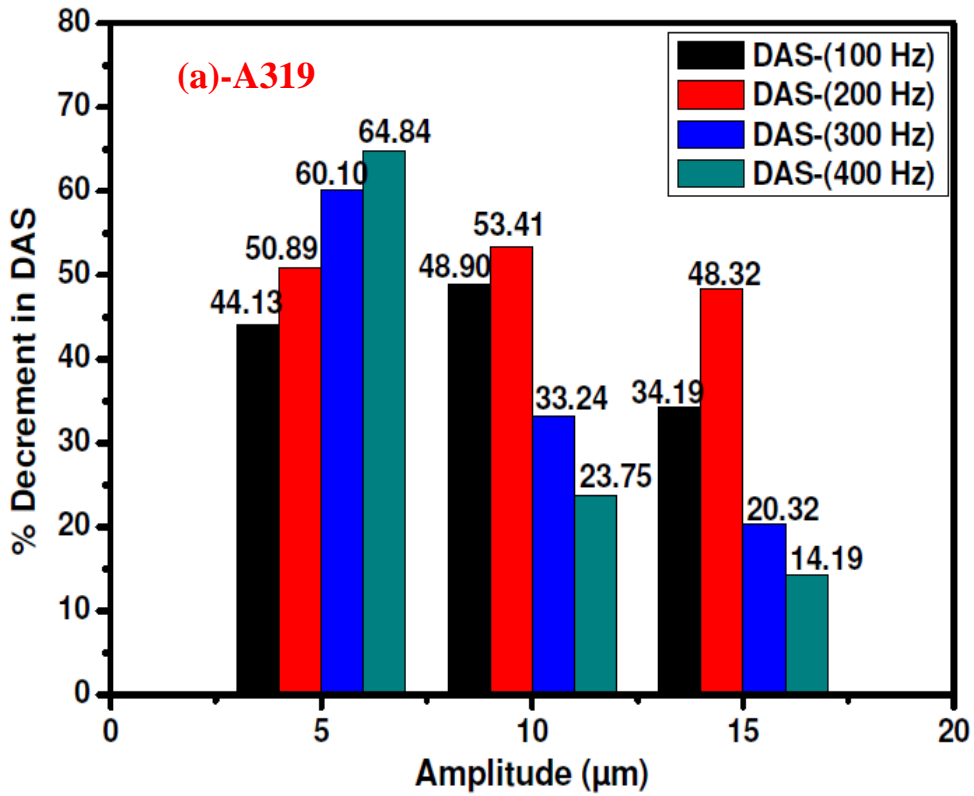


Figure 4.31 Comparison of percentage change in DAS (a) A319 and (b) A356 aluminum alloys Casting

### 4.5.3 Effect of Oscillation on Roundness Of Silicon Particle (%)

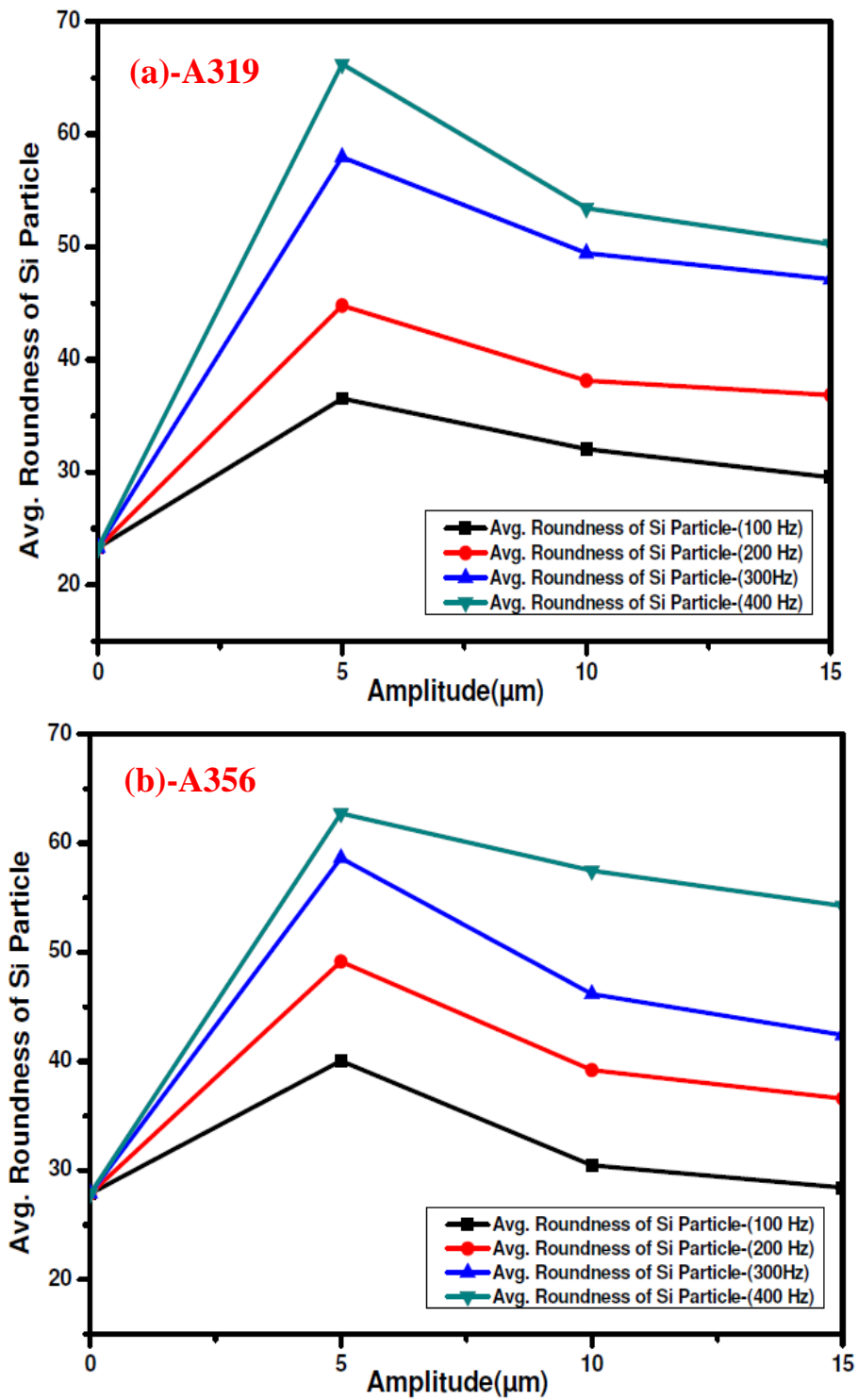
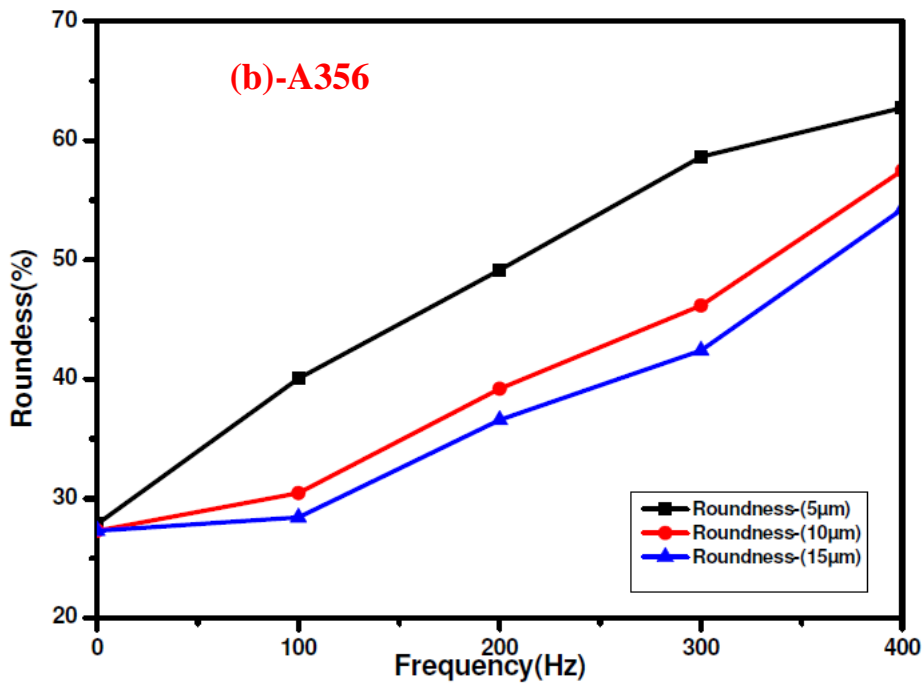
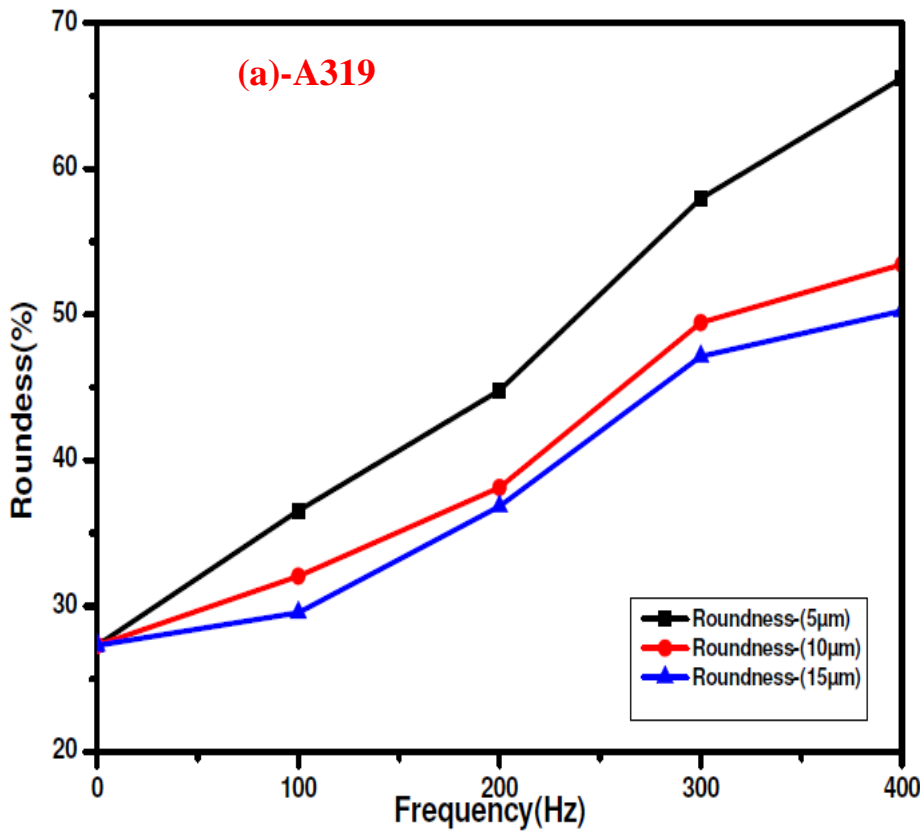


Figure 4.32 Effect of amplitude on roundness(%) of silicon particle of (a) A319 and (b) A356 aluminium alloys casting



**Figure 4.33 Effect of frequency on roundness(%) of silicon particle of (a) A319 and (b) A356aluminium alloys casting**

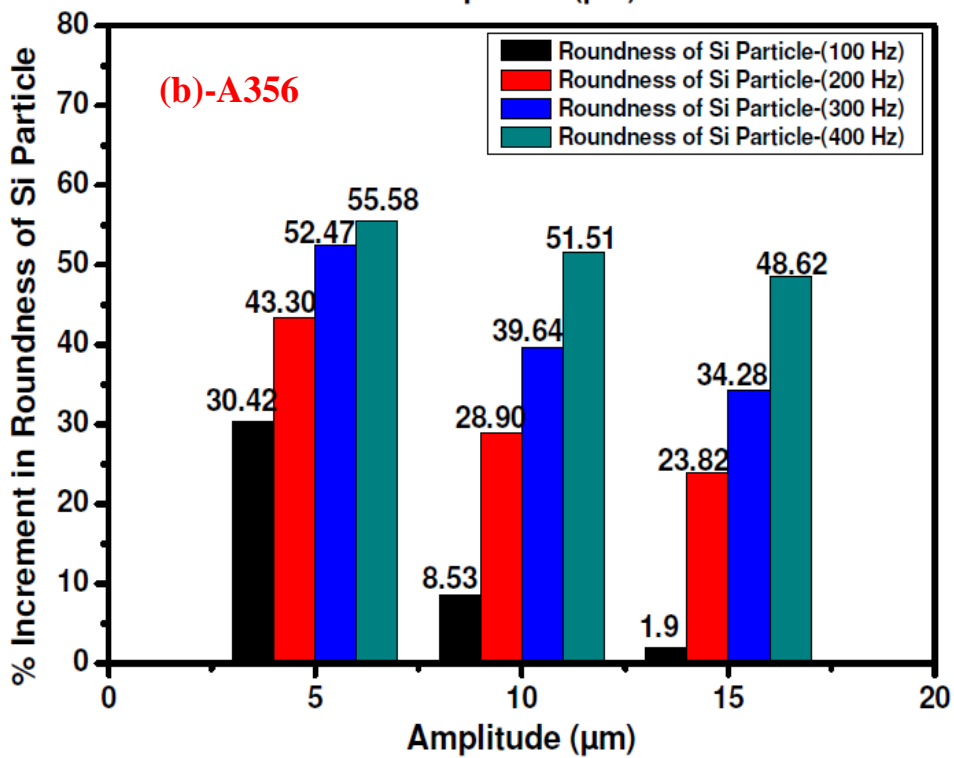
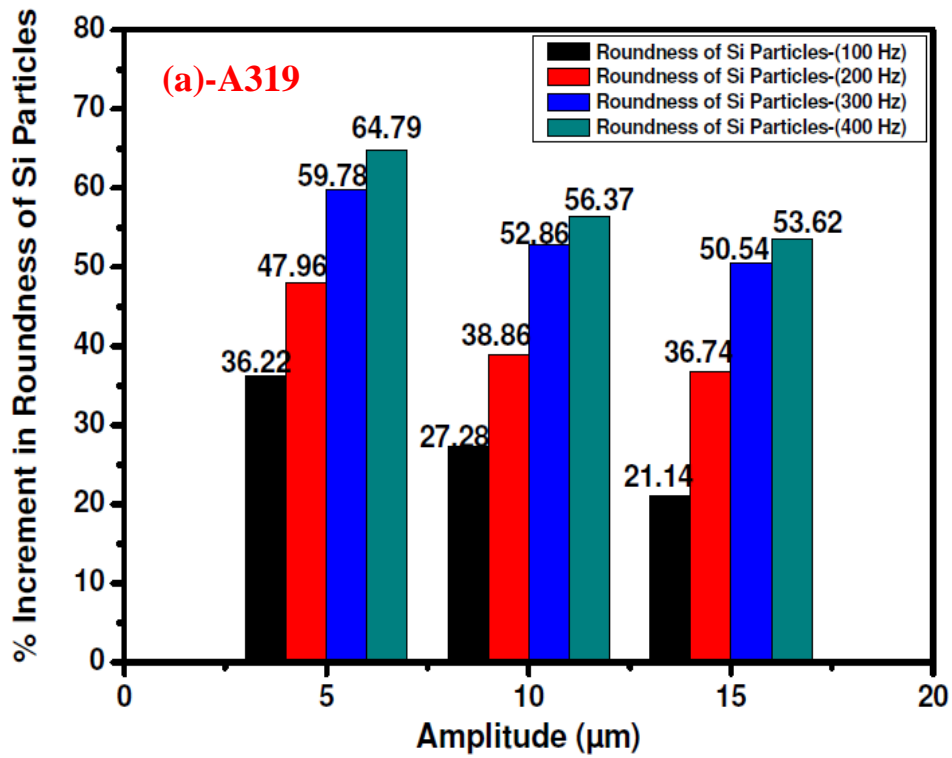


Figure 4.34 Comparison of percentage change in roundness of silicon particle (a) A319 and (b) A356 aluminum alloys casting

4.5.4 Effect of Oscillation on Average Of Area of Silicon Particle ( $\mu\text{m}^2$ )

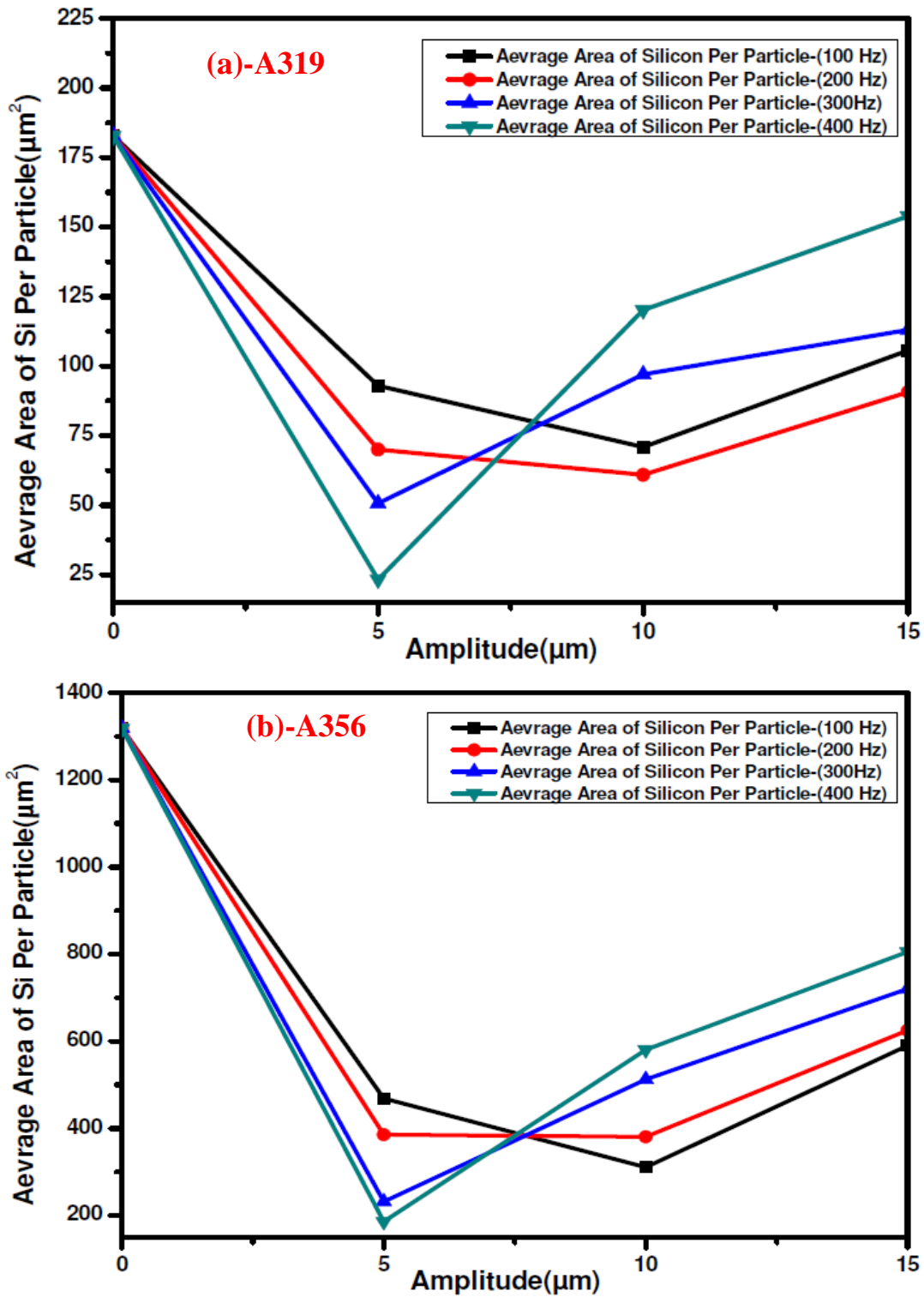


Figure 4.35 Effect of amplitude on area of silicon particle ( $\mu\text{m}^2$ ) of (a) A319 and (b) A356 aluminium alloys casting

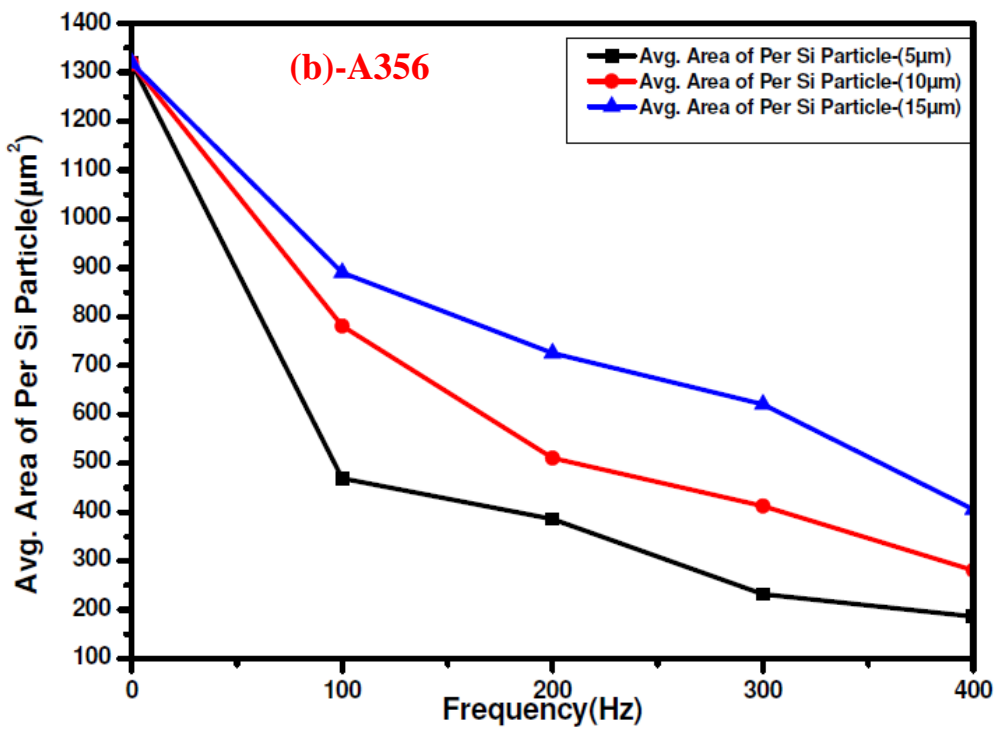
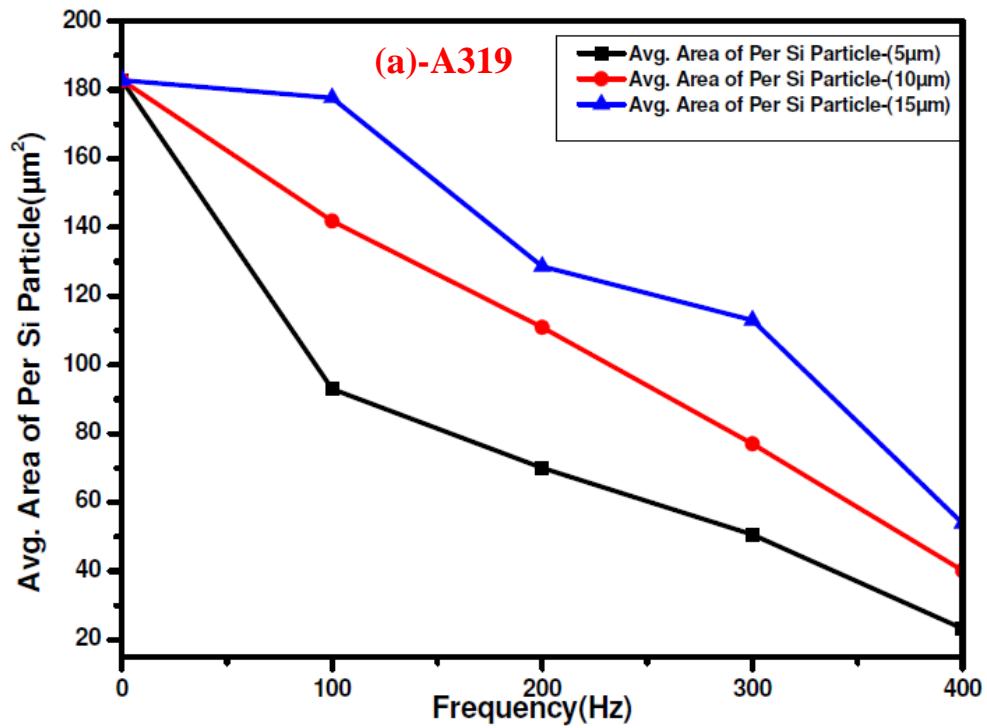


Figure 4.36 Effect of frequency on area of silicon particle(µm<sup>2</sup>) of (a) A319 and (b) A356 aluminium alloys casting

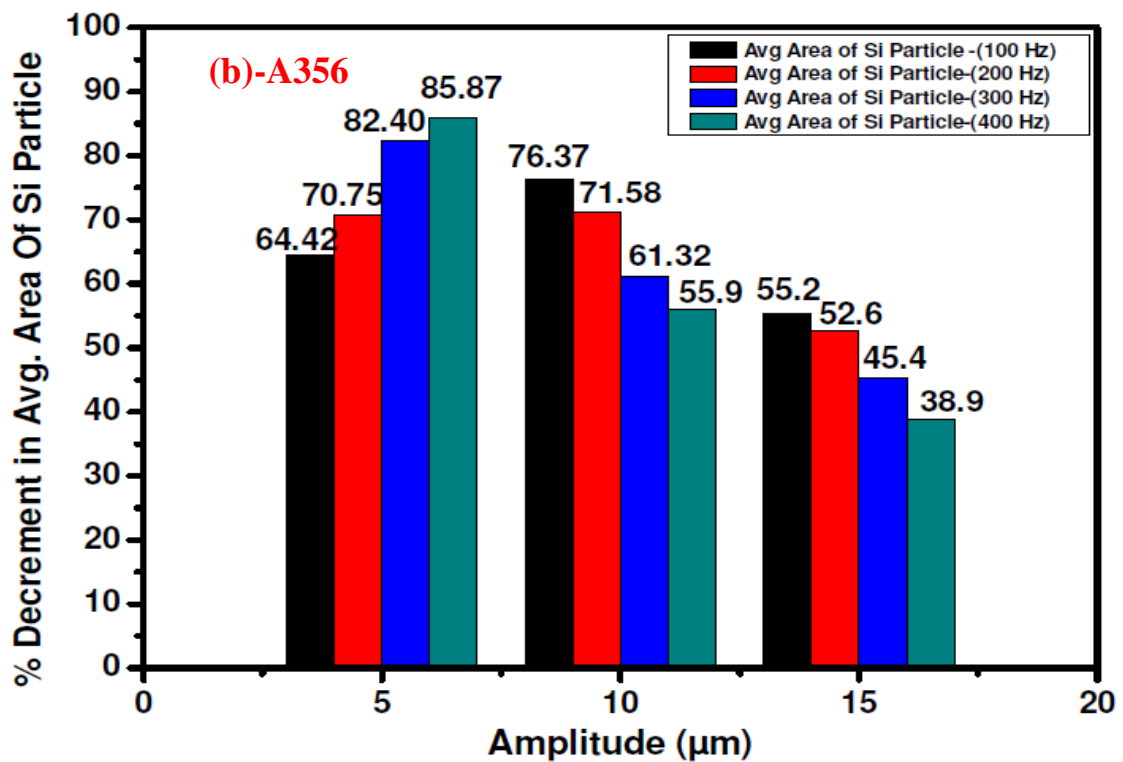
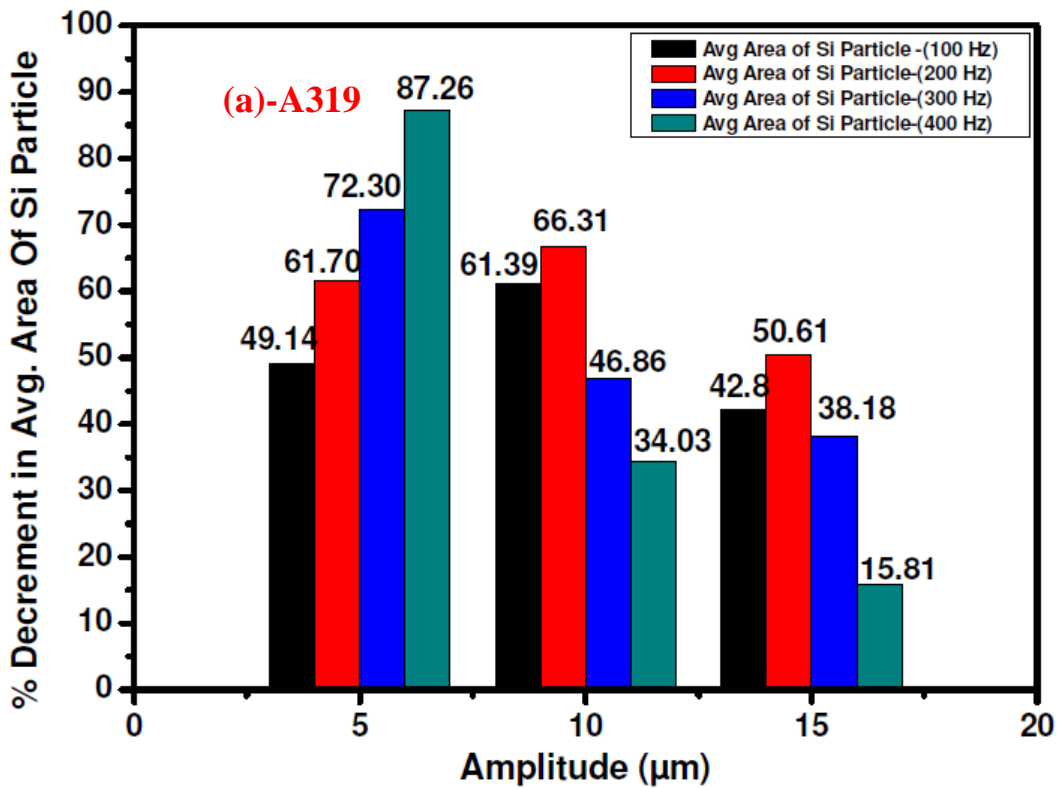


Figure 4.37 Comparison of percentage change in avg. area of silicon particle (a) A319 and (b) A356 aluminum alloys casting

#### 4.5.5 Effect of Oscillation on Aspect Ratio of Silicon Particle

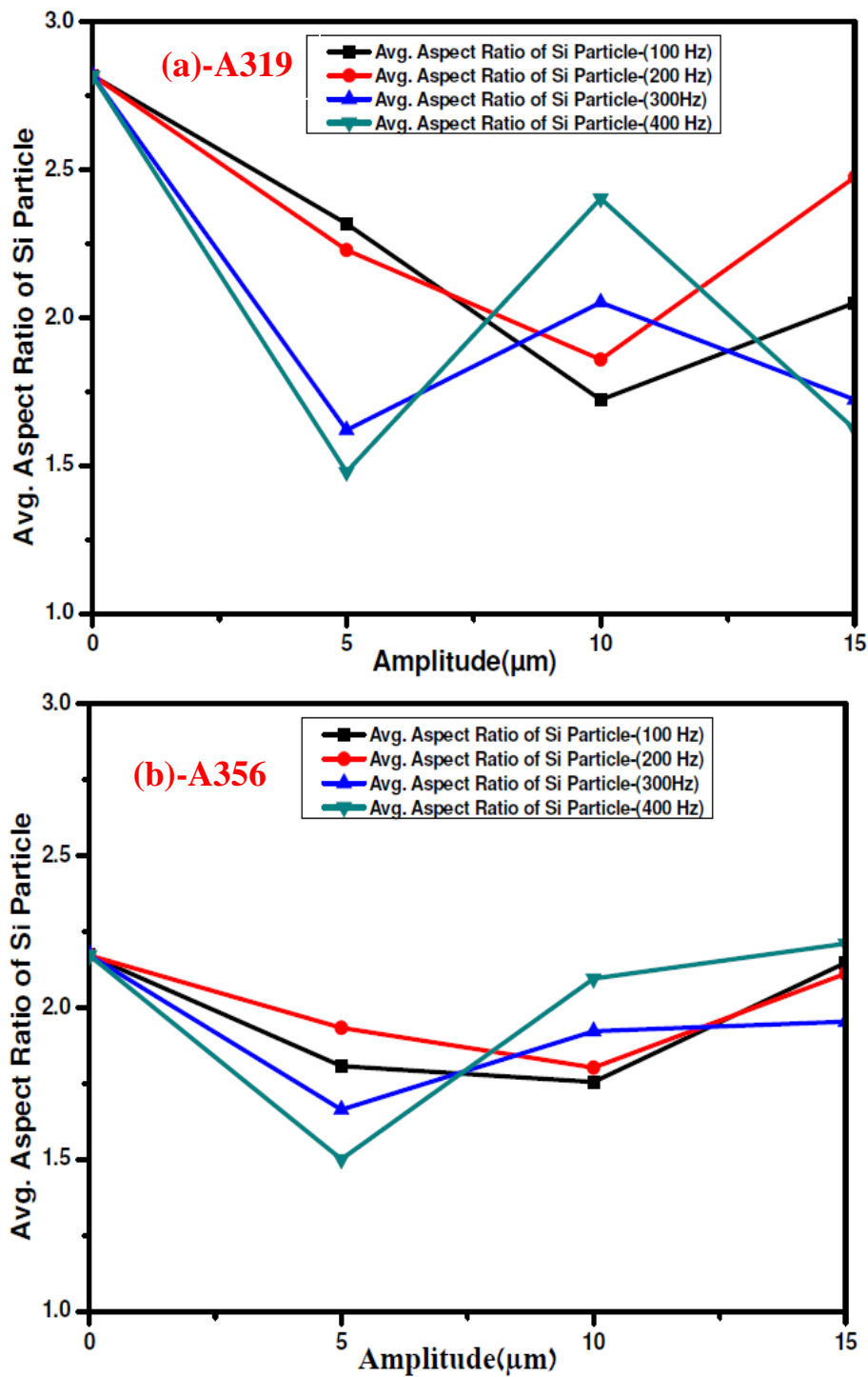


Figure 4.38 Effect of amplitude on aspect ratio of silicon particle of (a) A319 and (b) A356 aluminium alloys casting

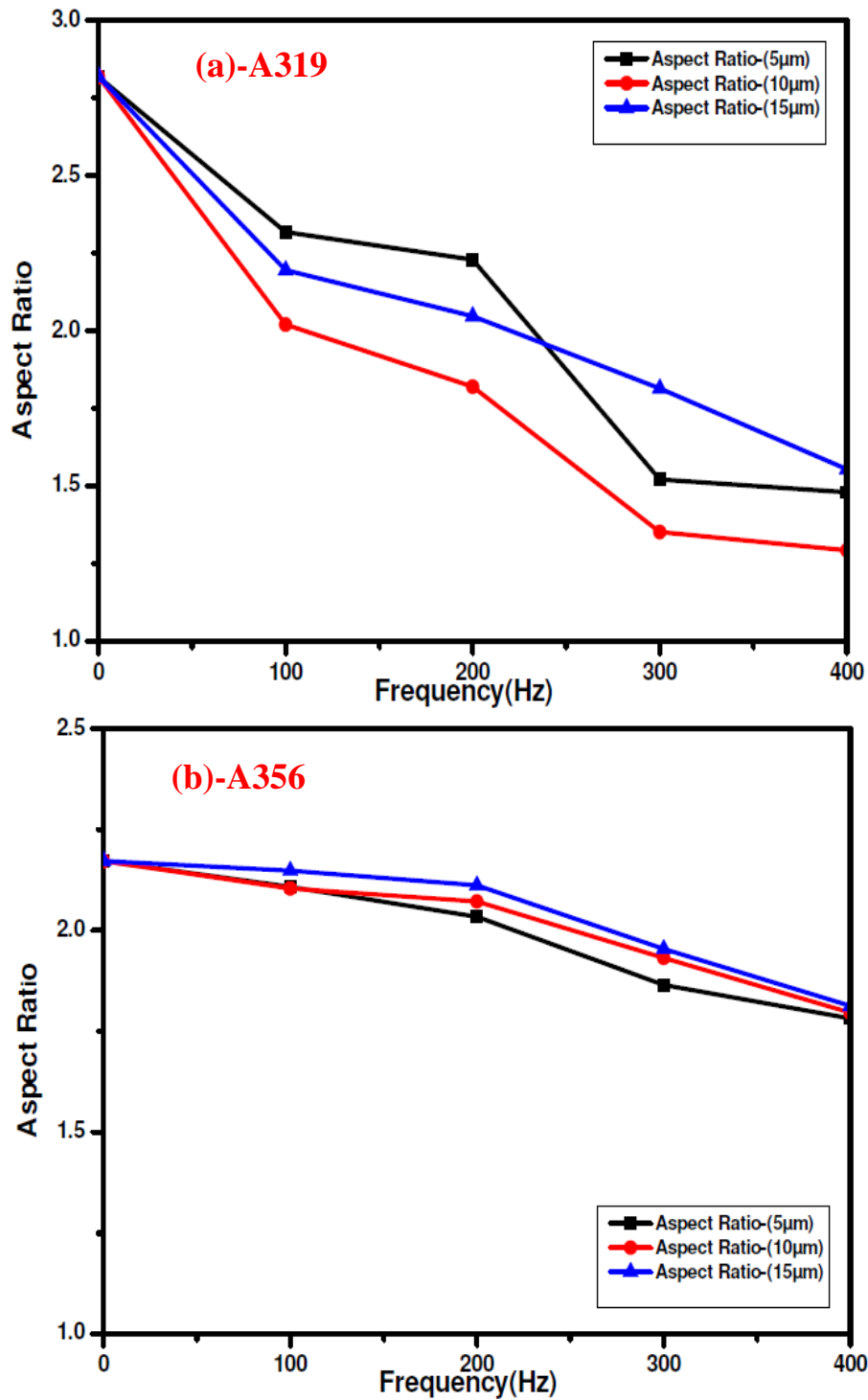
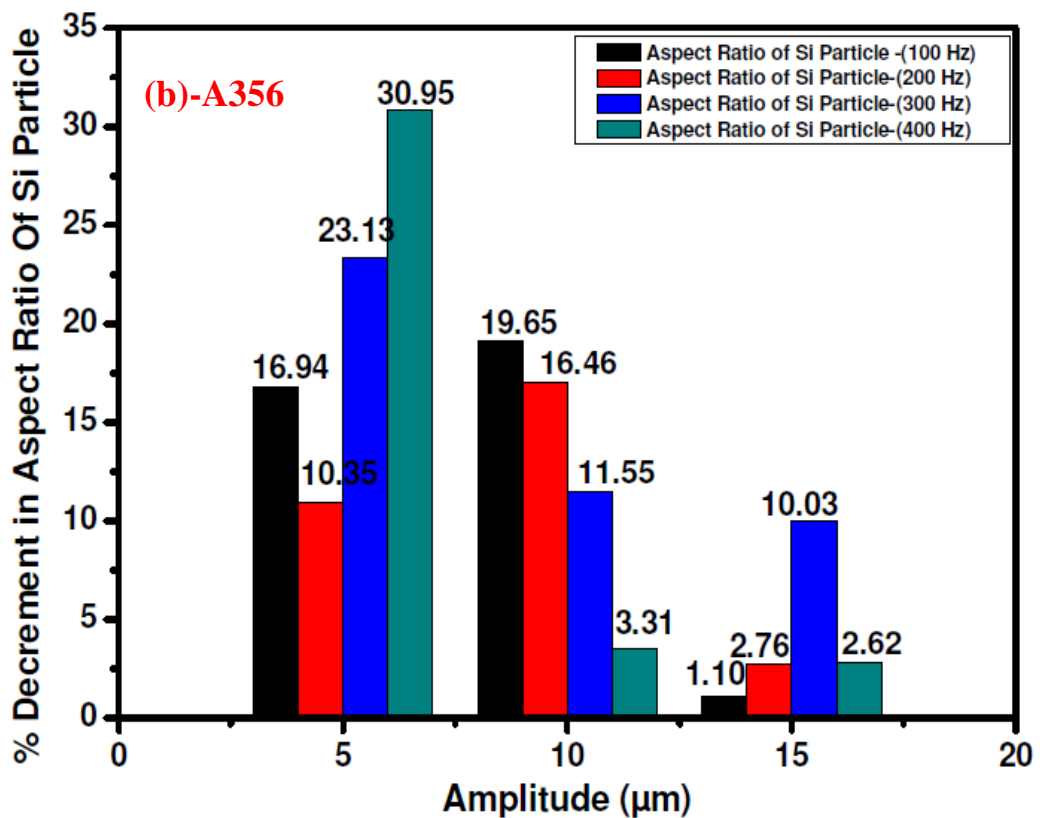
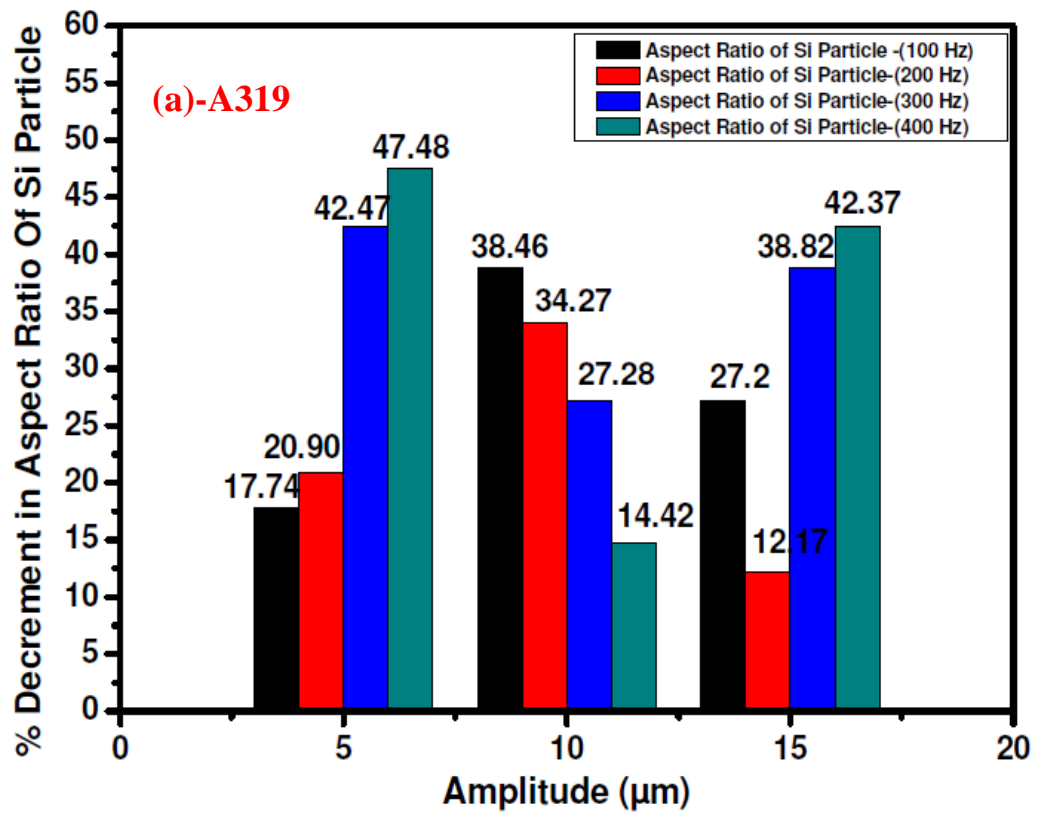


Figure 4.39 Effect of frequency on aspect ratio of silicon particles of (a) A319 and (b) A356 aluminium alloys casting



**Figure 4.40 Comparison of percentage change in aspect ratio of silicon Particle (a) A319 and (b) A356 aluminum alloys casting**

### 4.5.6 Effect of Oscillation on Porosity (%)

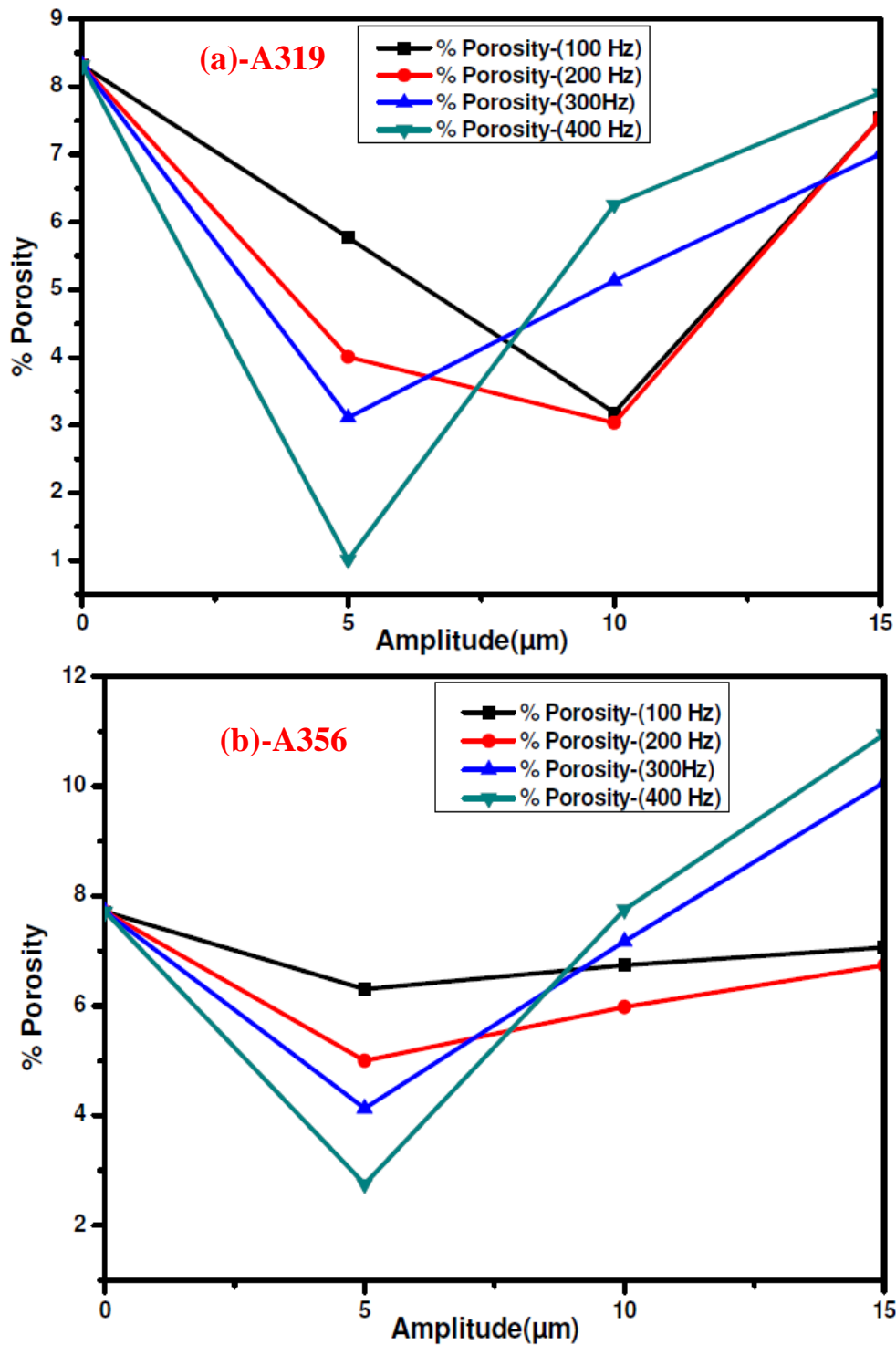
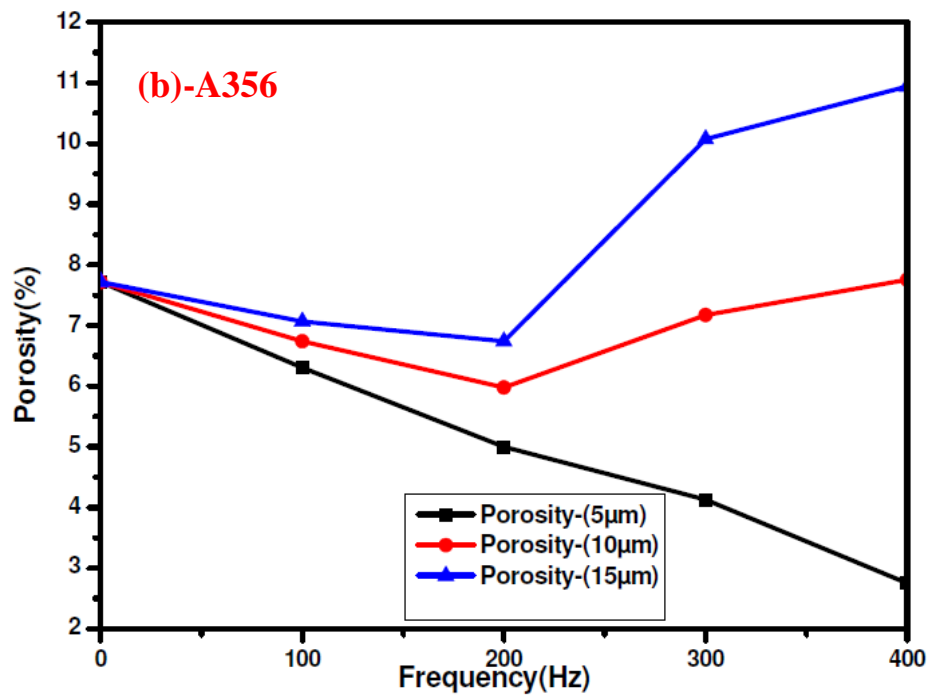
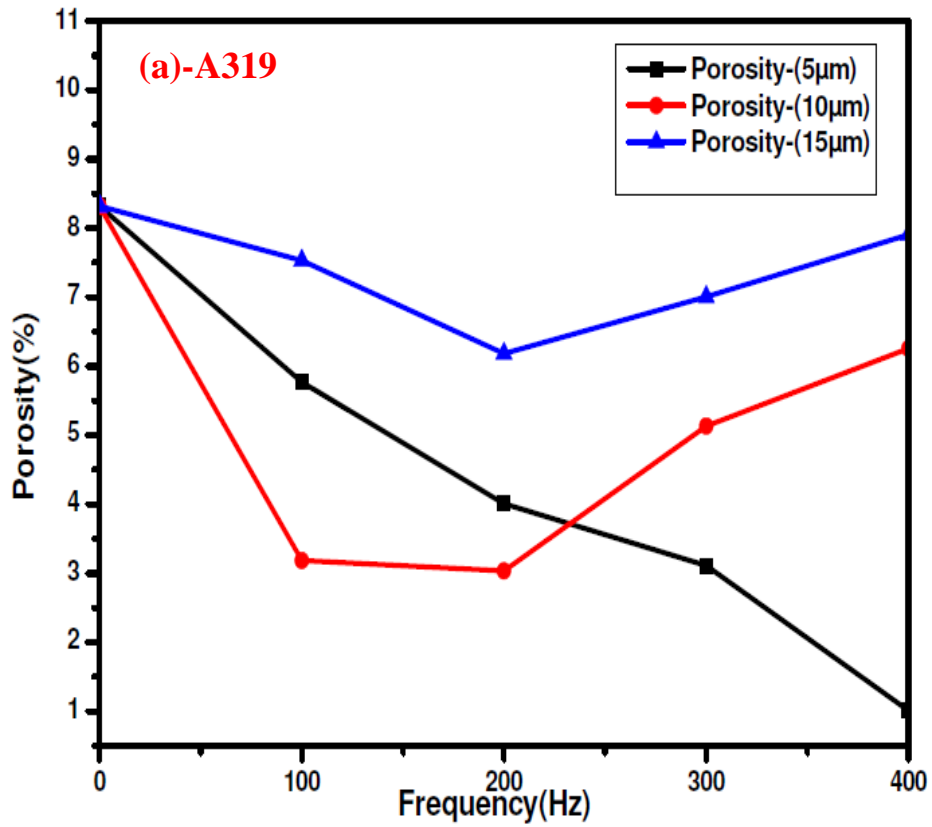


Figure 4.41 Effect of amplitude on porosity (%) of (a) A319 and (b) A356 aluminium alloys casting



**Figure 4.42 Effect of frequency on porosity (%) of (a) A319 and (b) A356 aluminium alloys casting**

## 4.6 Aspect Ratio of Silicon Particles

### 1) A319 Aluminum alloy Casting

The aspect ratio of silicon particles is improved by mold oscillation during the solidification and varies for oscillated test specimens when compared to stationary cast specimens. Variation of the aspect ratio with respect to amplitude and frequency of oscillation are shown in **Figure 4.39(a)** and **Figure 4.40(a)** respectively. The aspect ratio at stationary and at 100,200,300,400Hz with 5 $\mu$ m amplitude are 2.818, 2.318, 2.229, 1.521 and 1.48 respectively. Similarly, the aspect ratio of silicon particles at stationary and at 100,200,300,400Hz with 10 $\mu$ m amplitude are 2.818, 2.02, 1.82,1.352 and1.293 respectively and similarly for the aspect ratio of silicon particles at stationary and at 100,200,300,400Hz with 15 $\mu$ m amplitude are 2.818,2.195,2.047,1.814 and 1.554 respectively. It can be observed that in general the aspect ratio of silicon particles decreases with increase in frequency of oscillation and increase with increase in amplitudes of oscillation.

The percentage decrement in aspect ratio of silicon particles for oscillated test specimens when compared to stationary cast specimen are 47.88 % at 400Hz ,42.47% at 300Hz ,20.90% at 200Hz and 17.74% at 100Hz frequencies of oscillation with 5 $\mu$ m amplitude .Similarly, 39.92 % at 400Hz ,34.27 % at 300Hz ,16.28% at 200Hz and 10.46 % at 100Hz frequencies of oscillation with 10 $\mu$ m amplitude and 42.37 % at 400Hz ,38.82 % at 300Hz ,12.17% at 200Hz and 5.7 % at 100Hz frequencies of oscillation with 15 $\mu$ m amplitude. It can be observed from the **Figure 4.41(a)** that in general the % aspect ratio decrement increase with increase in frequency of oscillation and decrease with increase in amplitudes of oscillation.

## 2) A356 Aluminum alloy Casting

The aspect ratio of silicon particles is improved by mold oscillation during the solidification and varies for oscillated test specimens when compared to stationary cast specimens. Variation of the aspect ratio with respect to amplitude and frequency of oscillation are shown in **Figure 4.39(b)** and **Figure 4.40(b)** respectively. The aspect ratios at stationary and at 100,200,300 and 400Hz with 5 $\mu$ m amplitude are 2.5, 2.22, 2.17, 1.65 and 1.47 respectively. Similarly, the aspect ratio of silicon particles at stationary, and at 100,200,300 and 400Hz with 10 $\mu$ m amplitude are 2.5, 2.23, 2.19, 2.10 and 1.53 respectively and similarly for the aspect ratio of silicon particles at stationary and at 100,200,300 and 400Hz with 15 $\mu$ m amplitude are 2.5, 2.45, 2.30, 2.20 and 1.89 respectively. It can be observed that in general the aspect ratio of silicon particles decrease with increase in frequency of oscillation and increase with increase in amplitudes of oscillation.

The percentage decrement in aspect ratio of silicon particles for oscillated test specimens when compared to stationary cast specimens are 17.95% at 400Hz, 14.13% at 300Hz, 6.35% at 200Hz and 2.94% at 100Hz frequencies of oscillation with 5 $\mu$ m amplitude. Similarly, 17.31% at 400Hz, 11.46% at 300Hz, 4.55% at 200Hz and 1.65% at 100Hz frequencies of oscillation with 10 $\mu$ m amplitude and 16.62% at 400Hz, 10.03% at 300Hz, 2.76% at 200Hz and 1.10% at 100Hz frequencies of oscillation with 15 $\mu$ m amplitude. It can be observed from the **Figure 4.41(b)** that in general the % aspect ratio decrement increase with increase in frequency of oscillation and decrease with increase in amplitudes of oscillation.

## 4.7 Roundness of Silicon Particles

### 1) A319 Aluminum alloy Casting

The roundness of silicon particles is improved by mold oscillation during the solidification and varies for oscillated test specimens when compared to stationary cast specimens. Variation of the roundness with respect to amplitude and frequency of oscillation are shown in **Figure 4.33(a)** and **Figure 4.34(a)** respectively. The roundness of silicon particles at stationary and at 100,200,300,400Hz with 5 $\mu$ m amplitude are 27.311, 36.548, 44.8, 57.961 and 66.22% respectively. Similarly, the roundness of silicon particles at stationary and at 100,200,300,400Hz with 10 $\mu$ m amplitude are 27.311,32.056,38.132,49.452 and 53.43% respectively and similarly for the roundness of silicon particles at stationary and at 100,200,300,400Hz with 15 $\mu$ m amplitude are 27.311,29.56,36.851,47.132 and 50.241 respectively . It can be observed that in general the roundness of silicon particles increase with increase in frequency of oscillation and decrease with increase in amplitudes of oscillation.

The percentage increase in roundness of silicon particle(modified) for oscillated test specimens when compared to stationary cast specimens are 58.26 % at 400Hz ,39.96% at 300Hz ,26.50% at 200Hz and 13.01% at 100Hz frequencies of oscillation with 5 $\mu$ m amplitude .Similarly, the increase in 50.39 % at 400Hz ,29.41 % at 300Hz ,15.43% at 200Hz and 8.88 % at 100Hz frequencies of oscillation with 10 $\mu$ m amplitude and 41.65 % at 400Hz ,21.73 % at 300Hz ,10.65% at 200Hz and 4.53 % at 100Hz frequencies of oscillation with 15 $\mu$ m amplitude. It can be observed from the **Figure 4.35 (a)** that in general the percentage increase in roundness increases with increase in frequency of oscillation and decreases with increase in amplitudes of oscillation.

The optical microstructures of the eutectic zone have been obtained with different mold oscillation frequencies in order to demonstrate a substantial microstructure difference in

the size and morphology of eutectic silicon particles. In the microstructure obtained from the sample without vibration, it is clear that the rod-like silicon particles are observed, and the eutectic silicon particles show a non-uniform distribution, as shown in Fig. 6a. In contrast, with the application of mechanical vibration, by increasing vibration frequency up to 400 Hz, the eutectic silicon particles obviously exhibit a short rod and granular structure, and the coarse plate-like silicon particles have disappeared, and the sizes of eutectic silicon particles are much finer than those of the sample without vibration. These mechanisms are responsible for globular silicon particle and due to Globularisation of Silicon Particle there is appreciable increase in roundness of silicon particle of casting prepared under oscillatory conditions as compared to stationary casting.

## 2) A356 Aluminum alloy Casting

The roundness of silicon particles are improved by mold oscillation during the solidification and varies for oscillated test specimens when compared to stationary casted specimen. Variation of the roundness with respect to amplitude and frequency of oscillation are shown in **Figure 4.33(b)** and **Figure 4.34(b)** respectively. The roundness of silicon particles at stationary and at 100,200,300 and 400Hz with 5 $\mu$ m amplitude are 33.66, 52.76, 60.39, 67.42 and 71.57% respectively. Similarly, the roundness of silicon particles at 100,200,300 and 400Hz with 10 $\mu$ m amplitude are 45.93,56.70,63.02 and 66.85% respectively and similarly for the roundness of silicon particles at 100,200,300 and 400Hz with 15 $\mu$ m amplitude are 42.52,50.79,55.08 and 61.36 respectively . It can be observed that in general the roundness of silicon particles increase with increase in frequency of oscillation and decrease with increase in amplitudes of oscillation.

The percentage increase in roundness of silicon particle(modified) for oscillated test specimens when compared to stationary cast specimen are 142.47 % at 400Hz ,112.22%

at 300Hz ,64.03% at 200Hz and 33.28% at 100Hz frequencies of oscillation with 5 $\mu$ m amplitude .Similarly, the increase is 95.63 % at 400Hz ,81.06 % at 300Hz ,39.62% at 200Hz and 17.37 % at 100Hz frequencies of oscillation with 10 $\mu$ m amplitude and 83.95 % at 400Hz ,72.57 % at 300Hz ,72.57% at 200Hz and 8.23 % at 100Hz frequencies of oscillation with 15 $\mu$ m amplitude. It can be observed from the **Figure 4.35(b)** that in general the percentage increase in roundness increases with increase in frequency of oscillation and decreases with increase in amplitudes of oscillation.

#### **4.8 The Average Area of Silicon Particles**

##### **1) A319 Aluminum alloy Casting**

The average area of silicon particles of castings are improved due to mold oscillation during the solidification and varies for oscillated test specimens when compared to stationary cast specimens. Variation of the average area of silicon particle with respect to amplitude and frequency of oscillation are shown in **Figure 4.36(a)** and **Figure 4.37(a)** respectively. The average area of silicon particles at stationary and at 100,200,300,400Hz with 5 $\mu$ m amplitude are 182.787, 92.959, 69.99, 50.618 and 23.278 $\mu$ m<sup>2</sup> respectively. Similarly, the average area of silicon particles at stationary and at 100,200,300,400Hz with 10 $\mu$ m amplitude 182.787,141.855,110.922,77.02, and 40.151  $\mu$ m<sup>2</sup> respectively and similarly for the average area of silicon particles at stationary and at 100,200,300,400Hz with 15 $\mu$ m amplitude are 182.787,177.638,128.647,112.987 and 53.899  $\mu$ m<sup>2</sup> respectively . It can be observed that in general the ductility of casting decrease with increase in frequency of oscillation and increase with increase in amplitudes of oscillation during the solidification.

The percentage decrease in area of silicon particle(modified) for oscillated test specimens when compared to stationary cast specimens are 85.87 % at 400Hz ,82.40% at 300Hz

,70.75% at 200Hz and 64.42% at 100Hz frequencies of oscillation with 5 $\mu$ m amplitude .Similarly, 78.71 % at 400Hz ,68.72 % at 300Hz ,61.26% at 200Hz and 40.77 % at 100Hz frequencies of oscillation with 10 $\mu$ m amplitude and 69.26 % at 400Hz ,52.93 % at 300Hz ,44.99% at 200Hz and 32.48 % at 100Hz frequencies of oscillation with 15 $\mu$ m amplitude. It can be observed from the **Figure 4.38 (a)** that in general the area of silicon particle(modified) decreases with increase in frequency of oscillation and increases with increase in amplitudes of oscillation.

## 2) A356 Aluminum alloy Casting

The average area of silicon particles of castings are improved due to mold oscillation during the solidification and varies for oscillated test specimens when compared to stationary cast specimen. Variation of the average area of silicon particle with respect to amplitude and frequency of oscillation are shown in **Figure 4.36(b)** and **Figure 4.37(b)** respectively. The average area of silicon particles at stationary and at 100,200,300 and 400Hz with 5 $\mu$ m amplitude are 1318.47, 469.07, 385.61, 231.98 and 186.18 $\mu$ m<sup>2</sup> respectively. Similarly, the average area of silicon particles at stationary and at 100,200,300 and 400Hz with 10 $\mu$ m amplitude 1318.47, 780.85, 510.68, 412.41, and 280.7  $\mu$ m<sup>2</sup> respectively and similarly for the average area of silicon particles at stationary and at 100,200,300 and 400Hz with 15 $\mu$ m amplitude are 1318.47, 890.2, 725.18, 620.5 and 405.23  $\mu$ m<sup>2</sup> respectively. It can be observed that in general the average area of silicon particles of casting decrease with increase in frequency of oscillation and increase with increase in amplitudes of oscillation during the solidification.

The percentage decrease in area of silicon particle(modified) for oscillated test specimens when compared to stationary cast specimens are 87.26 % at 400Hz ,72.30% at 300Hz ,61.70% at 200Hz and 49.15% at 100Hz frequencies of oscillation with 5 $\mu$ m amplitude .Similarly, 78.04 % at 400Hz ,57.86% at 300Hz ,39.31% at 200Hz and 22.39% at 100Hz

frequencies of oscillation with 10 $\mu$ m amplitude and 70.51 at 400Hz ,38.18 % at 300Hz ,29.61% at 200Hz and 2.80 % at 100Hz frequencies of oscillation with 15 $\mu$ m amplitude. It can be observed from the **Figure 4.38 (b)** that in general the area of silicon particle(modified) decreases with increase in frequency of oscillation and increases with increase in amplitudes of oscillation.

## 2.9 The Average Grain Size

### 1) A319 Aluminum alloy Casting

The average grain size of  $\alpha$ -Al of castings are improved due to mold oscillation during the solidification and varies for oscillated test specimens when compared to stationary casted specimen. Variation of the grain size with respect to amplitude and frequency of oscillation are shown in **Figure 4.27(a)** and **Figure 4.28(a)** respectively. The average grain size of  $\alpha$ -Al at stationary and at 100,200,300 and 400Hz with 5 $\mu$ m amplitude are 55.85, 48.24, 40.72, 36.84 and 28.54 $\mu$ m respectively. Similarly, the grain size at stationary and at 100,200,300 and 400Hz with 10 $\mu$ m amplitude are 55.85, 52.35, 49.8, 42.48 and 37.52 $\mu$ m respectively and similarly for the average grain size of  $\alpha$ -Al at stationary and at 100,200,300 and 400Hz with 15 $\mu$ m amplitude are 55.85, 54.5, 50.85, 48.74 and 40.92 respectively. It can be observed that in general the average grain size of casting decreases with increase in frequency of oscillation and increase with increase in amplitudes of oscillation during the solidification.

The percentage decrease in grain size for oscillated test specimens when compared to stationary cast specimens are 48.89 % at 400Hz ,34.03% at 300Hz ,27.09% at 200Hz and 13.62% at 100Hz frequencies of oscillation with 5 $\mu$ m amplitude .Similarly, 32.82 % at 400Hz ,23.93 % at 300Hz ,10.83% at 200Hz and 6.2 % at 100Hz frequencies of oscillation with 10 $\mu$ m amplitude and 26.73 % at 400Hz ,12.73 % at 300Hz ,8.9% at 200Hz and 2.4 % at 100Hz frequencies of oscillation with 15 $\mu$ m amplitude. It can be

observed from the **Figure 4.29(a)** that in general the grain size decreases with increase in frequency of oscillation and increases with increase in amplitudes of oscillation.

## 2) A356 Aluminum alloy Casting

The average grain size of  $\alpha$ -Al of castings is improved due mold oscillation during the solidification and varies for oscillated test specimens when compared to stationary casted specimen. Variation of the grain size with respect to amplitude and frequency of oscillation are shown in **Figure 4.27(b)** and **Figure 4.28(b)** respectively. The average grain size of  $\alpha$ -Al at stationary and at 100,200,300 and 400Hz with 5 $\mu$ m amplitude are 49.19, 42.79, 36.15, 29.53 and 20.53 $\mu$ m respectively. Similarly, the micro-hardness at stationary and at 100,200,300 and 400Hz with 10 $\mu$ m amplitude are 49.19, 44.82, 41.6 34.72 and 24.4 $\mu$ m respectively and similarly for the average grain size of  $\alpha$ -Al at stationary and at 100,200,300 and 400Hz with 15 $\mu$ m amplitude are 49.19, 46.95, 43.58, 38.5 and 28.7 $\mu$ m respectively . It can be observed that in general the average grain size casting decreases with increase in frequency of oscillation and increase with increase in amplitudes of oscillation during the solidification.

The percentage decrease in grain size for oscillated test specimens when compared to stationary cast specimens are 58.26 % at 400Hz ,39.96% at 300Hz ,26.50% at 200Hz and 13.01% at 100Hz frequencies of oscillation with 5 $\mu$ m amplitude .Similarly, 50.39 % at 400Hz ,29.45 % at 300Hz ,15.43% at 200Hz and 8.88 % at 100Hz frequencies of oscillation with 10 $\mu$ m amplitude and 41.65 % at 400Hz ,21.73 % at 300Hz ,10.65% at 200Hz and 4.53 % at 100Hz frequencies of oscillation with 15 $\mu$ m amplitude. It can be observed from the **Figure 4.29(b)** that in general the percentage decrease in grain size increases with increase in frequency of oscillation and decrease with increase in amplitudes of oscillation.

## 4.10 Dendrite Arm Spacing

### 1) A319 Aluminum alloy Casting

The dendrite arm spacing of A319 of castings are improved due mold oscillation during the solidification and varies for oscillated test specimens when compared to stationary cast specimens. Variation of the dendrite arm spacing with respect to amplitude and frequency of oscillation are shown in **Figure 4.30 (a)** and **Figure 4.31 (a)** respectively. The dendrite arm spacing at stationary and at 100,200,300 and 400Hz with 5 $\mu$ m amplitude are 39.65, 22.15, 19.47, 15.82 and 13.94 $\mu$ m respectively. Similarly, the dendrite arm spacing at 100,200,300 and 400Hz with 10 $\mu$ m amplitude are 20.26, 18.47, 26.47 and 30.23 $\mu$ m respectively and similarly for the dendrite arm spacing of  $\alpha$ -Al at 100,200,300 and 400Hz with 15 $\mu$ m amplitude are 26.09, 20.49, 31.59 and 34.02 $\mu$ m respectively. It can be observed that in general the dendrite arm spacing of casting decreases with increase in frequency of oscillation and increase with increase in amplitudes of oscillation during the solidification.

The percentage decrease in dendrite arm spacing for oscillated test specimens when compared to stationary cast specimens are 64.84 % at 400Hz ,60.10% at 300Hz ,50.89% at 200Hz and 44.13% at 100Hz frequencies of oscillation with 5 $\mu$ m amplitude .Similarly, 23.75 % at 400Hz ,33.24 % at 300Hz ,53.41% at 200Hz and 48.90 % at 100Hz frequencies of oscillation with 10 $\mu$ m amplitude and 14.19 % at 400Hz ,20.32% at 300Hz ,48.32% at 200Hz and 34.19 % at 100Hz frequencies of oscillation with 15 $\mu$ m amplitude. It can be observed from the **Figure 4.32(a)** that in general the percentage decrease in dendrite arm spacing increases with increase in frequency of oscillation and decrease with increase in amplitudes of oscillation.

## 2) A356 Aluminum alloy Casting

The dendrite arm spacing A356 casting are improved due mold oscillation during the solidification and varies for oscillated test specimens when compared to stationary cast specimens. Variation of the dendrite arm spacing with respect to amplitude and frequency of oscillation are shown in **Figure 4.30 (b)** and **Figure 4.31 (b)** respectively. The average grain size of  $\alpha$ -Al at stationary and at 100,200,300 and 400Hz with 5 $\mu$ m amplitude are 45.76, 37.88, 29.47, 22.42 and 17.76 $\mu$ m respectively. Similarly, the dendrite arm spacing at 100,200,300 and 400Hz with 10 $\mu$ m amplitude are 26.68, 23.47, 26.77 and 28.2 $\mu$ m respectively and similarly for the dendrite arm spacing of  $\alpha$ -Al at, 100,200,300 and 400Hz with 15 $\mu$ m amplitude are 25.21, 22.86, 29.43 and 36.54 $\mu$ m respectively. It can be observed that in general the dendrite arm spacing casting decreases with increase in frequency of oscillation and increase with increase in amplitudes of oscillation during the solidification.

The percentage decrease in dendrite arm spacing for oscillated test specimens when compared to stationary cast specimens are 60.75 % at 400Hz ,51.00% at 300Hz ,35.59% at 200Hz and 17.22 % at 100Hz frequencies of oscillation with 5 $\mu$ m amplitude .Similarly, 38.37 % at 400Hz ,41.49 % at 300Hz ,48.71% at 200Hz and 41.69 % at 100Hz frequencies of oscillation with 10 $\mu$ m amplitude and 20.14 % at 400Hz ,36.68% at 300Hz ,39.12% at 200Hz and 38.35 % at 100Hz frequencies of oscillation with 15 $\mu$ m amplitude. It can be observed from the **Figure 4.32(b)** that in general the percentage decrease in dendrite arm spacing increases with increase in frequency of oscillation and decrease with increase in amplitudes of oscillation.

## 4.11 (%) Porosity

### 1) A319 Aluminum alloy Casting

The % Porosity of A319 of castings are improved due mold oscillation during the solidification and varies for oscillated test specimens when compared to stationary cast specimens. Variation of the dendrite arm spacing with respect to amplitude and frequency of oscillation are shown in **Figure 4.42 (a)** and **Figure 4.43 (a)** respectively. The % Porosity at stationary and at 100,200,300 and 400Hz with 5 $\mu$ m amplitude are 8.31, 5.76, 4.01, 3.10 and 1.01% respectively. Similarly, the % Porosity at 100,200,300 and 400Hz with 10 $\mu$ m amplitude are 3.18, 3.03, 5.13 and 6.25% respectively and similarly for the % Porosity of  $\alpha$ -Al at 100,200,300 and 400Hz with 15 $\mu$ m amplitude is 7.5, 6.18, 7.01 and 7.90% respectively. It can be observed that in general the % Porosity of casting decreases with increase in frequency of oscillation and increase with increase in amplitudes of oscillation during the solidification.

### 2) A356 Aluminum alloy Casting

The % Porosity of A319 of castings are improved due mold oscillation during the solidification and varies for oscillated test specimens when compared to stationary cast specimens. Variation of the dendrite arm spacing with respect to amplitude and frequency of oscillation are shown in **Figure 4.42 (b)** and **Figure 4.43 (b)** respectively. The % Porosity at stationary and at 100,200,300 and 400Hz with 5 $\mu$ m amplitude are 7.72, 6.30, 5, 4.13 and 2.75% respectively. Similarly, the % Porosity at 100,200,300 and 400Hz with 10 $\mu$ m amplitude is 6.73, 5.97, 7.17 and 7.75% respectively and similarly for the % Porosity of  $\alpha$ -Al at 100,200,300 and 400Hz with 15 $\mu$ m amplitude are 7.06, 6.74, 10.07 and 10.94% respectively. It can be observed that in general the % Porosity of casting decreases with increase in frequency of oscillation and increase with increase in amplitudes of oscillation during the solidification.

**GUO Hong-min, et al. [46]** investigated combined effects of vibration and grain refiner on the microstructure of semisolid slurry of hypoeutectic Al-Si alloy. They found that the primary  $\alpha$ -(Al) particles become finer and rounder with the increase of vibration frequencies. Intense convection can be produced in the melt by vibration during the solidification. Non-dendrite primary  $\alpha$ (Al) crystals become finer and rounder with the increase of vibration frequency. From combined effect vibration and grain refiner on the slurry can be prepared with EPD (equivalent particle diameter) of primary  $\alpha$ -(Al) about 90  $\mu\text{m}$  and ASC (average shape coefficient) above 0.5 under the vibration of 20 Hz.

**S. Wu et al. [48]** developed a method of introducing mechanical vibration during the isothermal holding period of hypo eutectic A356 alloy to prepare the semi-solid slurry and study the development of non-dendritic microstructure under the condition described above. The above method used mechanical vibration to agitate the melt this hold at a temperature below its liquidus in a crucible. Formation of the nucleation and development of a non-dendritic microstructure occurred within the semi-solid slurry due to melting convection by mechanical vibration together with under cooling of melts.

**C. Limmaneevichitr et al., [51]** studied about the metallurgical structure of A356 aluminum alloy solidified under mechanical vibration and suggested that formation of dendrite in the liquid alloy were consequently disturbed and fragmented by the mechanical vibration. This effect was enhanced when the vibration was introduced within an alloy with a larger solid part, as was observed with solidification at lower pouring temperatures. It was revealed that the introduction of mechanical vibration into the A356 melt with sufficient solid fraction before complete solidification successfully resulted in an as-cast structure emphasizing semi-solid morphology.

**N. Abu-Dheir et al. [57]** studied about the silicon morphology modification in the eutectic Al–Si alloy under mechanical mold vibration. The microstructure responsible is where the lamellar spacing tends to reduce and silicon morphology becomes fibrous with the increasing of the vibration amplitude as compared to gravity casting. However, it is also reported that by exceeding a critical value of vibration amplitude, the silicon tends to coarsen.

**S. Guo et al. [67]** observed the microstructural refinement of DC cast AZ80 Mg billets by low frequency electromagnetic vibration and the experimental results show that the grains have been greatly refined by applying electromagnetic vibration. The grains over the cross section of the billet tend to become homogenous under certain electromagnetic vibration conditions.

**W. Wang et al.[77]** investigated about the crystal nucleation and detachment from a chilling metal surface with vibration. They found that the exerting vibration to a chilling solid surface is an effective way to produce lots of nuclei for forming equiaxed grains microstructure by preventing the solidifying shell. Vibration during the solidification also helped to form and promote dendrites to break off and shower down not only from the free liquid surface along with from the chilling solid surface. To obtain finer equiaxed grains, it is necessary to increase synchronously vibration frequency as well as amplitude..

**Piwwonka T S [88]** reported the vibration is the primary reason during solidification a zone of low-melting liquid exists instantly adjacent to the main crystal growth. Nucleation can occur, and fragmented by vibration, banding results. This method further states that growth takes place from these new nuclei in such a way as to form a sandwich of liquid metal surrounded by solid metal, which is isolated from the liquid bath at the bore .

**P.A.O. Adegbuyi et al.[84]** recommended the each composition of Aluminum-Copper alloy's grain refinements that led to improved properties by mold vibration at different frequencies during solidification (Casting).Vibration enhances the number of grains produced, i.e., fine grain structure.

**Jiang, W., et al. [91]** found that the mechanical vibration significantly increased the mechanical properties and density of A356.The mechanical vibration has also significantly improved metallurgical properties such as the size, morphology, dispersion of  $\alpha$ -Al phase, eutectic silicon particles, and SDAS. They also found that with increasing vibration frequency, the grain size and SDAS continuously reduced, and the shape factor gradually improved with the increase of vibration frequency.

**Radjai et al. [87]** examined the impact of vibration on the refinement of Al - 17 wt.% Si and concluded that electromagnetic vibration caused a cavitation effect that broke the primary silicon particles into smaller pieces.

**Kumar, R., et al. [95]** were studied the impact of mold vibration during solidification of Al-Cu alloys and understand the change of metallurgical and mechanical properties of casting. The molten metal was poured into a graphite mold, and frequencies varied from 40 to 150 Hz. A casting was also made in un-vibrated condition to compare the results of castings with vibration. The experimental results showed notable grain refinement and increase in hardness of castings with mold vibration.They were consistent with the measured grain size, where the maximum strength and elongation correspond to the lowest grain size obtained under used vibration acceleration.

**Mizutani, Y., et al. [96]** in their study used the electromagnetic vibrations and temperature gradient to grain refinement of pure aluminum (99.7 mass%).The pure aluminum melt has been solidified under electromagnetic vibrations with a frequency range from 150 to 500 Hz. The grain has become small with the increase of frequency. In

the case of the stationary prepared casting specimen, the average grain sizes of each cross-section are dispersing widely, and the total average grain size is about 700  $\mu\text{m}$ . On the other hand, the average grain size reduces continuously by the imposition of electromagnetic vibrations with low frequencies until 500 Hz, and scattering for each cross-section diminishes. Particularly, grains are most refined at the frequency of 500 Hz, and the average grain size is about 200  $\mu\text{m}$ .

**Guo, H. M., et al. [97]** found the mechanical vibration during the solidification of AZ31 magnesium alloy casting can significantly enhance mechanical properties such as strength and elongation. With increasing vibration acceleration from 2.5 to 19  $\text{m s}^2$ , the ultimate tensile strength increased from 152 to 213 MPa, the yield strength increased from 71 to 122 MPa, and the elongation increased from 4.8 to 11.5 percent.

**Chaturvedi, V., & Pandel, U. [98]** studied the influences of mechanical vibrations on the mechanical properties of AZ91 magnesium alloy. This was tested at constant frequency of 40Hz and varied amplitude from 0 to 2 mm. Increased amplitude of mechanical vibration during solidification causes refinement of the grain in the alloy. Tensile strength improved upto a certain point with increasing amplitude and start decreasing with further increment in the amplitude of vibrations. This refinement of the grains also results in an increased percentage of elongation and hardness of the alloy samples.

**Jiang, W., et al.[99]** investigated the effects of vibration frequency on microstructure, mechanical properties, and fracture behavior of the A356 aluminium alloy. Obtained results showed that mold vibration frequency of 100 Hz, the grain size and SDAS decreased by 32 and 19 %, respectively, and the shape factor increased by 262 %, and the average length, width, and aspect ratio of the silicon particles decreased by 45, 6, and 42 %, respectively, compared to that of the sample without vibration. Meanwhile, the

tensile strength, yield strength, elongation, and hardness of the A356 alloy sample were, respectively, 35, 42, 57, and 28 % higher than those of the sample without vibration. In addition, the mechanical vibration changed the fractograph of the A356 alloy from a clear brittle fracture nature of the alloy without vibration to an obvious dimple fracture nature, and with the increase of vibration frequency, the dimples were very deep and well distributed with a high density. In addition, the mechanical vibration changed the fractograph of the A356 alloy from a clear brittle fracture nature of the alloy without vibration to an obvious dimple fracture nature, and with the increase of vibration frequency, the dimples were very deep and well distributed with a high density.

**Jianbo Yu et. al [102]** examined the effect of electromagnetic vibration on the microstructure of eutectic Al-Si alloy. Solidification structure of eutectic Al-Si alloy. They found that the eutectic microstructure has been refined by solely imposing high magnetic field but coarsened under the electromagnetic vibration. Polyhedral Silicon grains and nondendritic  $\alpha$ -Al developed when the electromagnetic vibration intensity was very strong convection.

**Patel, V. R. [103]** suggested that eutectic silicon particles in eutectic aluminium-silicon alloys can be modified with the help of mechanical mold vibration during the solidification. With the help of mold vibration during the solidification pattern of the eutectic silicon particles tends to become more uniform. The tensile strength and impact strength of vibratory prepared casting are higher than that of stationary prepared casting. Mold vibration method also affects the morphology of eutectic Si-particle and refinement of  $\alpha$ -Al dendrites of eutectic Al-Si alloy.

**Anilkumar, T., et al. [104]** investigated the influence of vibration during the solidification on the mechanical properties of the Al-Si alloy castings. Grain structure gets reduced, when the alloy is subjected to vibration frequency varies from 0 to 12Hz .

#### **4.12 SEM-Photograph of Tensile Fracture Surface of A319 and A356 Aluminum Alloys Casting**

This article introduces the topic of fractography and the interpretation of fracture surfaces. Fractography is the science of revealing loading conditions that caused the fracture by a three dimensional interpretation of the appearance of a broken component. An understanding of how cracks nucleate and grow microscopically to cause bulk (macro-scale) fracture is an essential part of fractography.

Some general types of macro-scale and micro-scale fractographic features, which are described in more detail. In summary form, the following are key features in distinguishing between monotonic versus fatigue fracture and ductile versus brittle fractures (on either a macro-scale or micro-scale), Becker, W. T., & Lampman, S. (2002)[110]:

1. Monotonic versus fatigue fracture: Beach marks and striations indicate fatigue, but their absence does not confirm fracture from monotonic loads. Fracture surfaces from fatigue do not always reveal beach marks and fatigue striations.
2. Macro-scale ductile versus brittle fracture: Macro-scale ductile fracture is revealed by obvious changes in cross section of the fracture part and/or by shear lips on the fracture surface. Macro-scale brittle fractures have fracture surfaces that are perpendicular to the applied load without evidence of prior deformation. Macro-scale fracture surfaces can have a mixed-mode appearance (brittle-ductile or ductile-brittle). The brittle-ductile sequence is more common on the macro-scale, while the appearance of the ductile portion is typically micro-scale in a ductile-brittle sequence.

3. Micro-scale ductile versus brittle fracture: Micro-scale ductile fracture is uniquely characterized by dimpled fracture surfaces due to micro-void coalescence. Micro-scale brittle fractures are characterized by either cleavage (transgranular brittle fracture) or intergranular embrittlement.

#### 4.12.1 SEM-Photograph of Tensile Fracture Surface of A319

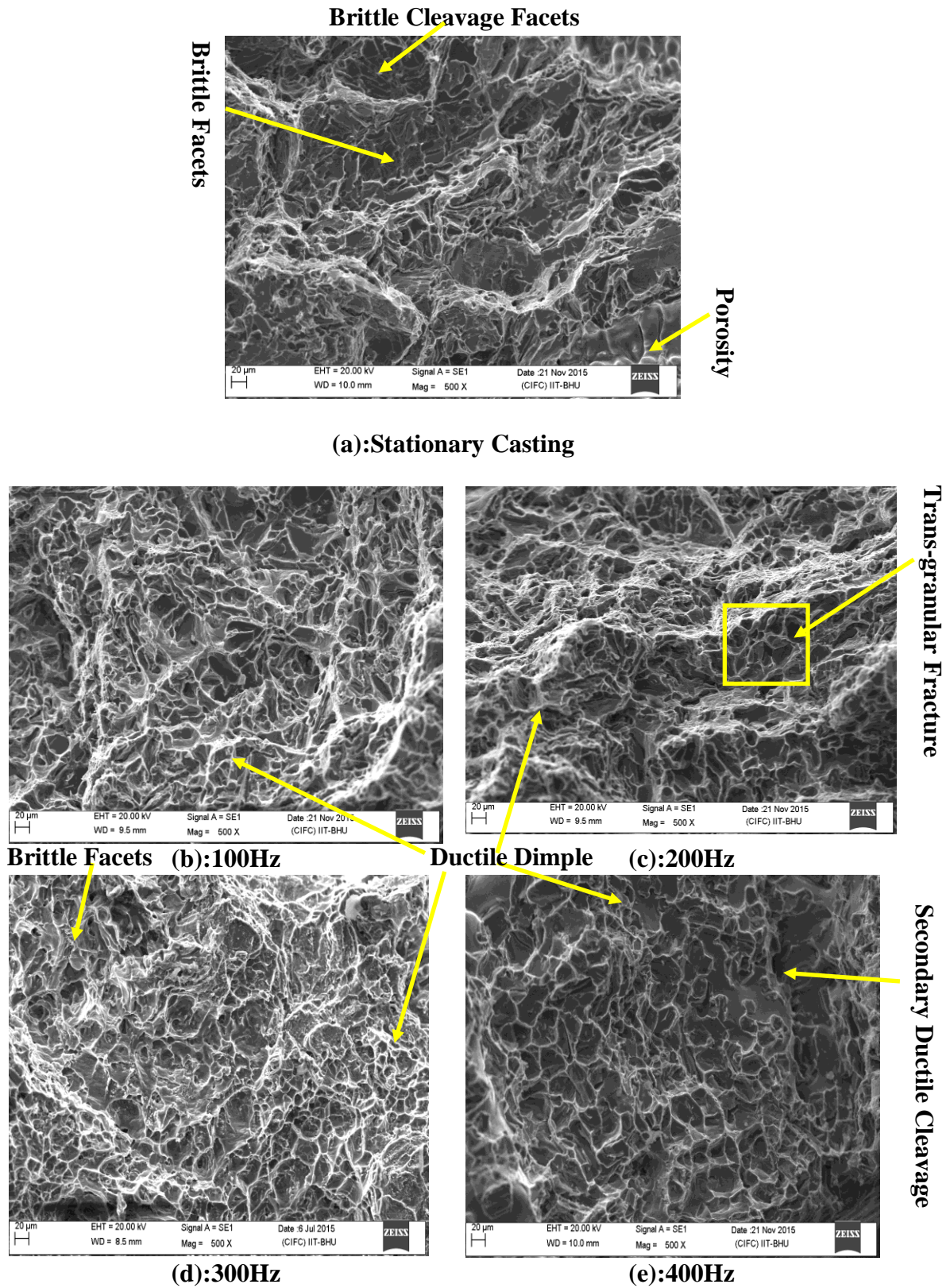


**Figure 4.43 SEM-photograph of tensile fracture surface of A319 order place with increase in frequency of mold oscillation (Constant Amplitude=5μm)**

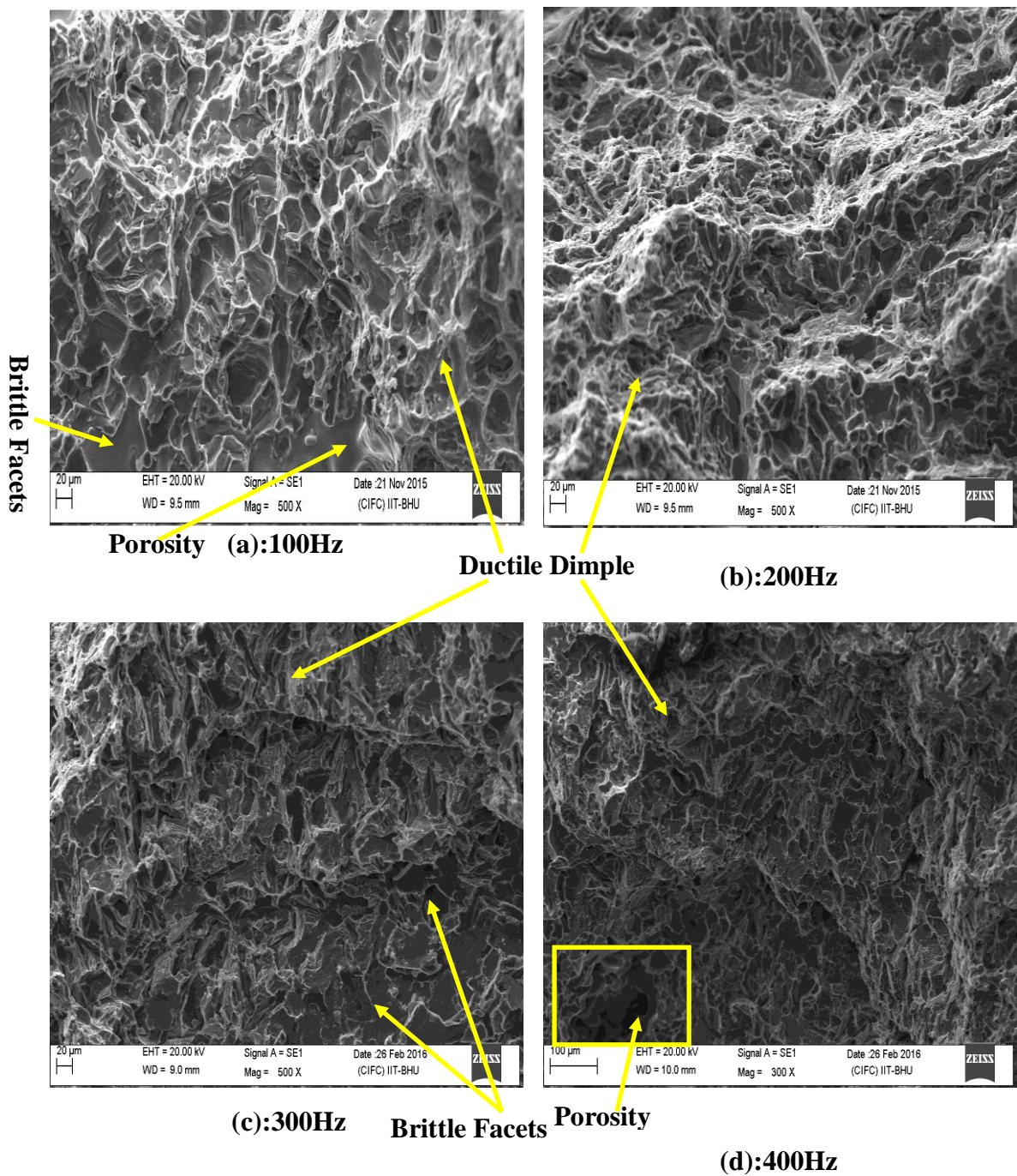
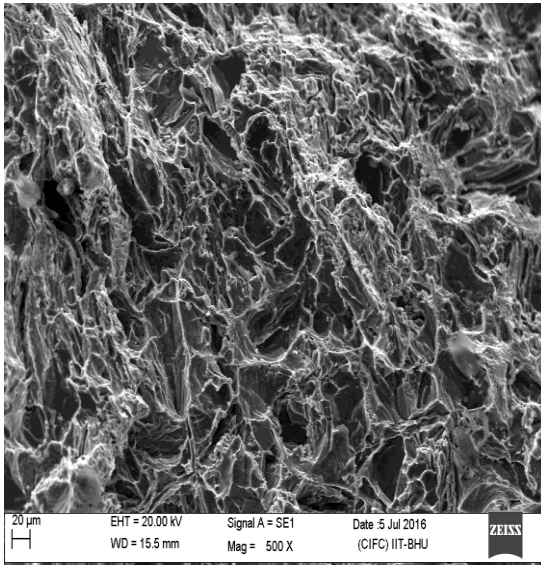
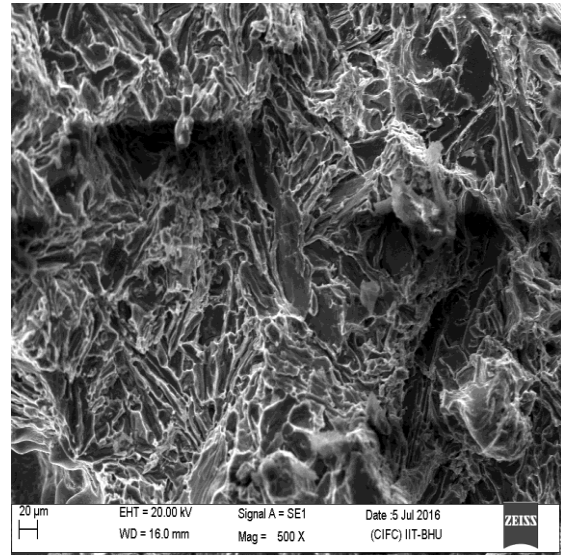


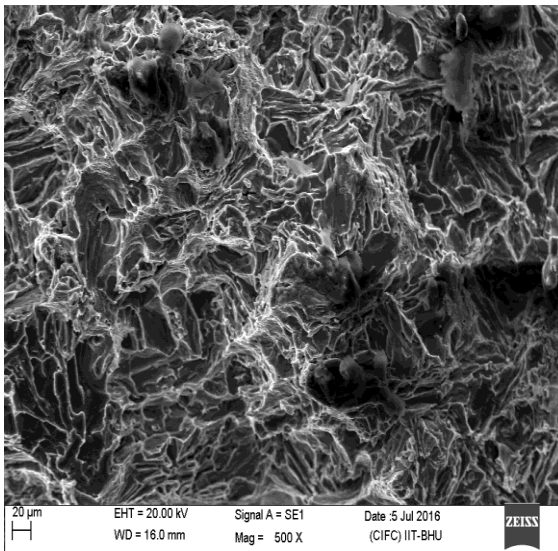
**Figure 4.44 SEM-photograph of tensile fracture surface of A319 order place with increase in frequency of mold oscillation(Constant Amplitude=10 $\mu$ m)**



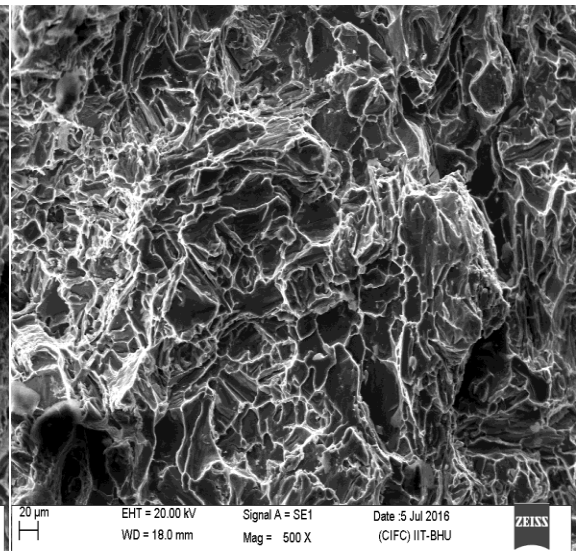
**(a):100Hz**



**(b):200Hz**



**(c):300Hz**



**(d):400Hz**

**Figure 4.45 SEM-photograph of tensile fracture surface of A319 order place with increase in frequency of mold oscillation(Constant Amplitude=15μm)**

4.12.2 SEM-Photograph of Tensile Fracture Surface of A356

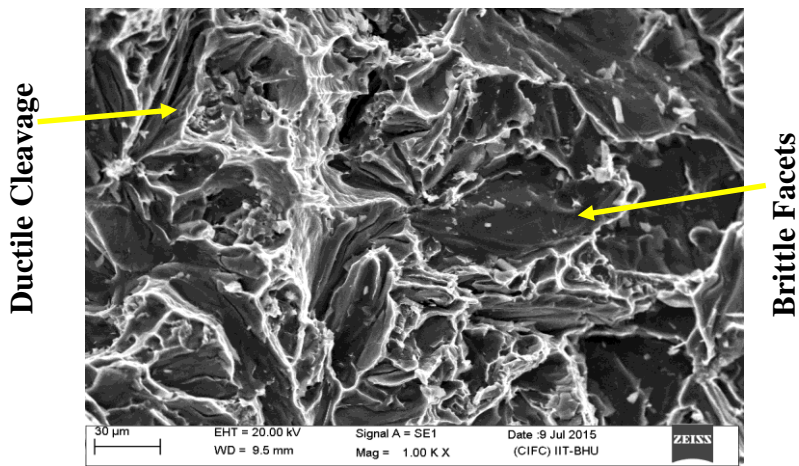
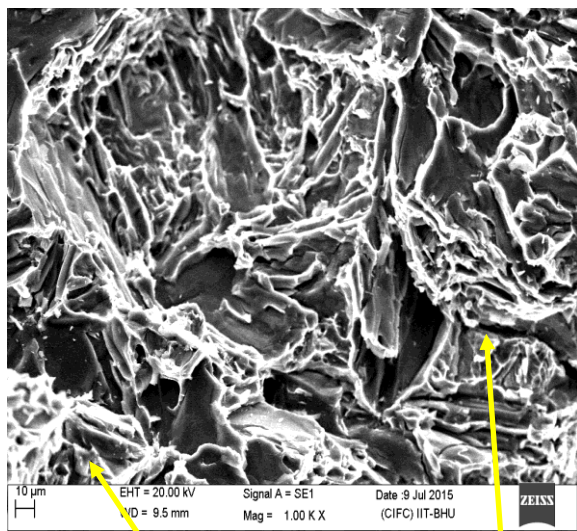
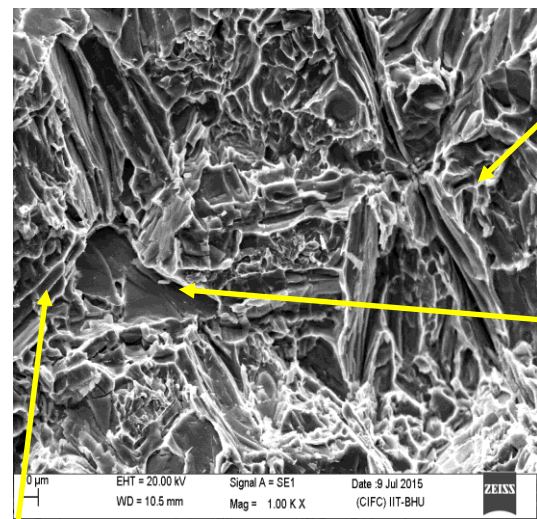


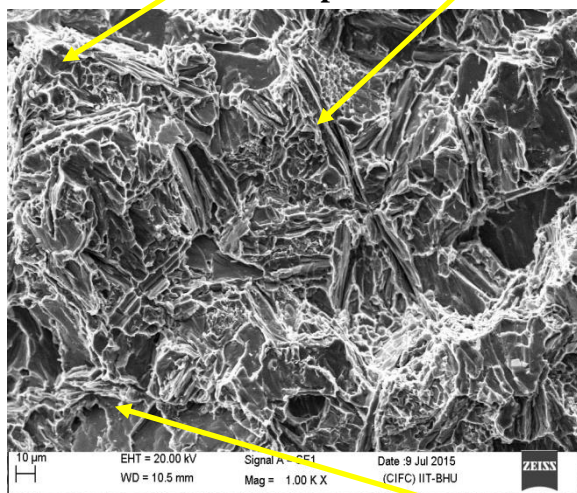
Figure (a): Stationary Casting



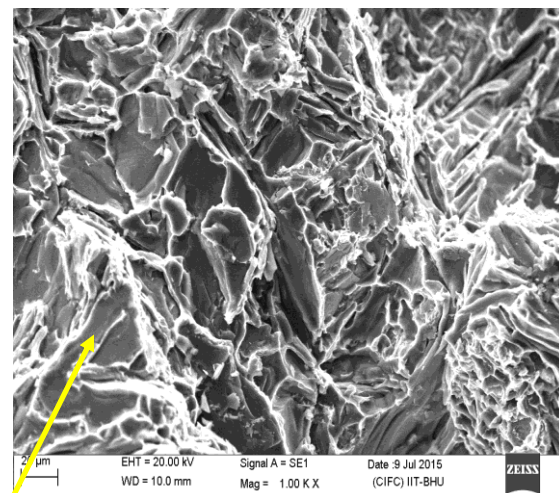
(b): 100Hz  
Ductile Dimple



(c): 200Hz

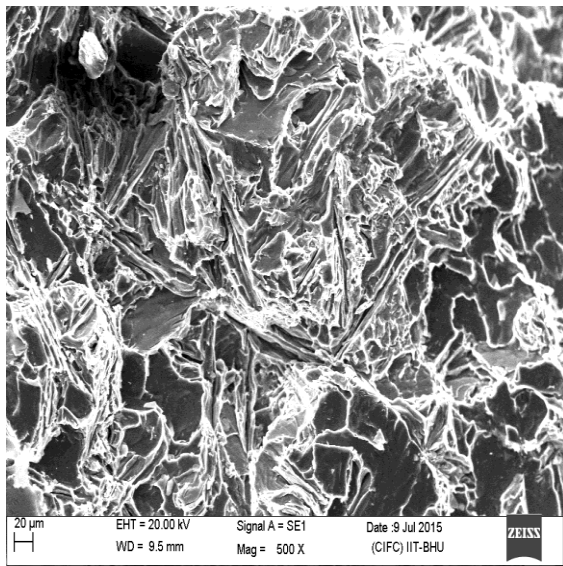


(d): 300Hz

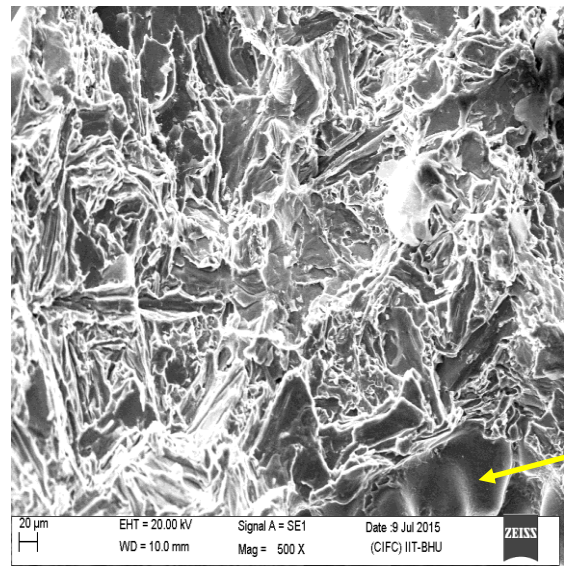


(e): 400Hz

Figure 4.46 SEM-Photograph of Tensile Fracture Surface of A356 order place with increase in Frequency of mold oscillation (Constant Amplitude=5μm)

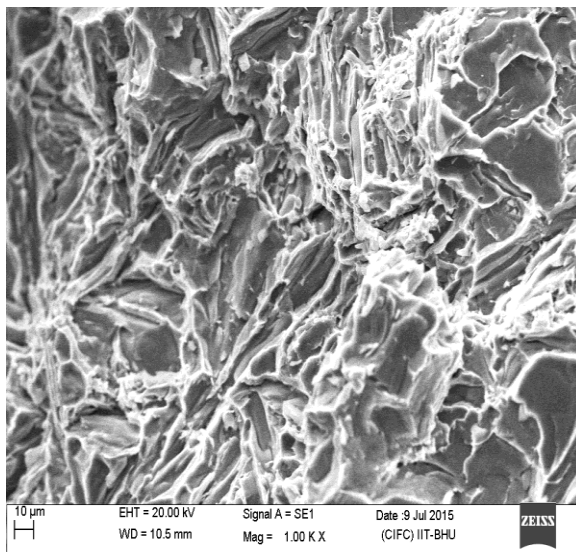


**(a):100Hz**

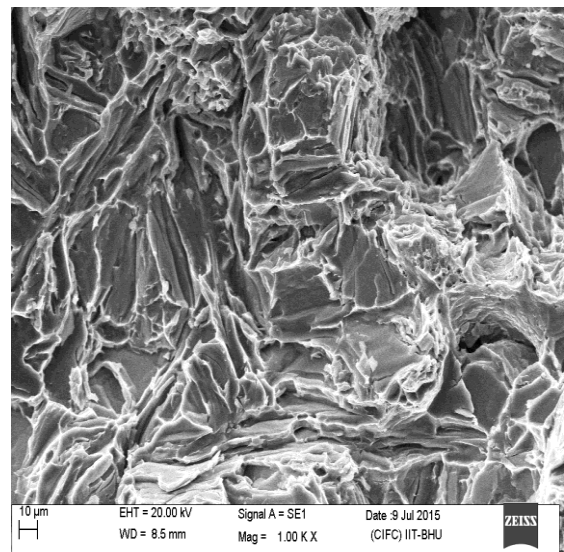


**(b):200Hz**

Porosity



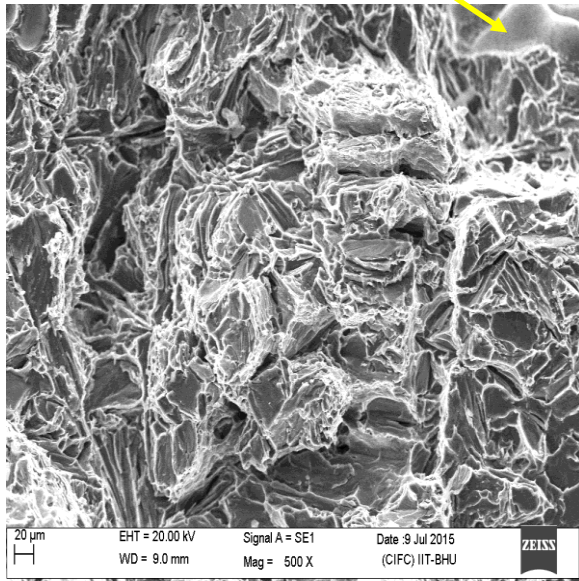
**(c):300Hz**



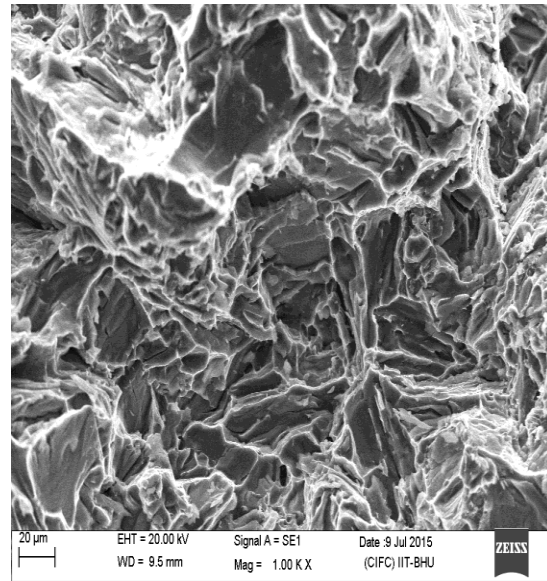
**(d):400Hz**

**Figure 4.47 SEM-Photograph of Tensile Fracture Surface of A356 order place with increase in Frequency of mold oscillation(Constant Amplitude=10µm)**

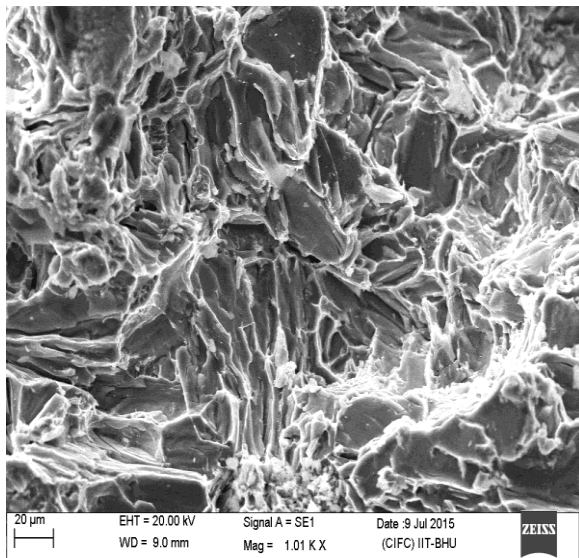
**Porosity**



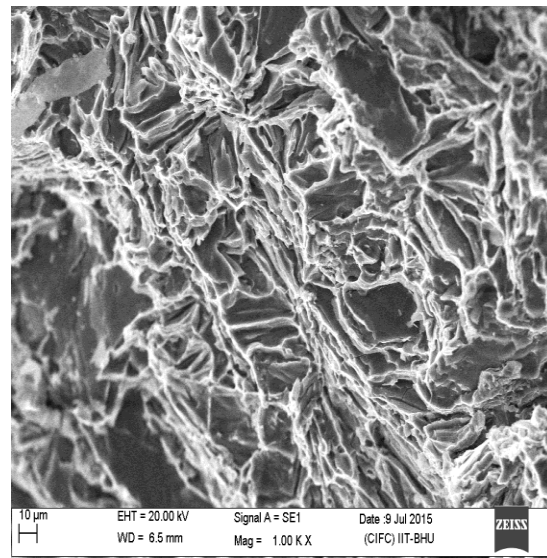
**(a):100Hz**



**(b):200Hz**



**(c):300Hz**



**(d):400Hz**

**Figure 4.48 SEM-Photograph of Tensile Fracture Surface of A356 order place with increase in Frequency of mold oscillation(Constant Amplitude=15μm)**

In this section of the chapter, I am trying to deal with various macroscopic aspects of tensile fracture. If fracture is associated with a failure case, it is necessary to identify its mode before the cause of failure can be determined. By fracture mode is meant the mechanism of crack propagation eventually leading to fracture. In principle, it is possible

to identify fracture mode from the microscopic appearance or morphology of resulting fracture surface. This is referred to as fractography. It is recalled that engineering products are never perfect; they unavoidably contain some of the cracks, defects or discontinuities eliminated or reduced by different fabrication methods.

#### **4.12.3 Evaluation of Tensile Fracture Surface (SEM Image) of A319**

The images of fracture surfaces of A319 aluminum alloy are shown in the Figure 4.44 to Figure 4.46 and SEM images of fractography obtained from the stationary and oscillatory modified castings are shown in **Figure 4.44 (a-e)** ordered in frequency range 0 to 400Hz of 5 $\mu$ m. Similarly **Figure 4.45(a-d)** and **Figure 4.46(a-d)** are also ordered in increasing frequency range 100 to 400Hz of 10 $\mu$ m and 15 $\mu$ m respectively. The positive effect of the mold oscillation during solidification was observed in both the microstructure and on the mechanical properties of the modified oscillatory casting. SEM image of the fracture surfaces are granular and shiny for primary and secondary cleavage. The secondary cleavage appear due to primary crack may be intercepted by an obstacle within the grain and secondary crack cleavage path shifted significantly. Fracture surfaces have mostly dimple and only few portion also have facets in oscillatory casted sample. Because of most portion of fracture surface have dimple, it is called ductile failure. This is possible only when fine grain size and fine dispersion of second phase particles within the material are achieved.

The SEM image of tensile fractured surface of A319 aluminium alloy casting obtained with different mold oscillation frequencies in order to demonstrate a substantial micro-fractographical difference in the size and morphology of formed surfaces after tensile test of specimens. The size and shape of the second phase silicon particles governs the nucleation and growth of crack in this type of alloys. SEM Images of Tensile Fractured Surfaces A319 Alloy in different conditions by the size, shape and distribution of silicon

particles have been investigated. Fine and spheroidised phases are known to contribute more to increased strength and ductility than the acicular and irregular shape particles. The size and shape of the second phase silicon particles Al governs the nucleation and growth of crack in this type of alloys. Small and homogeneously rounded evenly distributed eutectic silicon particles results in high ductility.

#### **4.12.4 Evaluation of Tensile Fracture Surface (SEM Image) of A356**

The images of fracture surfaces of A356 aluminum alloy are shown in the Figure 4.47 to Figure 4.49 and SEM images of fractography obtained from the stationary and oscillatory modified castings are shown in **Figure 4.47 (a-e)** ordered in frequency range 0 to 400Hz of  $5\mu\text{m}$ . Similarly **Figure 4.48(a-d)** and **Figure 4.49(a-d)** are also ordered in increasing frequency range 100 to 400Hz of  $10\mu\text{m}$  and  $15\mu\text{m}$  respectively. The SEM photographs of tensile fractured surface of A356 aluminum alloy casting achieved with different mold oscillation frequencies in order to show a significant micro-fractographical difference in the size and morphology of formed surfaces after tensile test of specimens. In the SEM image obtained from the stationary cast sample, it is clear that the mostly facets like areas are observed and rest area have ductile dimple and secondary cleavage show a non-uniform distribution.

The fracture surfaces of the A356 aluminum alloy obtained from the stationary and vibratory casting presented a clear, brittle fracture nature as a transgranular fracture mode due to its coarse microstructure in the stationary prepared cast samples. Whereas fractography of the A356 aluminum alloy casting solidified under vibratory conditions exhibited the distinct morphologies of the dimple fracture as an intergranular fracture mode because of a significant improvement in the microstructure. Fractography consists of dimples as well as flat surface which is evidence that the tensile specimen failed in a quasi-cleavage

These figures also reveal well faceted brittle appearance of silicon particles and black rounded areas, from which the hard second phase silicon particles seem to have been pulled out during the tensile loading. In all the cases it reveals a mixed mode of fracture consisting of fine dimples and intergranular decohesion fracture surfaces. Small dimples indicate that some plastic deformation has taken place prior to fracture. Cleavage formation may be attributed to the presence of hard and brittle  $Mg_2Si$  and  $NiSi_2$  in the case of A356 aluminium alloy casting.

With the application of mechanical vibration during the solidification, by increasing frequency of up to 400 Hz, the eutectic silicon particles clearly show a tiny rod and granular structure, and the coarse plate-like silicon particles have vanished and the sizes of eutectic silicon particles are finer than those of the sample without vibration

The microstructure of oscillatory castings of the alloy where high degree of refining of dendrite cells and eutectic silicon are seen. Other things being equal, the resistance to crack growth will be maximum in this type of microstructure and density of ductile dimple with secondary cleavage. The fracture surfaces appear granular, shiny, cleavage and Secondary cleavage clearly visible in SEM images. Elongated dimples, cleavage and secondary cleavage more than clearly visible due to dislocation pile up on oscillatory casting than stationary casting fracture surface. It favors to yield strength of oscillatory casting more than stationary casting. This is possible only when fine grain size and fine dispersion of second phase particles within the material are achieved.

**Das, P., et al. [106]** in their study found that structural defects, such as shrinkage porosity act as fracture initiation sites. After initiation, the crack progresses by breaking the eutectic Si particles. The fractured eutectic Si particles are capable of the formation of facets on the tensile specimen fracture surface of the rheocast A356 alloy. During the examination of the fractograph, the appearance of dimples in the fractograph implies the

void initiation at globular eutectic Si particles. The acicular shaped eutectic Si particles are responsible for facets. Grain refiner addition not only to reduce the grain size and improve the degree of sphericity of primary phase but also sets void initiation and growth as the dominant mechanism for fracture, as observed from the fracture surface. Whereas, mixed mode fracture has been observed in case of rheocast samples.

**Islam, S. T., et al. [107]** investigated the morphology of tensile fracture surface of A356 rheocasting. SEM image of low superheat casting implies quasi-cleavage fracture, as evident from the facets present in the fractograph. While rheocast using 45° slope shows mixed mode fracture behaviour. Dimples present in the fractograph originate due to the fracture of ductile primary Al phase, whereas fracture of eutectic Si particles causes facets.

**Zhang, G. H., et al. [108]** studied the nature of tensile fracture in heavily alloyed Al-Si piston alloy and found the overall fracture morphology at first sight was similar to that in Al alloys. The fracture surface was perpendicular to the tensile axis. There were a bunch of tiny black spots, which might be identified with difficulty at low magnification. These small spots sparkled when analysed by the unaided eye. From aforementioned information, we can conclude that these spots were small planes which could reflect light. At a slightly high magnification, a large proportion of the fracture surface exposed a brittle mode with a very large number of smooth planar facets. In these flat areas, the Si platelet might be torn off from the Al matrix, leaving a terrace with a smooth facet. These facets were more probably formed as a result of fracture of brittle Si phase crystals. On the other hand, some broken intermetallics might be found in this micrograph represented characteristics of the broken intermetallics. Severe breakup occurred at these intermetallics, which showed a flower-like morphology with no obvious cleavage facets. This means that the stress field of the main crack broke up the intermetallics because of

their poor deformation properties. That is to say, the crack propagated by the fracturing of the intermetallic itself, not by destroying the boundaries among the intermetallic particles and the Al–Si eutectic.

**Kumar, S., & Tewari, S. P. [109]** Observed the Tensile fracture surfaces by Scanning Electron Microscope (SEM) to identify the type of fracture of A356 aluminum alloy in different casting conditions. Photograph of tensile fracture surface under different frequencies of vibration of mold (melt treatment) during solidification of casting and post heat treatment. The SEM images of the tensile fracture surface of as cast under stationary condition exposes faceted, brittle appearance of silicon particle and black area form where hard second phase particle seem to have been pulled out during tensile loading. Fine dimples and intergranular decohesion fracture surfaces are also visible. This shows the mixed mode of fracture. Cleavage formation may be attributed to the presence of acicular silicon needles and hard and brittle  $Mg_2Si$  phase. The SEM images of the tensile- fractured surface of oscillated and heat treated alloy reveals cleavage fracture along with fine dimples. The smooth, shiny area and dimples patterns indicate a tendency near to ductile rupture. In the heat treated SEM images of tensile- fracture surface of stationary as cast as well as oscillated mostly reveals fine dimples than as cast and melt treated (oscillated) with few cleaves facets. This indicates that good plastic deformation has taken place prior to fracture i.e. ability of matrix to deform plastically has increased.

**Jiang, W., et al.[99]** investigated the influences of vibration frequency on microstructure, mechanical and fracture behavior of the A356 aluminum alloy. Received results revealed that mold vibration frequency of 100 Hz, the grain size, and secondary dendrite arms spacing (SDAS) reduced by 32 and 19 %, respectively compared to stationary casting. The morphological properties of Si particles such as aspect ratio, width, and the average length of the silicon particles decreased by 42, 6, and 45 %, respectively.

respectively. Shape factor increased by 262 % compared to that stationary prepared casting sample. Meanwhile, the yield strength, tensile strength, elongation, and hardness of the A356 alloy sample were, respectively 42, 35, 57, and 28 % higher than those of the sample without vibration. In addition, the mechanical vibration changed the fractograph of the A356 alloy from a clear brittle fracture nature of the alloy without vibration to an obvious dimple fracture nature, and with the increase of vibration frequency, the dimples were very deep and well distributed with a high density.

**Ouellet, P., & Samuel, F. H. [110]** examined the effect of Mg on the ageing behaviour of Al-Si-Cu 319 type aluminium casting alloys and found the fracture of intermetallic phases in the interdendritic regions is mostly brittle, with the formation of micro cracks at the Si, Cu, Fe-base intermetallics and aluminum interfaces. Fracture of the  $\alpha$ -aluminium dendritic network is always ductile as evidenced by the formation of long-sized dimples. However, their size is rather controlled by the type of the heat treatment applied. Ageing the quenched test bars at 150 °C leads to propagation of relatively deep micro-cracks into the matrix beneath the fracture surface. These cracks are mainly localized in the interdendritic regions.

**Ibrahim, M. F., et al. [111]** conducted study to the impact toughness and fractography of Al-Si-Cu-Mg base alloys and found the fracture surfaces of non-modified alloys consisted of long Si particles with cracks at their interiors. After addition of grain refiner Sr resulted in a dimple structure throughout the matrix. Increasing the Mg content up to 0.6% resulted in the appearance of fractured particles of Q-Al<sub>5</sub>Mg<sub>8</sub>Cu<sub>2</sub>Si<sub>6</sub> and p-Al<sub>8</sub>Mg<sub>3</sub>-FeSi<sub>6</sub> phases and also reported that the decreasing the cooling rate or increasing the aging temperature did not alter the fracture mechanism with respect to the alloy composition.

**Salleh, M. S., et al. [112]** in their research work, fracture surface characterization of A319 aluminium alloy of the tensile fracture samples was examined to determine the type

of fracture occurring during tensile loading. The SEM photographs of the fracture surfaces obtained from the fractured tensile samples of the as-cast, as-thixoformed, and thixoformed T6 was compared and found the fracture of the as-cast sample is a brittle fracture, while the as-thixoformed and thixoformed T6 exhibit ductile fractures. The thixoformed T6 alloy showed the maximum tensile elongation before failure, reporting an improvement in the ductility properties of the sample attributed to the T6 heat treatment. The as-cast sample exhibits a fracture of the large acicular Si particles, while the as-thixoformed and thixoformed T6 samples display a fine, well-dispersed dimple fracture.